

**MASTER**

**Mathematical analysis and visual representation of sound**

van Erning, L.J.T.O.

*Award date:*  
1979

[Link to publication](#)

**Disclaimer**

This document contains a student thesis (bachelor's or master's), as authored by a student at Eindhoven University of Technology. Student theses are made available in the TU/e repository upon obtaining the required degree. The grade received is not published on the document as presented in the repository. The required complexity or quality of research of student theses may vary by program, and the required minimum study period may vary in duration.

**General rights**

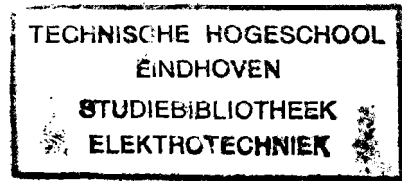
Copyright and moral rights for the publications made accessible in the public portal are retained by the authors and/or other copyright owners and it is a condition of accessing publications that users recognise and abide by the legal requirements associated with these rights.

- Users may download and print one copy of any publication from the public portal for the purpose of private study or research.
- You may not further distribute the material or use it for any profit-making activity or commercial gain

3090

3090 bse

**Mathematical Analysis and  
Visual Representation of Sound.**



**Leon van Erning**

**An investigation performed in the period january 1977 - december 1978 at the Laboratory of Medical Physics and Biophysics of the University of Nijmegen as part of the research of the group Neurophysics, under the responsibility of Prof. Dr. A.J.H. Vendrik and under the supervision of Dr. P.I.M. Johannesma and Prof. Dr. Ir. J.E.W. Beneken (University of Technology, Eindhoven).**

**Special thanks to: Ad Aertsen, Koos Braks, Jan Boezeman, Jan Bruijns, Bert Cranen, Wim van Deelen and Dik Hermes.**

## Contents

Summary	...1
Introduction	...3
1. Mathematical theory of signals	...6
1.1. Real signals	...9
1.2. Analytic signals	..11
1.3. The complex spectro temporal intensity density	..16
2. Visual representation of signals	..29
2.1. Real functions of a single variable	..29
2.2. Real functions of two variables	..30
2.3. Complex functions of two variables	..30
3. Methods	..34
3.1. Preprocessing	..34
3.2. Software implementation	..35
4. Results	..36
4.1. Artificial Signals	..36
4.2. Natural Signals	..57
Discussion	..62
References	..64

## Summary.

This report will give a description of some methods to analyse signals. The aim of these methods is to give a display of the information-bearing attributes of the signals. We will do this in terms of the distribution of intensity as a function of time and frequency. This distribution can be calculated in an analogue way by means of a spectral analyzer (a set of passband filters) or in a digital way by means of a running transform (dynamic or short-term spectrum). These methods are commonly used but they neglect the phase relations of the different frequency components. Because these relations may be important to the auditory system a new method is suggested: the calculation of the Complex Spectro Temporal Intensity Density Function (COSTID).

For this concept, signal description by means of the analytic signal is used. This enables us to define envelope and instantaneous phase of the signal; instantaneous frequency is then given by differentiation of the phase with respect to time. All these characteristics are directly related to the COSTID.

A visual representation of this complex function of time and frequency is constructed by coding the complex function by means of colours. Two different ways of colour-coding are presented here. They depend on the choice of real- and imaginary part or modulus and argument of the complex value:

rectangular and polar coding.

As for the software only a general description of the preprocessing (filtering, sampling) and the implementation is given. Program listings are available in the group Neurophysics.

The results are presented for several computer generated and one natural sound signal.

## Introduction.

The investigations described here are part of the research of the group Neurophysics. This research is within the study of brain and behaviour concerned with the auditory part of the nervous system of the frog *Rana temporaria* [1].

The basic question is the neural base of perception. In this context the more direct goal is the description of the stimulus-response relation for a single neuron in central auditory nuclei. By stimulus is meant the sound presented to the frog by means of an acoustic coupler attached to the eardrum. By response we mean the extracellular measurements of single unit activity: the action-potentials, spikes or neural events.

From earlier investigations it appeared that artificial sounds like tones, clicks and Gaussian white noise are less effective in central parts of the auditory system than they are in the more peripheral parts [2]. Therefore the stimulus ensemble was extended to natural sounds that may play a role in the normal behaviour of the animal.

Investigation of the characteristics of natural sounds is important for several reasons:

1. To characterize a system by means of correlation of input and output signal, it is necessary to know the characteristics of the input signal. The correlation depends

on the kind of input signal.

2. Stimulation with natural sounds under computer control can be done by digital to analogue conversion of the sampled natural sound or by controlling synthesizers and noise generators. This last method needs a parametric description of the natural sound.

3. To extract sound-parameters that can be used to characterize units in higher parts of the auditory system [4].

Though we mentioned only acoustic signals in the foregoing our methods are not limited to sound. Various other kinds of signals can be analyzed, i.e. EEG, EOG, etc.

Signal analysis can be made in time- and frequency domain separately, but there does exist also a method that considers signal properties in time and frequency combined. The theory of these methods is discussed in chapter 1.

As long as we are dealing with a real function of one or two variables we can make a display in two or (in perspective) three dimensions. But when the calculated signal function is a complex function of two variables, it is no longer possible to make a display of the total function in such a way. Therefore we came to a coding of complex values in colours. The two dimensional complex plane is mapped into the three dimensional colour range. The coding procedure is explained in chapter 2.

Chapter 3 gives insight in the selection of examples and the structure of the software that was developed.

For the need of checking the software and gaining insight in the representation of complex functions in a colour display, we made some runs with artificial signals. They consisted of pulses (rectangular, triangular and Gaussian), sines, cosines and amplitude and/or frequency modulated wave forms. In chapter 4 the results are given for a tone-pulse, that resembles an element from a frog vocalization, for combinations of these tones shifted in time and/or frequency and for an element taken from a frog vocalization.



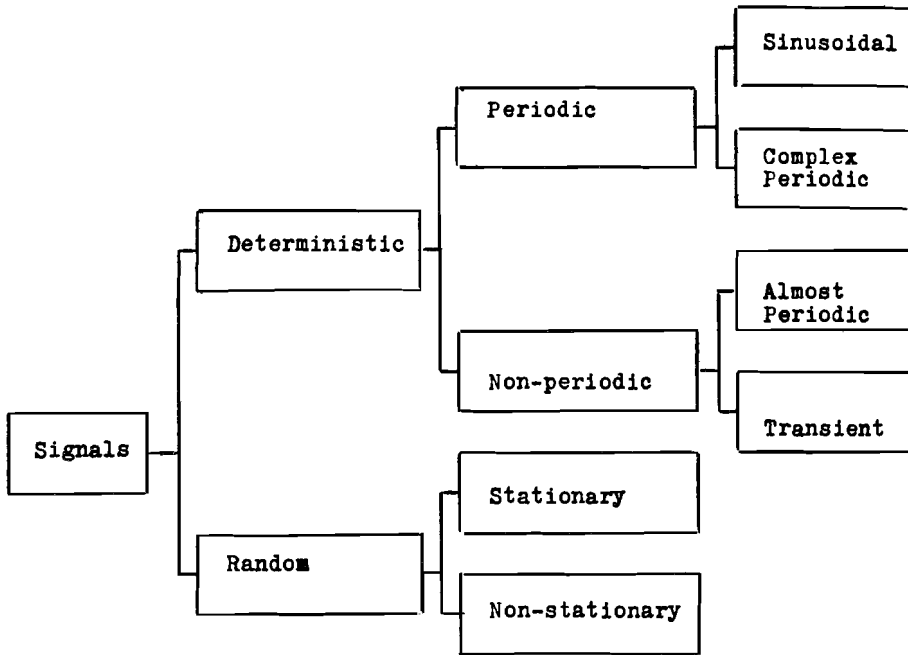


Fig. 1.1. Classification of data.

## Chapter 1

### Mathematical theory of signals.

In this chapter a review is given of some theoretical aspects of signal analysis. Although all signals are real (electrical voltages resulting from physical processes), analysis will be based on complex signals; this leads to considerable mathematical simplification.

The most general description of a signal is as a set of pairs of numbers  $\{x(t), t\}$ ,  $-A \leq x(t) \leq A$  and  $0 \leq t \leq T$ . The restriction on  $x(t)$  is allowed because measuring ranges are bounded and measuring time is also restricted. Because the type of signal may have an influence on the type of analysis, we shall first examine the various types of signals which are encountered in practice.

A fundamental division of physical data is into deterministic or random data.

Deterministic means that the relation between  $x(t)$  and  $t$  can be described by an explicit mathematical relationship. In general this implies that if an experiment producing specific data of interest can be repeated many times with identical results (within the limits of experimental error), then the data can generally be considered deterministic. Data representing deterministic phenomena can be categorized as being either periodic or non-periodic. Periodic data can be further categorized as being either sinusoidal or

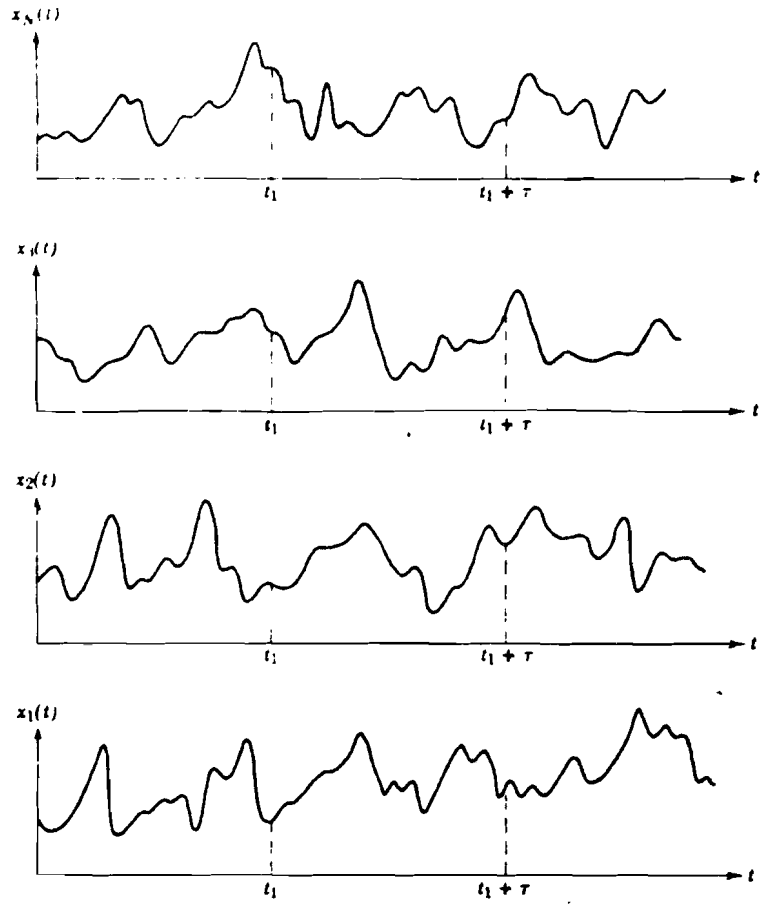


Fig. 1.2. Ensemble of sample functions

nonsinusoidal; non-periodic data as being " almost-periodic " or transient (fig. 1.1). Of course any combination of these forms may also occur.

Data representing a random phenomenon cannot be described by an explicit mathematical relationship, because each observation of the phenomenon will be unique. In other words, any given observation will represent only one of many possible results, which may have occurred. A single time history representing a random phenomenon is called a sample function. The set of all possible sample functions is called a random or stochastic process. Random processes may be categorized as being either stationary or nonstationary. For random processes, the properties of the phenomenon can hypothetically be described at any instant of time by computing average values over a subset of sample functions (also called the ensemble), which are realizations of the random process (fig. 1.2).

For the general case where mean

$$\mu_x(t) \triangleq \lim_{N \rightarrow \infty} \frac{1}{N} \sum_{k=1}^N x_k(t) \quad 1.1.$$

and the autocorrelation function

$$R_x(t, t+\tau) = \lim_{N \rightarrow \infty} \frac{1}{N} \sum_{k=1}^N x_k(t) x_k(t+\tau) \quad 1.2.$$

vary as time  $t$  varies, the random process  $\{x(t)\}$  is said to be nonstationary. For the special case where  $\mu_x(t)$  and  $R_x(t, t+\tau)$  do not vary as time  $t$  varies, the random process  $x(t)$  is said to be weakly stationary or stationary in the wide sense. For the case where all ensemble averages (moments) and joint

moments are time invariant, the random process  $\{x(t)\}$  is said to be **strongly** stationary or stationary in the strict sense.

The concept of stationarity, as defined above relates to the ensemble averaged properties of a random process. In practice, however, data in the form of individual signal waveforms resulting from a random phenomenon are frequently referred to as being stationary or non-stationary. A slightly different concept of stationarity is involved here. When a signal waveform is referred to as being stationary, it is generally meant that the properties computed over short time intervals do not vary "significantly" from one interval to the next. The word significantly is used here to mean that observed variations are greater than would be expected owing to normal statistical sampling variations. Many physical signals as speech, frog vocalizations, etc. are non-stationary signals. We find, for example, that any signal derived from a process involving the Doppler effect cannot be analyzed in terms of a constant frequency content since this will be found to vary with time. Now a measure for the non-stationarity can be the change of the power spectrum when this spectrum is calculated for sequential signal parts with more or less overlap. For the segmentation of the natural sounds to analyze, we selected by looking at a visual display of the total signal waveform mostly those parts with a temporal envelope starting and ending at zero. These segments will further on be referred to as "the" signal.

1.1. Real Signals.

Functions of a rather general nature can be described by the development in a set of orthogonal functions  $\{g_i(t)\}$ . In this way such an "arbitrary" function can be approximated by a finite number of coefficients [3] provided the function satisfies certain conditions.

A continuous set of orthonormal functions is given by

$$\int_a^b dt g_\mu(t) g_\nu(t) = \delta(\mu - \nu) \quad 1.1.1.$$

where the Dirac-"function"  $\delta(s) = 0$  for  $s \neq 0$

$$\text{and } \int_{-\infty}^{+\infty} ds \delta(s) = 1$$

(In the rest of this report we will omit integration boundaries that reach from  $-\infty$  to  $+\infty$ ).

Now a time function can be expressed as

$$x(t) = \int d\nu c_\nu g_\nu(t) \quad 1.1.2.$$

$$\text{where } c_\nu = \int dt x(t) g_\nu(t) \quad 1.1.3.$$

If  $\int dt |x(t)| < \infty$  we can take

$$g_\nu(t) = e^{-i\nu t} = \cos(\nu t) - i \sin(\nu t) \quad 1.1.4.$$

which results in the Fourier- transform; an orthogonal expansion of the signal in harmonic functions. These functions form an important class of functions because they are the

eigenfunctions of linear systems. In hearing, not only the temporal structure of the signal is of interest, but also its spectral composition. Investigations have shown that the ear may perform a continuous frequency analysis. Therefore an analysis in the frequency domain may lead to find related characteristics of the auditory part of the nerve system.

We recall some properties of the Fourier transform to demonstrate how they change as we use an analytic signal instead of a real signal.

$$\text{Fourier transform: } \check{x}(\omega) = \int dt e^{-i\omega t} x(t) \quad 1.1.5.$$

where "  $\int dt e^{-i\omega t}$  " is a linear operator on  $x(t)$ ;

$$\text{The inverse transform: } x(t) = \frac{1}{2\pi} \int d\omega e^{i\omega t} \check{x}(\omega) \quad 1.1.6.$$

$$\text{Since } \check{x}(-\omega) = \check{x}^*(\omega) \quad 1.1.7.$$

it follows, that only one half of the spectrum fully specifies the signal  $x(t)$ . Now we can write equation (1.1.6) in the form:

$$x(t) = \frac{1}{2\pi} \int_{-\infty}^0 d\omega e^{i\omega t} \check{x}(\omega) + \frac{1}{2\pi} \int_0^{\infty} d\omega e^{i\omega t} \check{x}(\omega) \quad 1.1.8.$$

Changing the variable  $\omega$  to  $-\omega$  in the first integral and use of equation (1.1.7.) gives

$$x(t) = \frac{1}{2\pi} \int_0^{\infty} d\omega e^{-i\omega t} \check{x}^*(\omega) + \frac{1}{2\pi} \int_0^{\infty} d\omega e^{i\omega t} \check{x}(\omega) \quad 1.1.9.$$

But equation 1.1.9. can also be written as

$$x(t) = \frac{1}{2\pi} \int_0^{\infty} d\omega \operatorname{Re} \left\{ 2\check{x}(\omega) e^{i\omega t} \right\} \quad 1.1.10.$$

Inspection of equation (1.1.10.) shows that a complex signal can be found from the real signal by omitting the negative frequencies and doubling the amplitude of the positive frequencies. We see that  $x(t)$  is the real part of the complex signal  $\xi(t)$ , if

$$\xi(t) = \frac{1}{\pi} \int_0^{\infty} d\omega e^{i\omega t} \check{x}(\omega) \quad 1.1.11.$$

For the spectrum of  $\xi(t)$  we may write

$$\begin{aligned} \check{\xi}(\omega) &= 0 && ; \omega < 0 \\ &= \check{x}(\omega) && ; \omega = 0 \\ &= 2\check{x}(\omega) && ; \omega > 0 \end{aligned} \quad 1.1.12.$$

Obviously the imaginary part of  $\xi(t)$  is given by

$$\check{x}(t) = \frac{1}{\pi} \int_0^{\infty} d\omega \operatorname{Im} \left\{ \check{x}(\omega) e^{i\omega t} \right\} \quad 1.1.13.$$

So we see that we can also represent  $x(t)$  by means of a complex signal without any loss of information, this brings us to the next part of this chapter.

## 1.2. Analytic Signals.

As mentioned before the aim of this analysis is the description of natural stimuli used in the investigations of



the auditory system of the frog.

For the classification of neurons the sensitivity to frequency and intensity are widely used. As long as pure tones are used "the" frequency is well defined. Natural sounds however contain different frequency components. In addition the number of frequency components and their magnitude may vary with time. The response of some neurons suggests that it may also be important to study the phase relations between the frequency components in the natural stimuli [17].

The description of a signal in terms of an instantaneous amplitude ("envelope") and instantaneous frequency is possible with the analytic signal. A concept that was introduced by Gabor and Ville [6, 11, 9]. If we assume the signal to contain no DC- component or

$$\dot{x}(0) = \int dt x(t) = 0 ; \text{ we have the analytic signal:}$$

$$\xi(t) = x(t) + i\tilde{x}(t) \quad 1.2.1.$$

where  $\tilde{x}(t)$  is the Hilbert transform of  $x(t)$ . Both  $x(t)$  and  $\tilde{x}(t)$  are real functions of time. The Hilbert transforms or reciprocity formulas are defined as

$$\tilde{x}(t) = \frac{1}{\pi} \int ds \frac{x(s)}{t-s} \quad 1.2.2.a$$

and 
$$x(t) = \frac{-1}{\pi} \int ds \frac{\tilde{x}(s)}{t-s} \quad 1.2.2.b$$

The integrals being understood as Cauchy principal values [7]. The functions  $x(t)$  and  $\tilde{x}(t)$  form a Hilbert pair and have the following properties [8, 9]

1) Each function of a pair has the same intensity or "norm"

$$I = \int x^2(t) dt = \int \tilde{x}^2(t) dt \quad 1.2.3.$$

2) The functions forming a pair are orthogonal,

$$\int x(t)\tilde{x}(t) dt = 0 \quad 1.2.4.$$

3) The Fourier spectra  $\check{x}(\omega)$  and  $\check{\tilde{x}}(\omega)$  of  $x(t)$  and  $\tilde{x}(t)$  are related as

$$\begin{aligned} \check{\tilde{x}}(\omega) &= i \check{x}(\omega) && ; \omega < 0 \\ &= 0 && ; \omega = 0 \\ &= -i \check{x}(\omega) && ; \omega > 0 \end{aligned} \quad 1.2.5.$$

For the Fourier spectrum of the analytic signal we then get

$$\begin{aligned} \check{\xi}(\omega) &= 0 && ; \omega < 0 \\ &= \check{x}(\omega) && ; \omega = 0 \\ &= 2\check{x}(\omega) && ; \omega > 0 \end{aligned} \quad 1.2.6.$$

This is the same result as we found for the Fourier spectrum of the complex signal in the previous part of this chapter. So we can construct an analytic signal by making the negative frequency components of the real signal equal to zero.

It should be noted here that in general complex signals are not necessary analytic signals. Complex signals are only analytic if their negative frequency components are equal to zero. Given an arbitrary complex signal

$$\rho(t) = x(t) + i y(t) = r(t)e^{i\varphi(t)} \quad 1.2.7.$$

This is in general not analytic for arbitrary  $x(t)$  and  $y(t)$  or  $r(t)$  and  $\varphi(t)$ . The necessary and sufficient condition is

$$\dot{\rho}(\omega) = 0 \quad ; \omega < 0 \quad 1.2.8.$$

Which is equivalent with

$$x(t) = \operatorname{Re}\{\rho(t)\} = r(t) \cos\varphi(t) \quad 1.2.9.$$

and 
$$y(t) = \operatorname{Im}\{\rho(t)\} = r(t) \sin\varphi(t) \quad 1.2.10.$$

being Hilbert-transforms. This implies  $y(t) = \mathcal{H}\{x(t)\}$  or using eq. (1.2.2.b)

$$r(t)\sin\varphi(t) = \frac{1}{\pi} \int ds \frac{r(s)\cos\varphi(s)}{t-s} = r(t)\sin\varphi(t) \otimes \frac{1}{\pi t} \quad 1.2.11.$$

where  $\otimes$  denotes convolution.

The first equality applies if

$$\int ds r(s) \frac{\cos\varphi(s)}{t-s} = r(s) \int ds \frac{\cos\varphi(s)}{t-s} \quad 1.2.12.$$

which is (approximately) correct if  $r(t)$  varies slowly with respect to  $\cos\varphi(t)$  for all  $t$ . This result forms a special form of a theorem given by Bedrosian [3]. It states that, if  $r(t)$  and  $\cos\varphi(t)$  are real functions with non-overlapping spectra and with the frequency band of  $r(t)$  below that of  $\cos\varphi(t)$ ,

$$\begin{aligned} \mathcal{H}\{r(t) \cos\varphi(t)\} &= r(t) \mathcal{H}\{\cos\varphi(t)\} \\ &= r(t) \sin\varphi(t) \end{aligned} \quad 1.2.13.$$

Basically the concept of modulation in communication rests

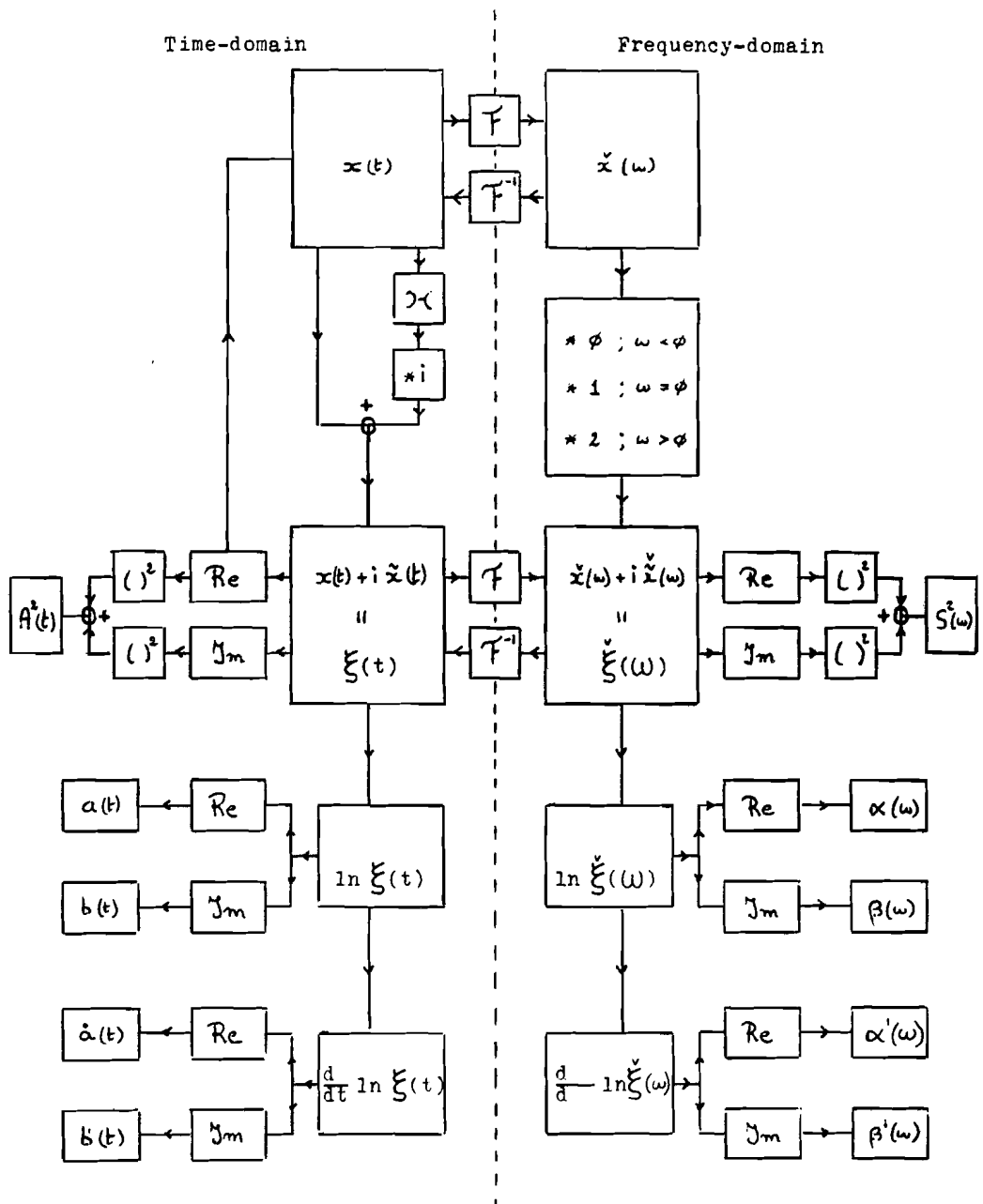


Fig. 1.2.1. Relations between real signal, analytic signal and signal parameters in time and frequency domain.

on this same assumption, as the modulating signal is supposed to have a frequency band below that of the carrier-signal. One considers three important types of modulation: amplitude-, phase- and frequency- modulation. In all three of them the modulated quantity is defined to depend linearly on the modulating signal. Now it is clear that we cannot speak of a modulating signal, when we are describing a signal that is not the output of a modulator, but just an arbitrary waveform, although we feel intuitively that we can speak of the amplitude, phase and frequency of a signal. Therefore let us define a number of signal-parameters related to the analytic signal.

$$\xi(t) = x(t) + i \tilde{x}(t) = e^{a(t) + ib(t)} \quad 1.2.14.$$

$$\text{and } \check{\xi}(\omega) = e^{\alpha(\omega) + i\beta(\omega)} ; \omega \geq 0 \quad 1.2.15.$$

$a(t)$  :  
the temporal  
logarithmic amplitude

$\alpha(\omega)$  :  
the spectral  
logarithmic amplitude

$b(t)$  :  
the temporal phase

$\beta(\omega)$  :  
the spectral phase

$\dot{a}(t)$  :  
the relative temporal  
amplitude change

$\alpha'(\omega)$  :  
the relative spectral  
amplitude change

' refers to  $\frac{d}{dt}$

' refers to  $\frac{d}{d\omega}$

$\dot{b}(t)$  :  
the temporal phase change or  
instantaneous frequency

$\beta'(\omega)$  :  
the spectral phase change or  
slope of phase characteristic

Additionally we define

$A(t) = e^{a(t)}$  :  
the temporal envelope

$S(\omega) = e^{\alpha(\omega)}$  :  
the spectral envelope.

### 1.3. The Complex Spectro Temporal Intensity Density Function.

Until now we considered signal properties either in time- or frequency domain. Although the concept of instantaneous frequency appears to supply a connection between the two domains, it does not represent a full description of time-frequency relations. It gives only information about the change of the temporal phase and disregards the effect of amplitude changes on the spectrum of the signal. As mentioned before the spectrum only represents how a signal is built up with harmonic components, but does not represent how the relations between these components vary with time. Because of this lack of phase information in the power spectrum, the temporal characteristics of the signal waveform may change without any effect on the power-spectrum. An ensemble of different waveforms may have the same power-spectrum. But, as the change of phase relations with time may be important to auditory neurons, the question arises how we can analyse signal properties in both the time- and the frequency domain. This now can be done in various ways.

By passing the signal through a bank of bandpass filters (spectral analyzer [21]) or calculation of the power-spectrum of temporal windowed signal parts [4], it is possible to get an impression of the change of signal properties as a function of the spectral band selected and the temporal window, respectively [14]. As Gabor's uncertainty relation [11] applies

to these concepts, we can only talk about an approximation of the time-dependent spectrum. Filters cannot have both short impulse responses and narrow bandwidth. So a band of fixed bandwidth filters cannot provide both good spectral and good temporal resolution. Exactly parallel limitations on resolution apply when short term spectral analysis is performed. In the latter case the window length should always be made as long as possible for good spectral resolution, but it will normally be limited by how rapidly the signal itself is changing. In calls of the frog *Rana temporaria*, individual elements last  $\approx 21$  msec. Now this is a possible window length, if one is interested in the spectral composition of the individual elements in these calls.

Now a concept is presented that does not suffer from the restrictions mentioned above. Several concepts involve both time and frequency and have been introduced into signal theory by different authors, Gabor[11] being one of the first. The account of Rihaczek unifies several of these concepts in terms of the complex energy density function [15.] Although we will use the mathematical expression given by Rihaczek, we introduce a different name, because it represents not really an energy : The Complex Spectro Temporal Intensity Density Function (COSTID). This function is defined as

$$\Xi(\omega, t) = \xi^*(\omega) e^{-i\omega t} \xi(t) \quad 1.3.1.$$

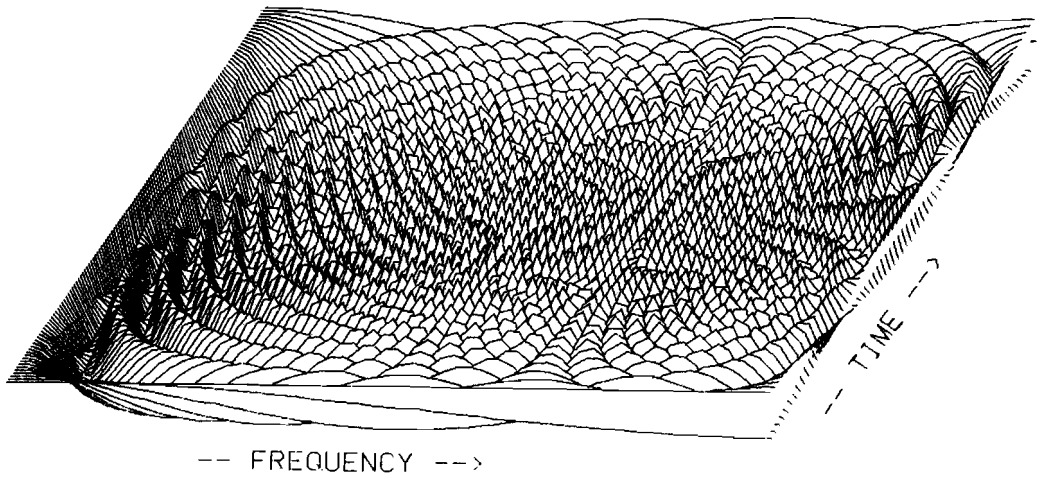


Fig. 1.3.1.a. Real part of  $\exp(-i2\pi ft)$ :  $\cos 2\pi ft$ .

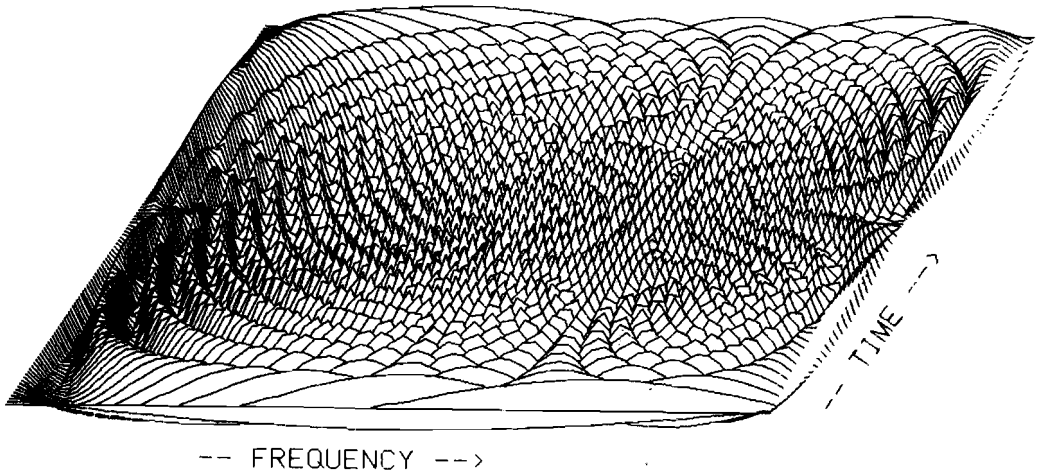


Fig. 1.3.1.b. Imaginary part of  $\exp(-i2\pi ft)$ :  $-\sin 2\pi ft$ ;  
time: from 0. to 5.12 msec, frequency: from 0. to 12500 Hz.



where  $\xi(t)$  is the analytic signal  
 $\xi(\omega)$  is the Fourier transform of  $\xi(t)$  and  
 $e^{-i\omega t}$  is a function that relates temporal and  
 spectral functions (fig. 1.3.1.).

That this function represents indeed the distribution of the  
 signals intensity over its spectral and temporal components,  
 may become clear in studying the properties of the COSTID.

Properties of the COSTID - function :

a) The temporal intensity  $|\xi(t)|^2$  is given by spectral  
 integration of the COSTID - function.

$$\frac{1}{2\pi} \int d\omega \Xi(\omega, t) = \xi(t) \frac{1}{2\pi} \int d\omega \xi^*(\omega) e^{-i\omega t} =$$

$$\xi(t) \xi^*(t) = I(t) \quad 1.3.2.$$

$I(t)$  is the square of the temporal envelope  $A(t)$ .

b) The spectral intensity  $|\xi(\omega)|^2$  is given by temporal  
 integration of the COSTID - function

$$\int dt \Xi(\omega, t) = \xi^*(\omega) \int dt \xi(t) e^{-i\omega t} =$$

$$\xi^*(\omega) \xi(\omega) = J(\omega) \quad 1.3.3.$$

$J(\omega)$  is the square of the spectral envelope  $S(\omega)$ .

c) The total intensity of the signal  $I$  is given by temporal  
 and spectral integration

$$\frac{1}{2\pi} \iint dt d\omega \Xi(\omega, t) = \int dt |\xi(t)|^2 = I_T$$

$$= \int d\omega |\xi(\omega)|^2 = J_\Omega \quad 1.3.4.$$

d) The COSTID - function is independent of the absolute phase  
 of the signal. This implies that the COSTID - function of

$$\xi(t) = \alpha \xi_0(t) + \sqrt{1 - \alpha^2} \check{\xi}_0(t) \quad 1.3.5.$$

is independent of  $\alpha$ . Substitution of

$$\check{\xi}_0(t) = \mathcal{H}(\{\xi_0(t)\}) = -i \xi_0(t) \quad 1.3.6.$$

and  $\check{\xi}(\omega) = (\alpha - i\sqrt{1 - \alpha^2}) \check{\xi}_0(\omega)$  1.3.7.

gives 
$$\begin{aligned} \Xi(\omega, t) &= (\alpha + i\sqrt{1 - \alpha^2}) \check{\xi}_0^*(\omega) e^{-i\omega t} \\ &\quad * (\alpha - i\sqrt{1 - \alpha^2}) \xi_0(t) = \Xi_0(\omega, t) \end{aligned} \quad 1.3.8.$$

e) The COSTID - function is non-linear. Given the analytic signals  $\xi_1(t)$  and  $\xi_2(t)$ , we can calculate the COSTID - function of either signal

$$\xi_1(t) \rightarrow \Xi_1(\omega, t) \quad \text{and} \quad \xi_2(t) \rightarrow \Xi_2(\omega, t)$$

Calculation of the COSTID - function for a signal

$$\xi_3(t) = \xi_1(t) + \xi_2(t)$$

results in the COSTID - function

$$\begin{aligned} \Xi_3(\omega, t) &= \Xi_1(\omega, t) + \check{\xi}_1^*(\omega) e^{-i\omega t} \xi_2(t) \\ &\quad + \check{\xi}_2^*(\omega) e^{-i\omega t} \xi_1(t) + \Xi_2(\omega, t) \end{aligned} \quad 1.3.9.$$

In c) we saw that the total signal intensity could be found by integration over the whole time- frequency plane. Now we can ask what the result is, if we integrate only over a part of that plane. The COSTID - function can be expressed in terms of modulus and argument

$$\Xi(\omega, t) = |\check{\xi}(\omega)| e^{-i\beta(\omega)} e^{-i\omega t} |\xi(t)| e^{ib(t)} \quad 1.3.10.$$

By introducing  $\check{\nu}(\omega, t) = \omega t + \beta(\omega) - b(t)$ , the argument or phase of the COSTID - function, we can write

$$\Xi(\omega, t) = |\check{\xi}(\omega)| |\xi(t)| e^{-i\check{\nu}(\omega, t)} \quad 1.3.11.$$

The COSTID - function, being a distribution function, the intensity concentrated in a region  $\Omega, T$  is given by

$$I(\Omega, T) = \int_{\Omega} d\omega \int_T dt |\check{\xi}(\omega)| |\xi(t)| e^{-i\check{\nu}(\omega, t)} \quad 1.3.12.$$

Using the fact that the spectral and temporal envelopes vary only slowly with respect to  $e^{-i\check{\nu}(\omega, t)}$ , we see that significant contributions to the integral can only come from points where the argument  $\check{\nu}(\omega, t)$  changes slowly as function of  $\omega$  and  $t$ . This leads to the equations :

$$\frac{\partial \check{\nu}(\omega, t)}{\partial t} = 0 \quad \longrightarrow \quad \omega = \dot{b}(t) \quad 1.3.13.$$

$$\frac{\partial \check{\nu}(\omega, t)}{\partial \omega} = 0 \quad \longrightarrow \quad t = -\beta'(\omega)$$

So a trajectory in the time-frequency plane may be found, on which  $\omega$  and  $t$  are related by (1.3.13.) and the signal has a local maximum in its intensity.

Signal parameters defined for the analytic signal can be calculated from  $\ln \Xi(\omega, t)$  according to the following diagram :

$$\ln \Xi(\omega, t)$$

	Re	Im
$\frac{\partial}{\partial t}$	$\dot{a}(t)$	$-(\omega + \dot{b}(t))$
$\frac{\partial}{\partial \omega}$	$\alpha'(\omega)$	$-t - \beta'(\omega)$

The last property of the COSTID - function that we will give here is the normalized first moment of the COSTID - function with respect to  $\omega$  or  $t$ . They are given by

$$\Omega(t) = \frac{\int d\omega \omega \Xi(\omega, t)}{\int d\omega \Xi(\omega, t)} \tag{1.3.14a}$$

$$T(\omega) = \frac{\int dt t \Xi(\omega, t)}{\int dt \Xi(\omega, t)} \tag{1.3.14b}$$

Now it appears that the first normalized moments are simply related to the signal parameters we defined for the analytic signal

$$\begin{aligned} \Omega(t) &= \frac{\int d\omega \omega \Xi(\omega, t)}{\int d\omega \Xi(\omega, t)} = \frac{i}{\xi^*(t)} \frac{d \xi^*(t)}{dt} = \frac{i}{1} \frac{d}{dt} \ln \xi^*(t) \\ &= \dot{b}(t) + i \dot{a}(t) \end{aligned} \tag{1.3.15}$$

and

$$\begin{aligned} T(\omega) &= \frac{\int dt t \Xi(\omega, t)}{\int dt \Xi(\omega, t)} = \frac{i}{\xi(\omega)} \frac{d \xi(\omega)}{d\omega} = \frac{i}{1} \frac{d}{d\omega} \ln \xi(\omega) \\ &= -\beta'(\omega) + i \alpha'(\omega) \end{aligned} \tag{1.3.16}$$

So these relations may be diagrammed as

	Re	Im
$\Omega(t)$	$\dot{b}(t)$	$\dot{a}(t)$
$T(\omega)$	$-\beta'(\omega)$	$\alpha'(\omega)$

The relation between the COSTID - function and short-term spectra made in analogue or digital way.

When considering the analysis of signal waveforms with time varying parameters the rate of change of these parameters is often of prime importance [20]. If these changes are slow enough to permit the signal to be considered as stationary over a finite period of time, the conventional stationary methods of analysis over such a small section of the signal time-history can be applied. This is the general principle behind the many forms of local, instantaneous and evolutionary spectral analysis.

The ideal with this form of analysis is to determine (for example) a power/ frequency distribution defined at a unique instant in time. An early attempt to define a time varying spectrum in terms of a Fourier transform was made by Page [14]. He recognized that the time variation is invariably a slow one in terms of the constituent signal frequencies and defined what he called an Instantaneous Power - Spectrum, a differential of time. This spectrum depends only on the past history of the signal and not on its future values, which are implied in the classical definition of the Fourier transform [20].

He proposed a "running transform" :

$$P_t(\omega) = \left| \int_{-\infty}^t ds e^{-i\omega s} x(s) \right|^2 \quad 1.3.17.$$

His instantaneous power spectrum was defined as the rate of change with time of  $P_t(\omega)$ :

$$p(\omega, t) = \frac{\partial}{\partial t} P_t(\omega) \quad 1.3.18.$$

By defining

$$\check{x}_t(\omega) = \int_{-\infty}^t ds e^{-i\omega s} x(s) \quad 1.3.19.$$

the equations (1.3.17.) and (1.3.18.) can be easily be manipulated into the alternative form

$$p(\omega, t) = 2 \operatorname{Re} \left\{ \check{x}_t^*(\omega) e^{-i\omega t} x(t) \right\} \quad 1.3.20.$$

Ackroyd [13] has derived a general expression for the energy distribution in the time and frequency domain

$$e(\omega, t) = x(t) \operatorname{Re} \left\{ \check{x}(\omega) e^{i\omega t} \right\} \quad 1.3.21.$$

Now  $\operatorname{Re} \left\{ \check{x}_t(\omega) e^{i\omega t} \right\}$  is the response to  $x(t)$  of a filter, whose impulse response is

$$h(t) = u(t) \cos \omega_0 t \quad 1.3.22.$$

where  $u(t)$  is the unit step function. This impulse response is physically realizable in the sense that it is zero for negative  $t$ . The transfer function corresponding to this impulse response is

$$\check{h}(\omega) = \frac{i\omega}{\omega_0^2 - \omega^2}, \quad 1.3.23.$$

while the non-physically realizable impulse response, that Ackroyd used, for the derivation of (1.3.21.) was at  $\omega_0$

$$\check{h}(\omega) = \pi \left\{ \delta(\omega + \omega_0) + \delta(\omega - \omega_0) \right\} \quad 1.3.24.$$

So the "ideal" filter of (1.3.24.) was replaced by the less perfect, but realizable, filter of eq.(1.3.23.) except for a scale factor. Therefore  $p(\omega, t)$  can be thought of as an approximation to  $e(\omega, t)$  with poorer spectral resolution.

Although eq.(1.3.21.) seems to have the same form as the COSTID - function it is not possible thusfar to express in a simple way the energy density function in terms of the COSTID - function. For the output of the spectral analyzer and the results of the short time spectra method this can be done.

#### Relation between COSTID - function and output of real-time spectral analyzer.

Starting with a short description of the real-time spectral analyzer, that was built in the electronic laboratory of the departement of medical physics and biophysics, we will only pay attention to the data path. All control-systems are omitted in fig. 1.3.2.

The first section is formed by a filterbank, consisting of 45 1/3-octave filters, covering the frequency range from 2 Hz up to 50 kHz. Their behaviour is that of a 6-th order

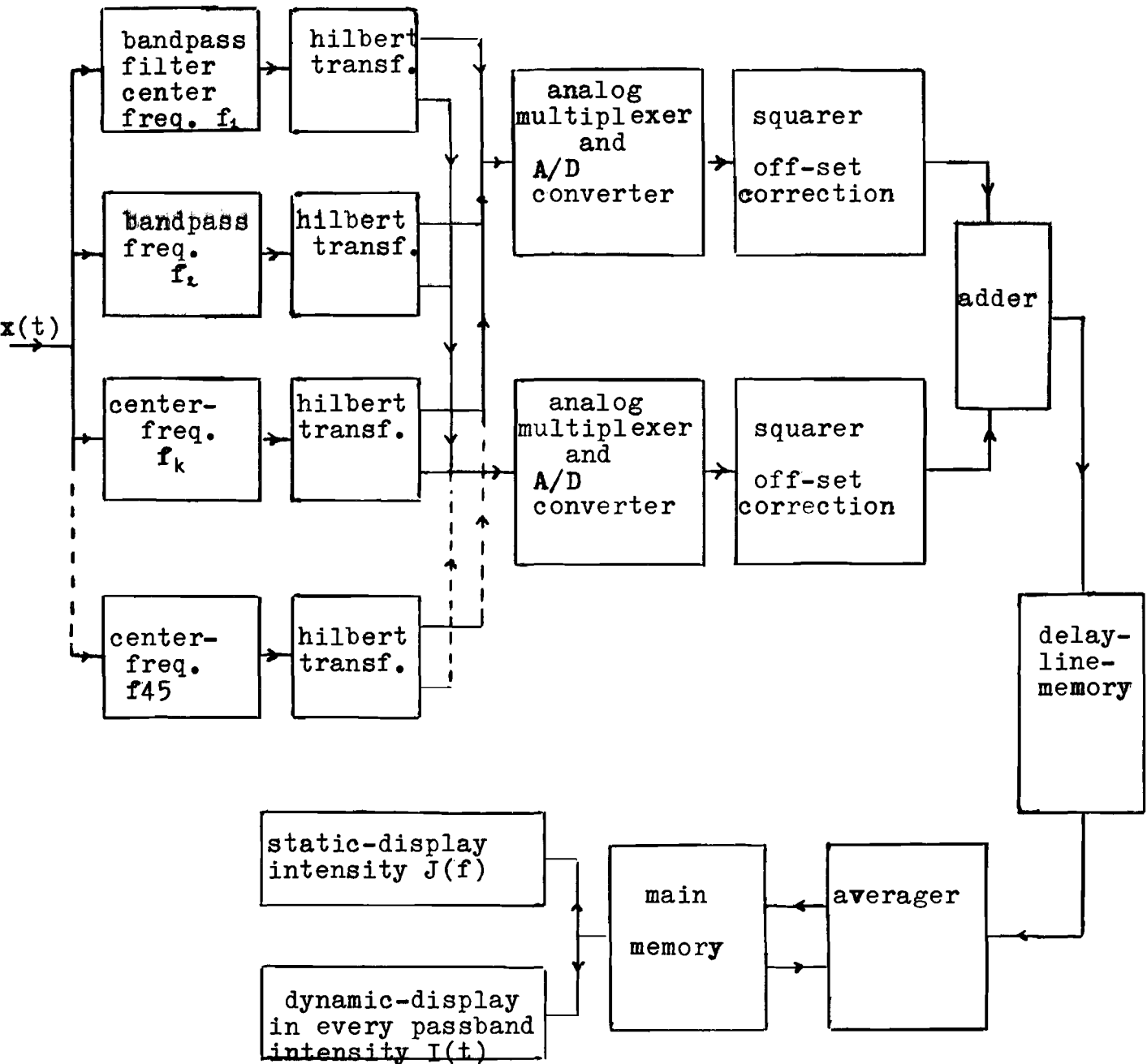


Fig. 1.3.2. Data-path in real-time spectral analyzer.



Chebyshev-filter with an effective bandwidth of  $0.205 \cdot f_k$  ( $f_k$  being the center frequency of the k-th filter). To avoid misinterpretations due to the different bandwidths, an energy correction can be made.

Second section : the Hilbert-transformer.

As the Hilbert-transformer can only produce two outputs with a phase difference of approximately 90 degrees over a limited frequency range, a slight deviation may occur in the (squared) detected amplitude. However, in normal operation an averaging occurs because the output of the preceding  $1/3$  octave filter contains a multiple of frequencies around  $f_k$ , each with their own phase, and so the error is reduced (for  $\varphi = 0.5^\circ$  less than  $10^{-2}$ ).

The third section contains an analogue multiplexer and A/D converter. The multiplexing is done to reduce the number of necessary A/D converters, squares and adders. The A/D converter has an accuracy of 9 bits. Assuming a maximal signal value of 5 Volts and accepting a percentage of errors in the least significant bit of 1%, the signal to noise ratio should be 69 dB (in practice 40 dB can be reached).

The fourth and fifth section, respectively square and add the data. Before squaring, the DC- offset is corrected because an undesired DC- offset may reduce the dynamic range of the analyzer. As long as the DC- offset is below the quantization level the dynamic range will be 54 dB.

The sixth section is formed by a delay-line-memory in order to have also access to the analyzed signal prior to

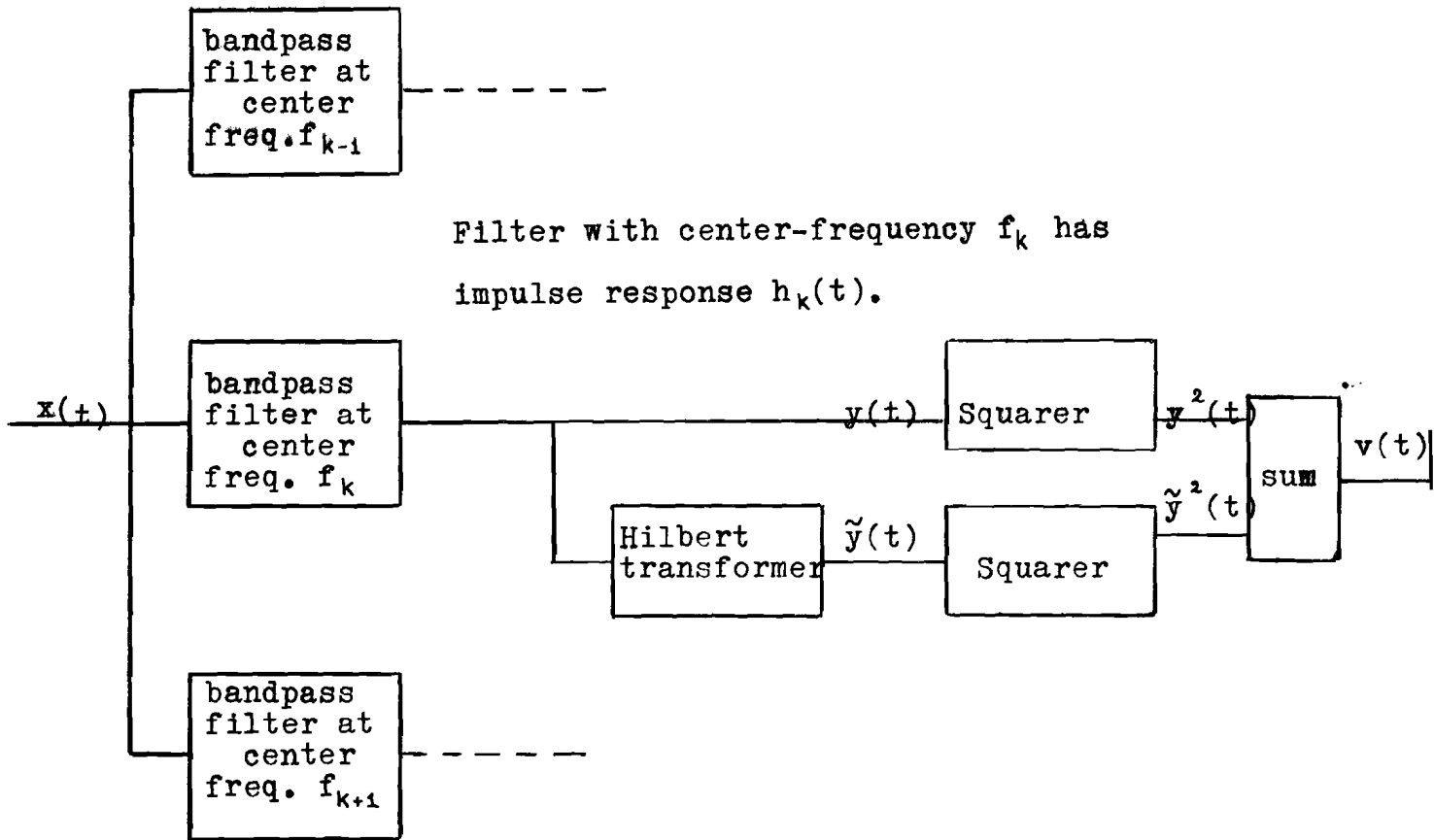


Fig. 1.3.3. Functional block-diagram of data-path in the real-time spectral analyzer.

a trigger-occurrence. The delay-line contains 4096 locations of 18 bits. Triggering can be done external (neural events), manual and internal. The data being stored in the delay-line-memory makes it possible to select  $p\%$  pre-trigger data and  $(100 - p)\%$  after trigger data.

Section seven and eight are respectively averager and main-memory. The objective of the averager is to average the data that is related to several neural events but also to reduce the variance of the detected envelope. The averaging is performed on a running base : the weighting factor is continuously adjusted to the number of averages already executed.

The last two sections represent the display of the data in a static display and a dynamic display. The static display gives the intensity as a function of frequency. The dynamic display gives for every band selected the temporal intensity as a function of time. In chapter 4 these displays will be given for signals that resemble elements out of a vocalization of the frog *Rana Temporaria*.

Now for the derivation of the relation between the output of the real-time spectral analyzer and the COSTID - function we will refer to a simplified version of fig. 1.3.2., namely fig. 1.3.3.

For the analyzer output  $v(t)$  for passband  $k$ , the following relations can be given.

$$v(t) = y^2(t) + \tilde{y}^2(t) \quad 1.3.25.$$

If  $\eta(t) = y(t) + i \tilde{y}(t)$  we get

$$v(t) = \eta(t)\eta^*(t) = \frac{1}{2\pi} \int \eta(t)\check{\eta}^*(\omega) e^{-i\omega t} d\omega \quad 1.3.26.$$

Now we will express  $\eta(t)$  and  $\check{\eta}^*(\omega)$  in terms of  $\xi(t) = x(t) + i \tilde{x}(t)$  and  $\varphi_k(t) = h_k(t) + i \check{h}_k(t)$  respectively in  $\check{\xi}^*(\omega)$  and  $\check{\varphi}_k^*(\omega)$ , this gives

$$\eta(t) = 1/2 \int \xi(t-\tau) \varphi(\tau) d\tau \quad 1.3.27.$$

$$\check{\eta}^*(\omega) = 1/2 \check{\xi}^*(\omega) \check{\varphi}_k^*(\omega) \quad 1.3.28.$$

Substitution in equation (1.3.26.) gives

$$\begin{aligned} v(t) &= \frac{1}{2\pi} \int 1/2 \left\{ \int \xi(t-\tau) \varphi_k(\tau) d\tau \right\} 1/2 \check{\xi}^*(\omega) \check{\varphi}_k^*(\omega) e^{-i\omega t} d\omega \\ &= \frac{1}{8\pi} \iint d\omega d\tau \Xi(\omega, t-\tau) \Xi(\omega, \tau) \quad 1.3.29. \end{aligned}$$

We see that for every passband the output of the real-time spectral analyzer is thus simply the temporal convolution of the COSTID - function of the input signal and the COSTID - function of the corresponding bandpass filter.

Relation between COSTID - function and the results of the short-time spectra method.

In the foregoing part our signal  $x(t)$  was convoluted with the impulse response of the filters  $f_k(t)$ . In this part  $x(t)$  is multiplied with the window function  $w(t)$ , that is

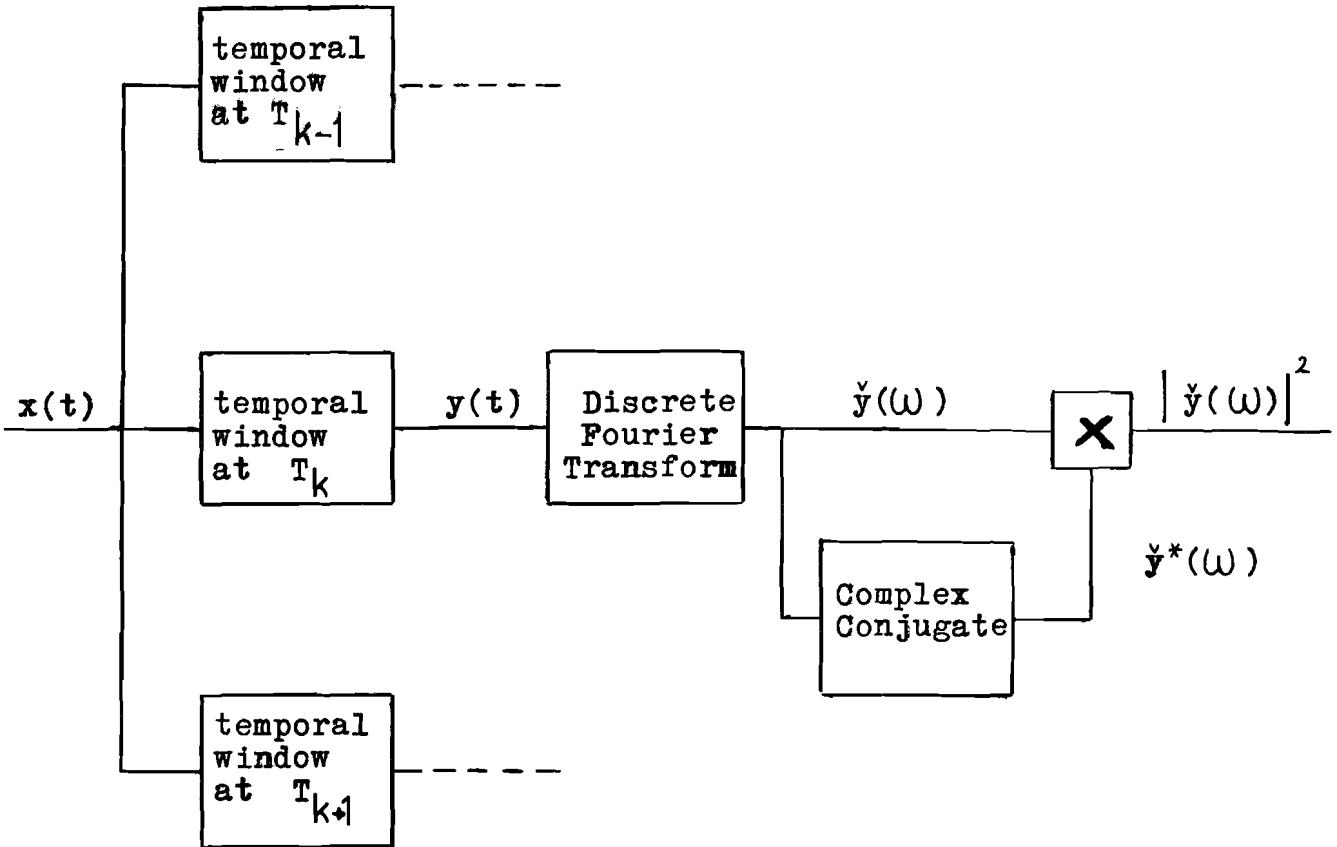


Fig. 1.3.4. Functional block-diagram of the short-time spectrum method.

translated to some point  $T_k$ . The resulting part of the signal waveform will be referred to as a sequence. For every sequence the Fourier transform is calculated (fig. 1.3.4.). As we consider the power spectrum in this case, we use

$$|\check{y}(\omega)|^2 = \check{y}(\omega) \check{y}^*(\omega) \quad 1.3.30.$$

If  $\eta(t) = y(t) + i \check{y}(t)$  we get

$$\begin{aligned} |\check{y}(\omega)|^2 &= 1/4 \check{\eta}(\omega) \check{\eta}^*(\omega) = 1/4 \int dt \check{\eta}^*(\omega) e^{-i\omega t} \eta(t) \\ &= 1/4 \int dt \Xi_{\eta}(\omega, t) \end{aligned} \quad 1.3.31.$$

which is non negative. Otherwise in using

$$\check{\eta}(\omega) = 2\pi \int \check{\xi}(\omega - s) \check{\psi}(s) ds \quad 1.3.32.$$

where

$$\check{\xi}(t) = x(t) + i \check{x}(t) \quad 1.3.33.$$

and

$$\check{\psi}(t) = w(t) + i \check{w}(t) \quad 1.3.34.$$

the convolution of the COSTID - function of the signal and the temporal window function with respect to the frequency is found to be

$$|\check{y}(\omega)|^2 = \frac{1}{8\pi} \iint d\omega dt \Xi_{\xi}(\omega - \nu, t) \Xi_{\psi}(\nu, t).$$

In chapter 4 we will give some results of the short-time power spectrum method for three computer generated signals.

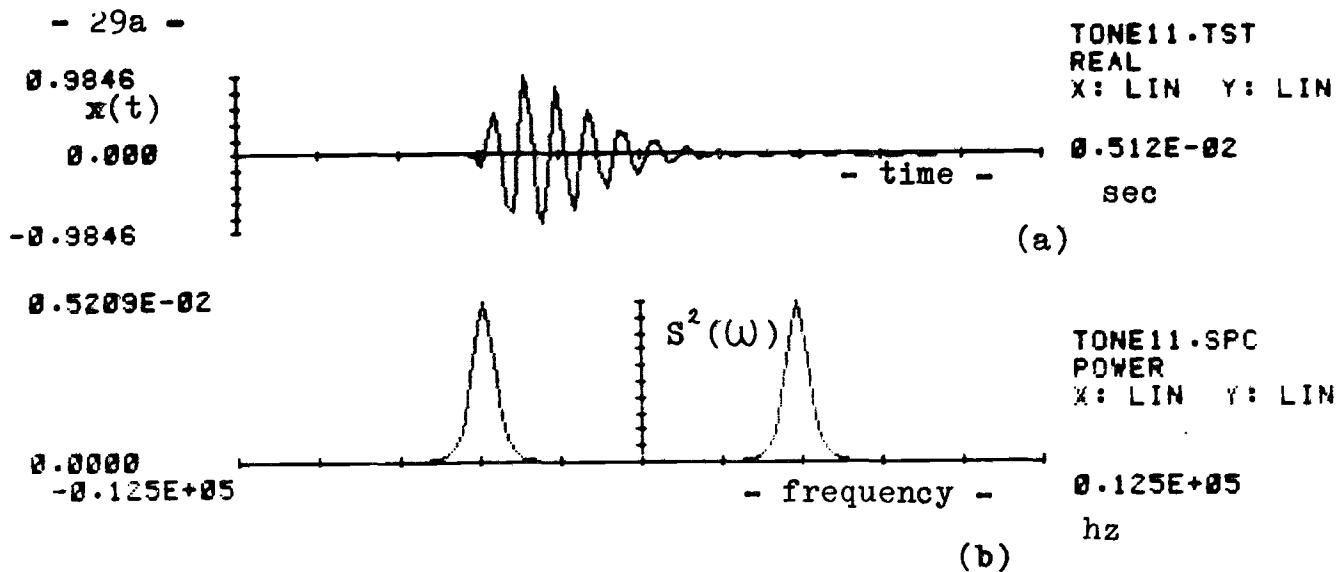


Fig. 2.1. Two dimensional display; (a) Real time signal (gamma-tone); (b) Corresponding power spectrum.

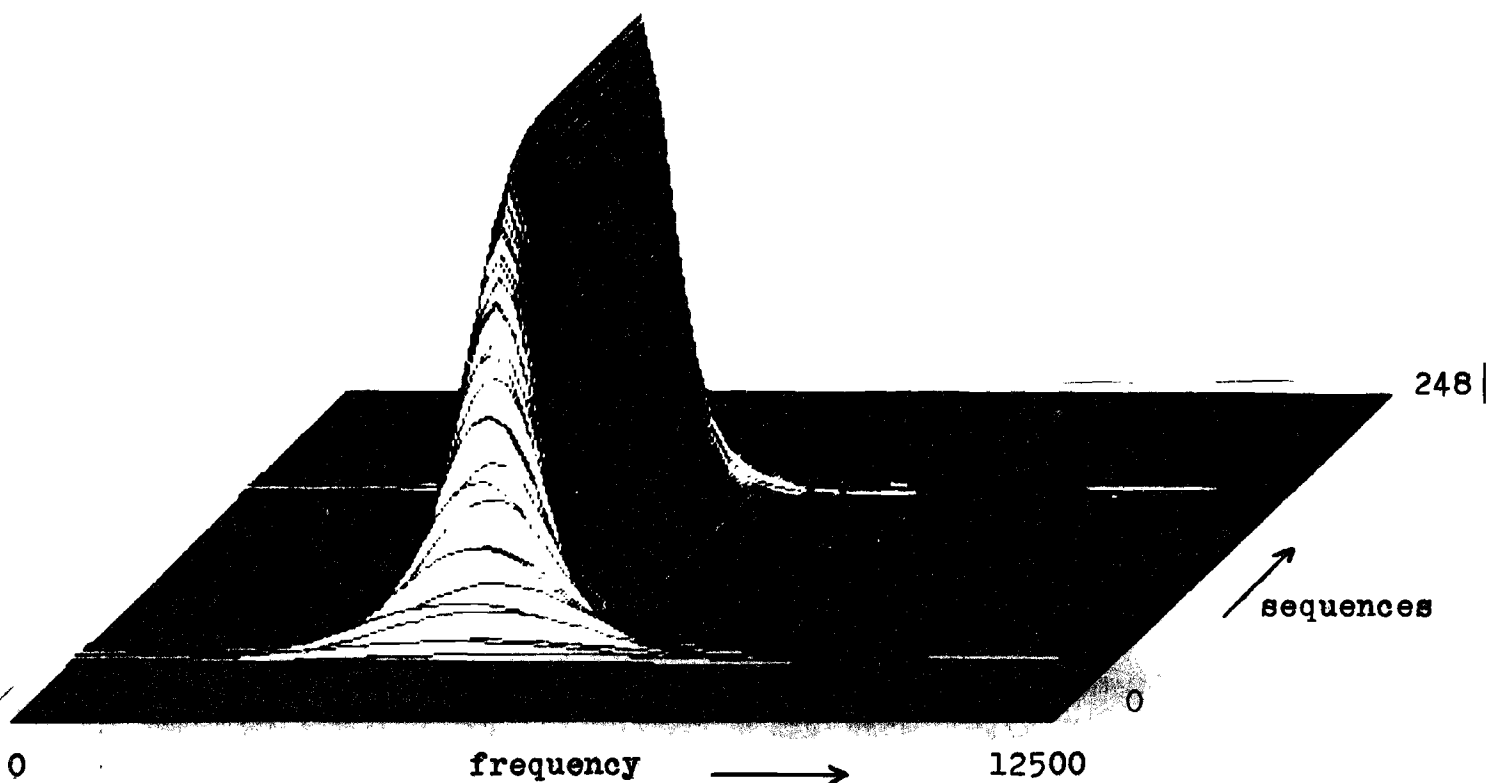


Fig. 2.2. Three dimensional display; Short-time power spectrum of the signal of fig. 2.1.

window length : 5.12 msec, window shift : 40 μ sec

## Chapter 2

### Visual Representation of Signals.

In this chapter we will come to the description of a method to display a complex function of two variables by means of a colour representation. Though the variables in the displays are time and frequency, the actual dimensions of the variables are not relevant for the display techniques.

#### 2.1. Real functions of a single variable.

To display a real function of a single variable only two axes are needed. One for the variable and the other for the corresponding function value. It is obvious that this method can also be used for the real-, imaginary part, modulus or argument of a complex function of a single variable. Though in a number of cases it becomes difficult to interpret results, that are given in two plots, but belong to the same function. This first method is used for : the real-, imaginary part, modulus or argument of the analytic signal or its Fourier transform (the signal spectrum). See example of fig. 2.1.: a real time-signal and its power spectrum. (the text refers to the computer-file: TONE11.TST, the display mode: REAL, POWER and the scaling of horizontal X and vertical Y axis:LIN= linear.



POWER OF SPECTRUM LINEAR SEQUENCE DURATION: 5.12 MSEC  
RECTANGULAR TIME-WINDOW TIME INCREMENT : 0.400E-01MSEC  
TIME FILE :TONE11.NEU FREQUENCY RESOL. : 195. HZ  
COMMENT :DYNAMIC SPECTRUM OF GAMMA TONE SPECTRUM FILENAME: TONE11.DYN  
SYMB-LEV: 0= 0.332E+09 1= 0.249E+09 == 0.166E+09 += 0.030E+08

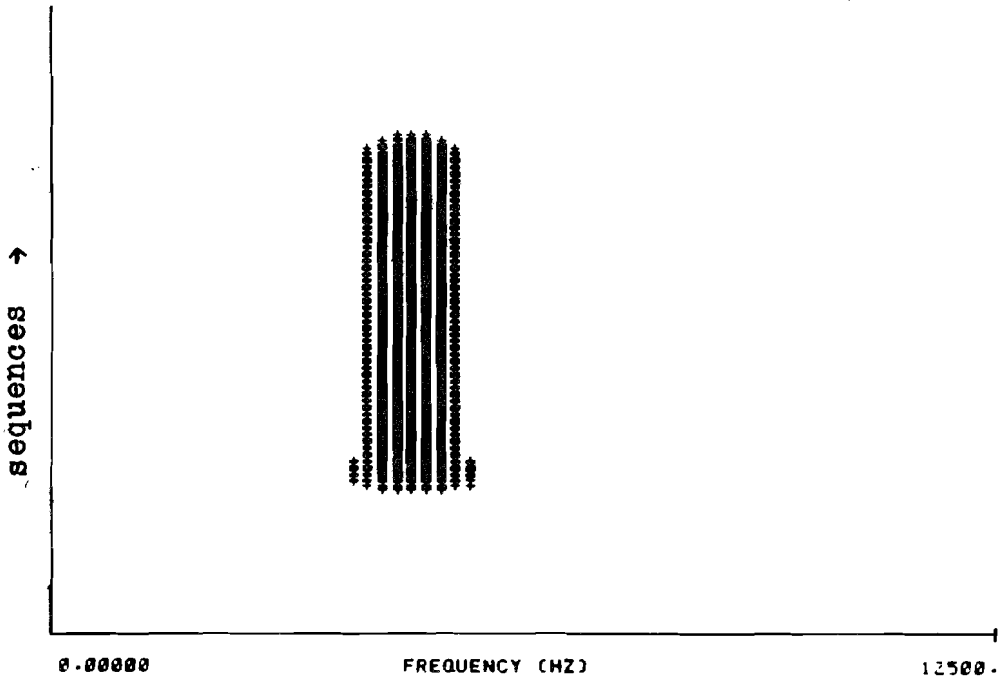


Fig. 2.3. " Sonogram " of dynamic spectrum of fig. 2.2.

POWER OF SPECTRUM LINEAR SEQUENCE DURATION: 5.12 MSEC  
NUMBER OF SEQUENCES : 248 TIME INCREMENT : 0.400E-01MSEC  
RECTANGULAR TIME WINDOW FREQUENCY RESOL. : 195. HZ  
TIME FILE :TONE11.NEU SPECTRUM FILENAME: TONE11.DYN  
COMMENT :DYNAMIC SPECTRUM OF GAMMA TONE  
SYMB-LEV: 0= 0.332E+09 1= 0.249E+09 == 0.166E+09 += 0.030E+08

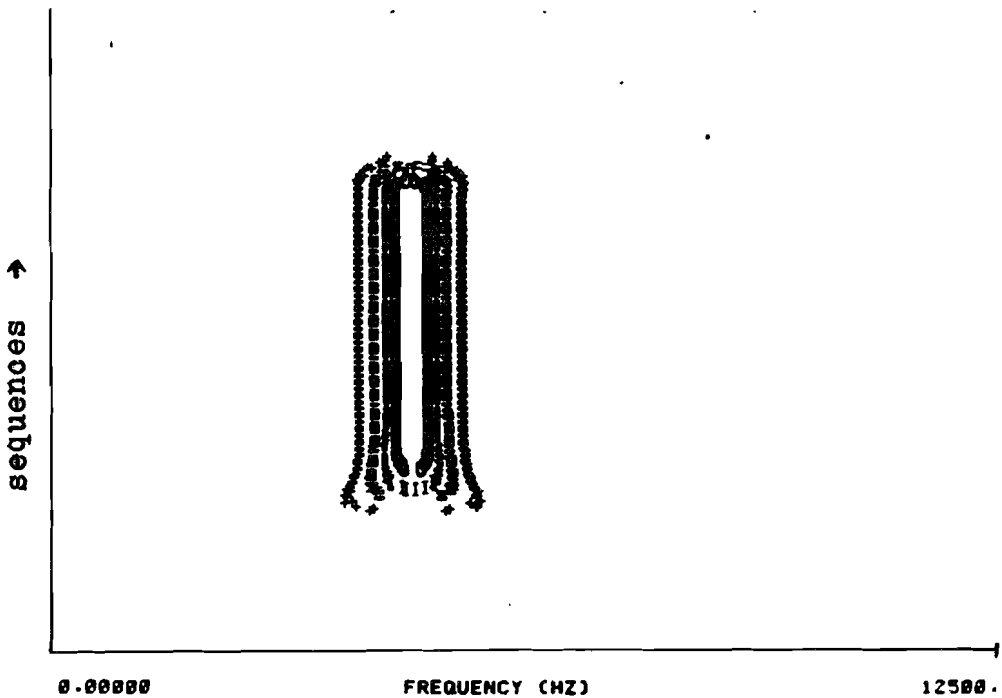


Fig. 2.4. " Level-display of dynamic spectrum of fig. 2.2.

## 2.2. Real functions of two variables.

For the display of a real function of two variables three dimensions are needed. By making a virtual three dimensional plot, this problem can be solved [4] (fig. 2.2.). Otherwise it is possible to display only cross-sections of the function. The cross-sections can be made rectangular to one of the variable axes and result in displays as described in 2.1. If a cross-section is made parallel to the plane of the axes, two possibilities remain :

- 1) the function values above the cross-section plane can be projected into this plane (fig. 2.3.)
- 2) display only the points where the function crosses the cross-section plane. (fig. 2.4.)

For these last two methods a normal two dimensional display is made with the variables along the axes and the corresponding projection or level-crossing is indicated by a certain symbol.

The displays discussed in this part are used for the output data of the spectral analyzer and for the short-time or running power spectra.

## 2.3. Complex functions of two variables.

Because the COSTID - function is a complex function of both

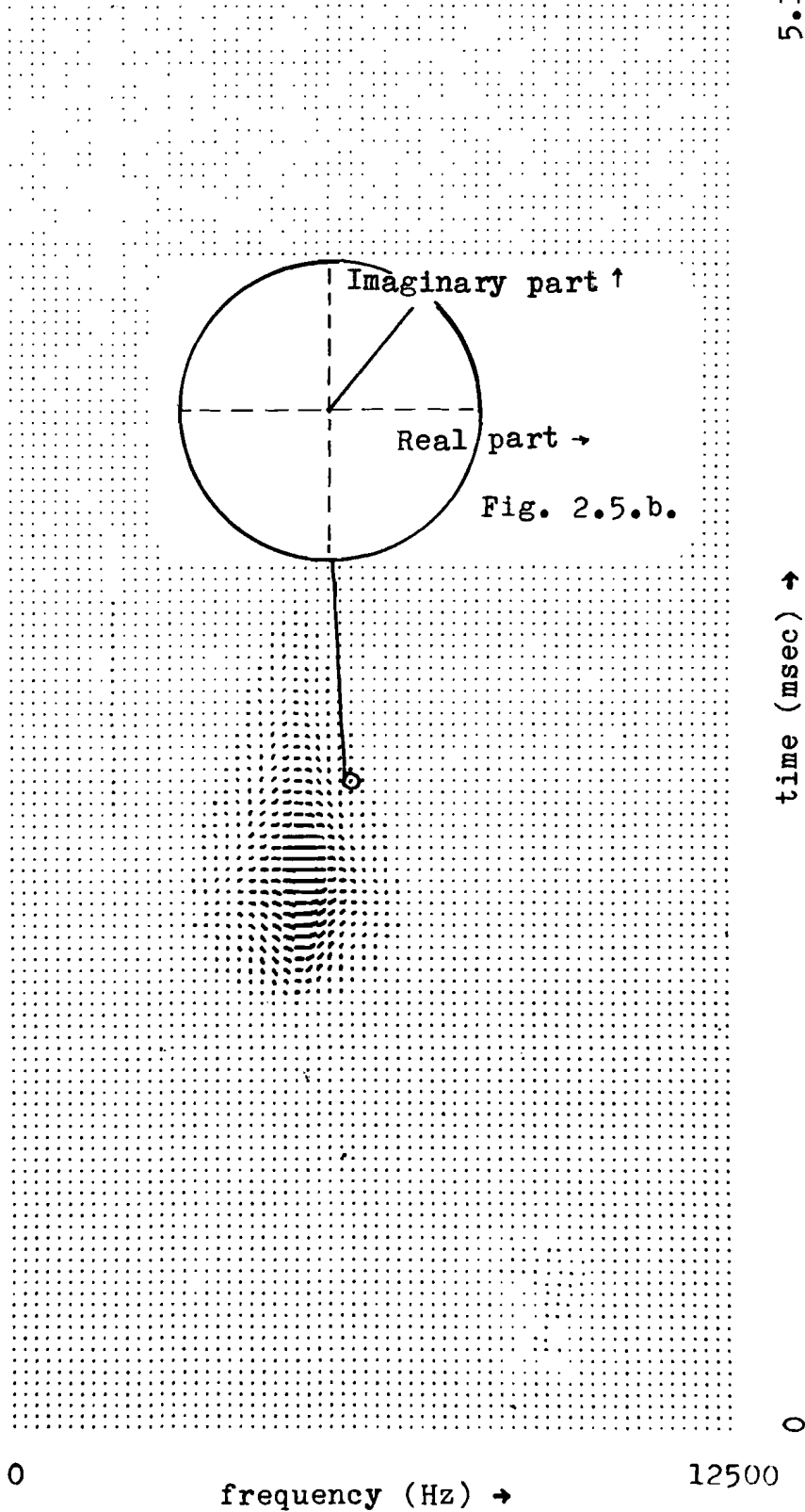


Fig. 2.5.a. An example of a vector-display; COSTID-function of a single gamma-tone. In b. an enlargement of the vector in a point ( $f= 5859$  Hz,  $t= 2.32$  msec) is given.

time and frequency additional display methods have been developed, as it was too difficult to interpret the results if only one aspect of this function was displayed.

We displayed the complex function in two ways :

1) By means of a vector-display. For this we made a two dimensional display with time along one and frequency along the other axis. Then for every  $(f,t)$  pair we calculated the modulus and argument and displayed a vector with length and direction depending on respectively modulus and argument of the COSTID - function value at  $(f,t)$ . This method however has the disadvantage that the vectors range into the regions of others and make the display unclear.(fig. 2.5.)

2) By making use of a colour display. The key to this kind of display is the mapping of the complex values into a colour range. It is obvious that we need not consider the entire plane but only that part, that contains the data points. Therefore we calculate at first the modulus for all data points and select the greatest. Now it comes to the choice of the colours for the segments or parts of the circle with a radius that equals the maximal modulus.

The choice of the colour distribution is done in two ways :

0) by making the colourrange a function of the real and imaginary part

1) by making the colourrange a function of the modulus and

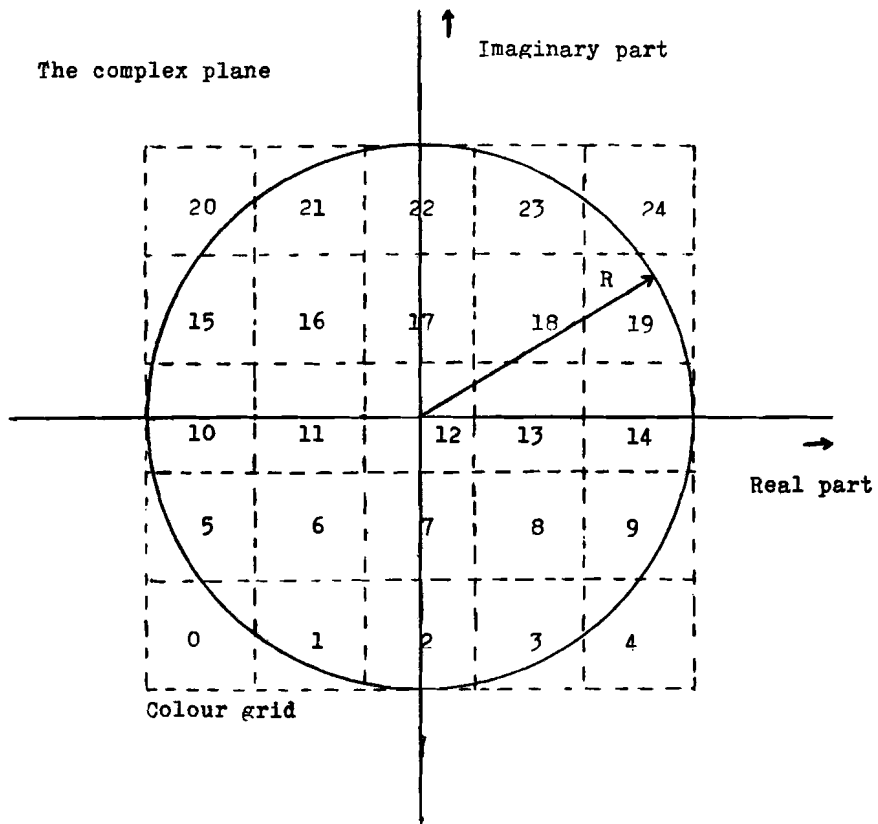


Fig. 2.3.1. Example for  $n=25$  of a grid for the XY-coding.

argument.

The first one is called XY -coding; the second R $\phi$ -coding.

Now suppose that the maximal modulus was R for our data and look at :

0) The XY-coding.(fig. 2.3.1.)

The essence of this way of coding is the fact, that we place a grid over the circle with radius R. This grid can be seen as a matrix with values from 0 to n-1. Where n is the number of different colours. This implies that we have a resolution of  $\sqrt{n}$  values for the real- and also for the imaginary axis ( $\sqrt{n}$  has to be an integer). Now we label every complex value with the corresponding grid number. So this results in only one real value for a class of complex values. It should be noted however that the resulting display can only be interpreted, if we have the possibility of looking at the coloured grid in combination with the coded display of the complex function values. At this point the choice of the colours is still open. This gives us the possibility of manipulating with the colours to investigate what colour choice is optimal for the perception of the signal features one wants to study. These investigations are the subject of further research [19]. We have considered only the case of an increasing red brightness on the real axis in positive direction and an increasing green brightness for the imaginary axis. This results in a yellow colour for the values with great positive real- and imaginary part and black for the values with great negative real- and imaginary part.

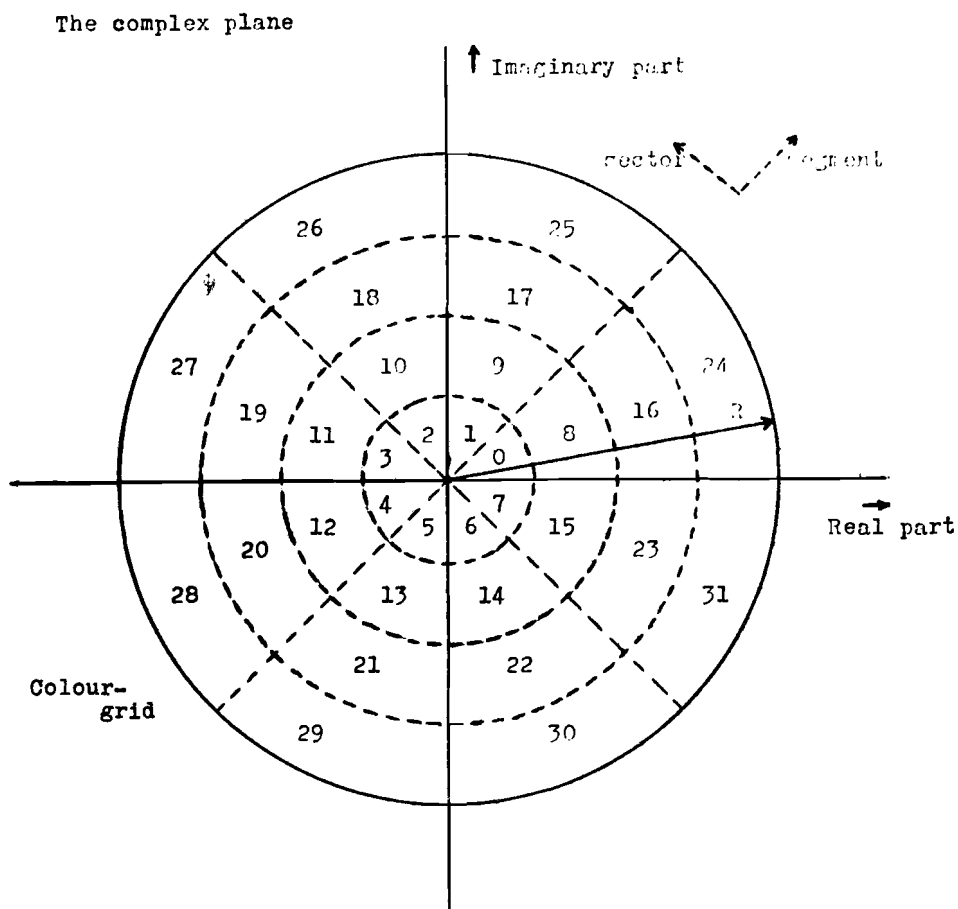


Fig. 2.3.2. Example for  $n=32$  of a grid for the RQ-coding.

1) The R- $\theta$ -coding. (fig. 2.3.2.)

In this procedure a segmented circle is placed over the circle with radius R in which all the complex data points for the display are concentrated. The colour circle consists of segments and sectors. The sectors determine the resolution for the argument of the complex value and the number of segments determine the resolution for the modulus. In this coding we tried to keep the brightness constant, while varying the hue, as a function of the argument of the complex value, and the saturation, as a function of the modulus. If we have again n different colour values (number of colours), we get  $\frac{n}{m}$  values for the modulus in the case of m segments ( $\frac{n}{m}$  has to be an integer).



## Chapter 3

### Methods.

#### 3.1. Preprocessing.

All manipulations with the signals before sampling of the analogue waveform are categorized as preprocessing.

First there is the selection of some calls out of a number of recorded frog vocalizations. The recordings were made by D. Hermes at the laboratory of Medical Physics and Biophysics of the University of Nijmegen. He used B&K type 4134 microphones and recorded the signal on audiotape with an Otari MX 5050 taperecorder at a speed of 38 cm/sec.

After the selection has been accomplished the signal was lowpass filtered with a Krohn-hite 3343 filter, (-3dB point at 5000 Hz) and copied to an FM-tape by means of an instrumental recorder of Hewlett-Packard (3968 A, recordingspeed at 15 inch/sec.).

Now the signal is played back at a speed of 15/16 inch/sec and sent to the sampling device through the Krohn-hite filter (now -3dB points for highpass at 2.2 Hz and lowpass 310 Hz). In this way the bandwidth is reduced by a factor 16 from 5 kHz to 312,5 Hz. At a rate of 1562,5 samples/sec the signal is sampled by the LPS 11 system of a PDP 11/45 computer which has a 12 bit A/D converter. For the original signal this implies that it is sampled 5 WT (25000 samples/sec).

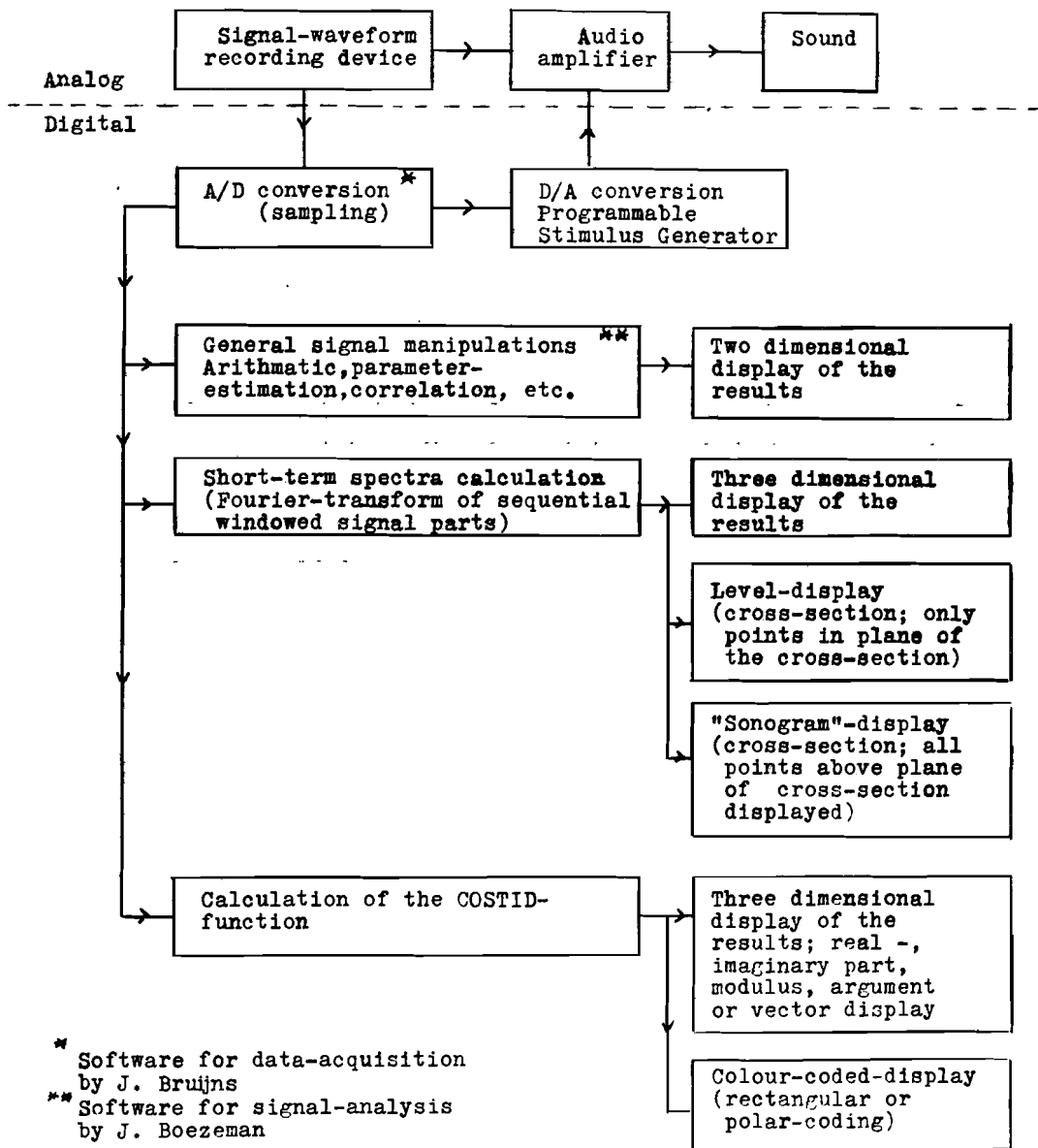


Fig. 3.2.1. Diagram of the developed software.

### 3.2. Software implementation.

The software implementation is explained in the diagram of fig. 3.2.1., which contains partly also software of J. Bruijns, J. Boezeman and N. de Jong. A full description of the software is not relevant here, but for those readers, who want more information, the listings, program descriptions and tests are available. The programs are written in Fortran IV plus and used on a PDP-11/45 computer operating under RSX 11-D.

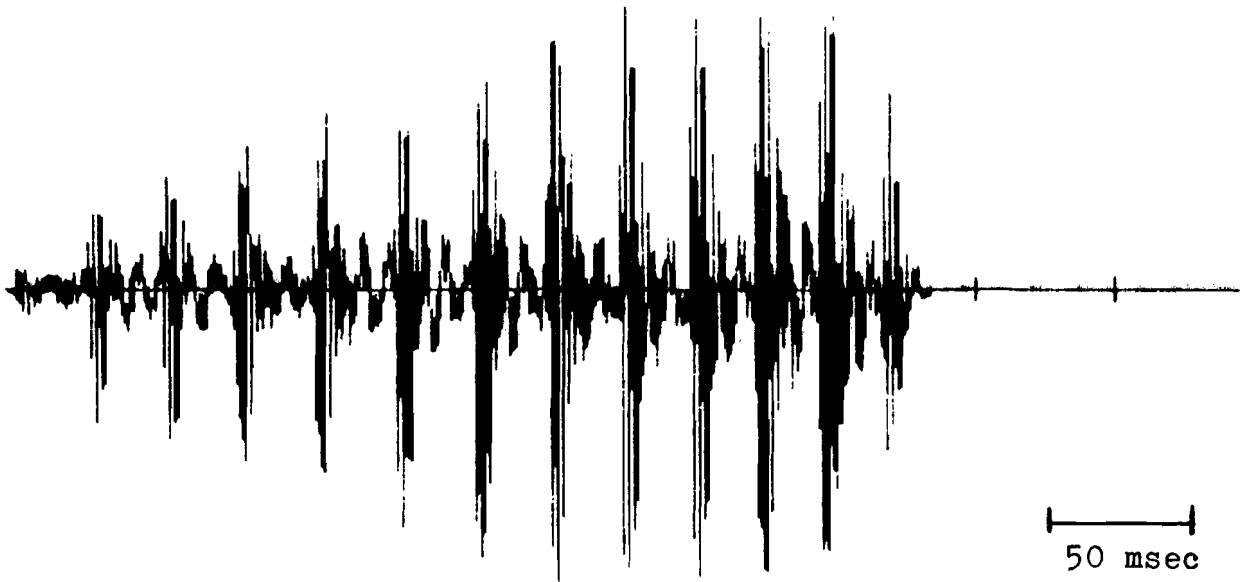


Fig.4.1.a B-call of Irish frog *Rana Temporaria*

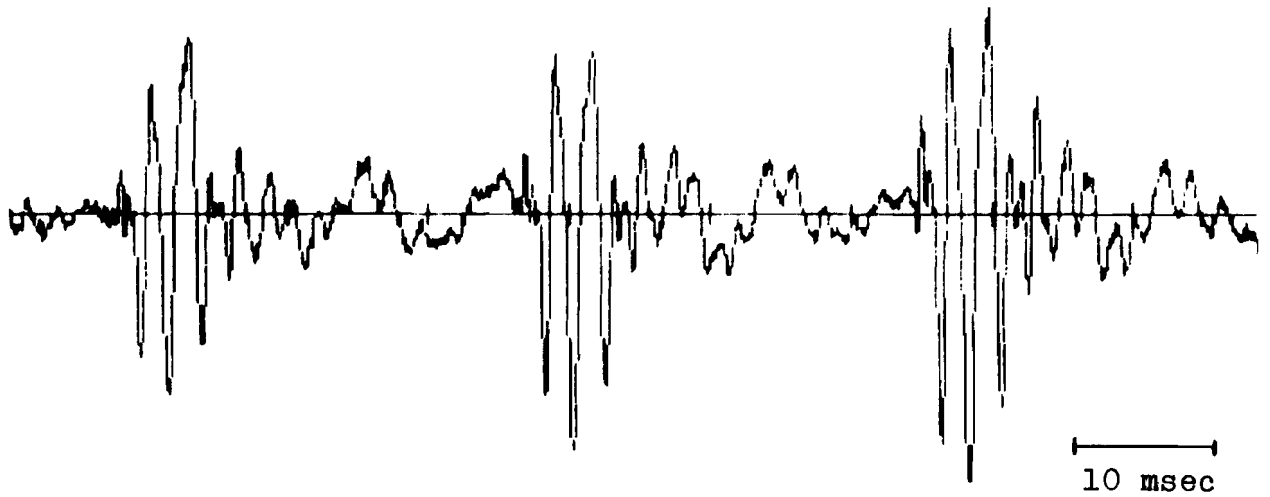


Fig. 4.1.b Fourth, fifth and sixth element

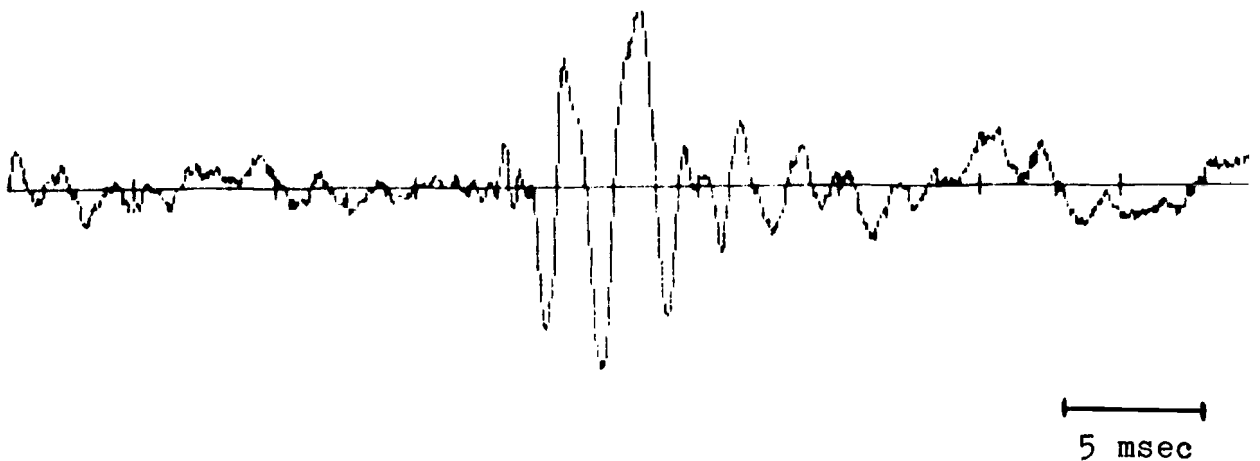


Fig. 4.1.c Fourth element

## Chapter 4

### Results.

In this chapter results are presented for the COSTID - function of some sound signals. The COSTID was calculated for several computer generated "simple" signals (sines, Gaussian pulses, etc) for the purpose of software testing, but also to have some reference for the interpretation of the results for natural sounds. In the first part the results are presented for the COSTID of an artificial signal that resembles an element out of a frog call and in the second part for the COSTID of an element of a B-call of the Irish frog *Rana Temporaria*.

#### 4.1. Artificial Signals.

When looking at the elements in a call of the frog *Rana Temporaria*, one gets the impression, that they are simple amplitude "modulated" signals (fig. 4.1.). Now for an element out of a call a simple approximation was chosen [1]

$$S_n(t) = A_n(t) \cos (\omega_n t + \varphi_n), \text{ for the } n\text{-th element.}$$

Considering this waveform for only one element we will drop the index  $n$  and define the parameters :

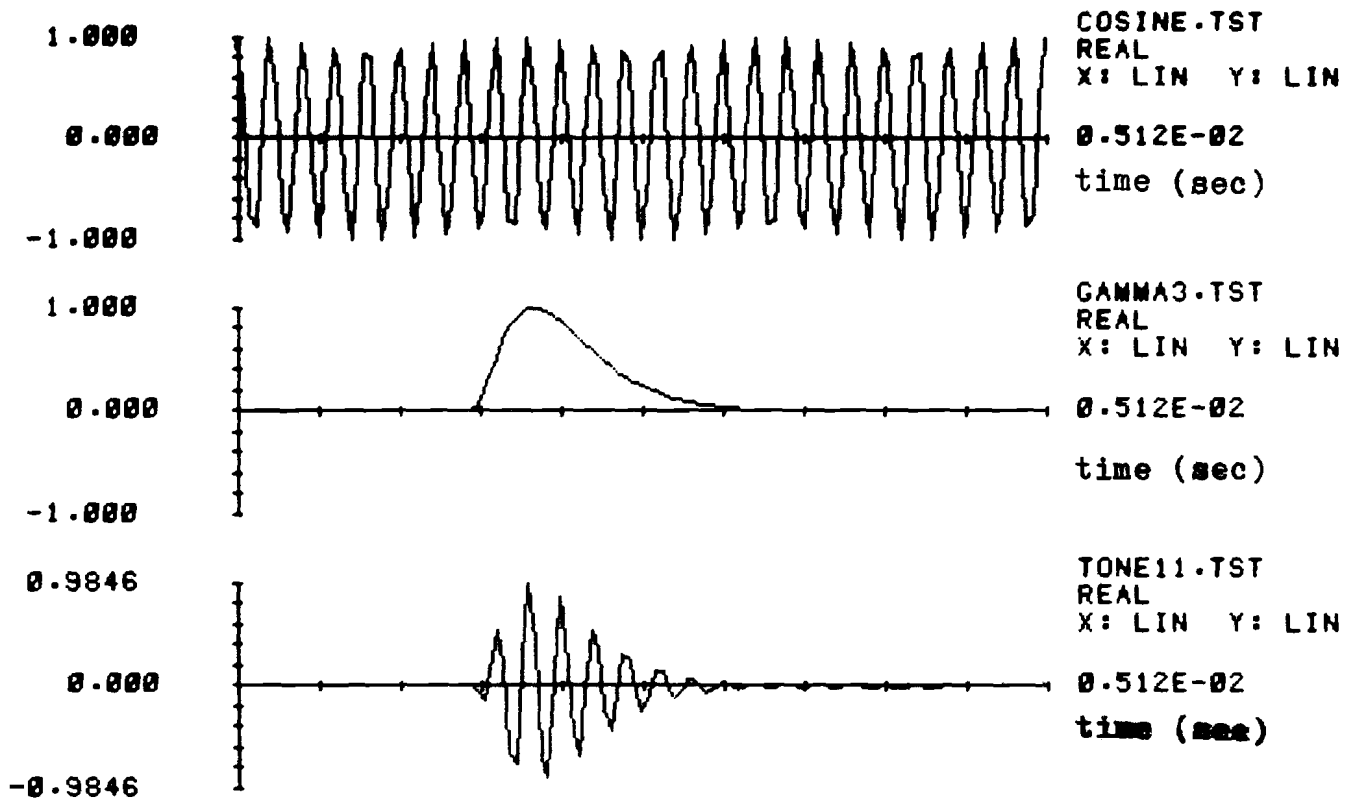


Fig. 4.2. The construction of a gamma-tone by multiplying a cosine waveform (the carrier) with a gamma-envelope.

the envelope :  $A(t) = A t^{\gamma-1} e^{-\frac{t}{\beta}}$ , called a gamma-envelope  
( $\gamma$  - envelope)

the carrier-frequency  $f_c = \frac{\omega}{2\pi}$   
and the phase-term  $\varphi$

This signal will be referred to as a gamma-tone and we generated a signal waveform with the parameters :

$$A = 1, \quad \gamma = 3, \quad \beta = 0.0025, \quad \omega = 2\pi 4882.8125$$

and  $\varphi \approx 0.85 * \pi$  .

The carrier-frequency is not of the same order as that of the approximated "frequency" in the natural frog-call-element ( $\approx 600$  Hz), because we wanted the results for a gamma-tone, that was approximately in the "middle" of the time-frequency plane under consideration ( $t : 0 - 5.12$  msec ;  $f : 0 - 12.5$  kHz). The signal is constructed by multiplying a cosine-waveform with a gamma-envelope (fig. 4.2.).

On the following pages we will now give for this signal :

- 1) the temporal and spectral representation of its analytic signal
- 2) the COSTID - function in a three-dimensional display, a vector-display and a representation with xy- and  $r\varphi$  colour coding.

Time domain

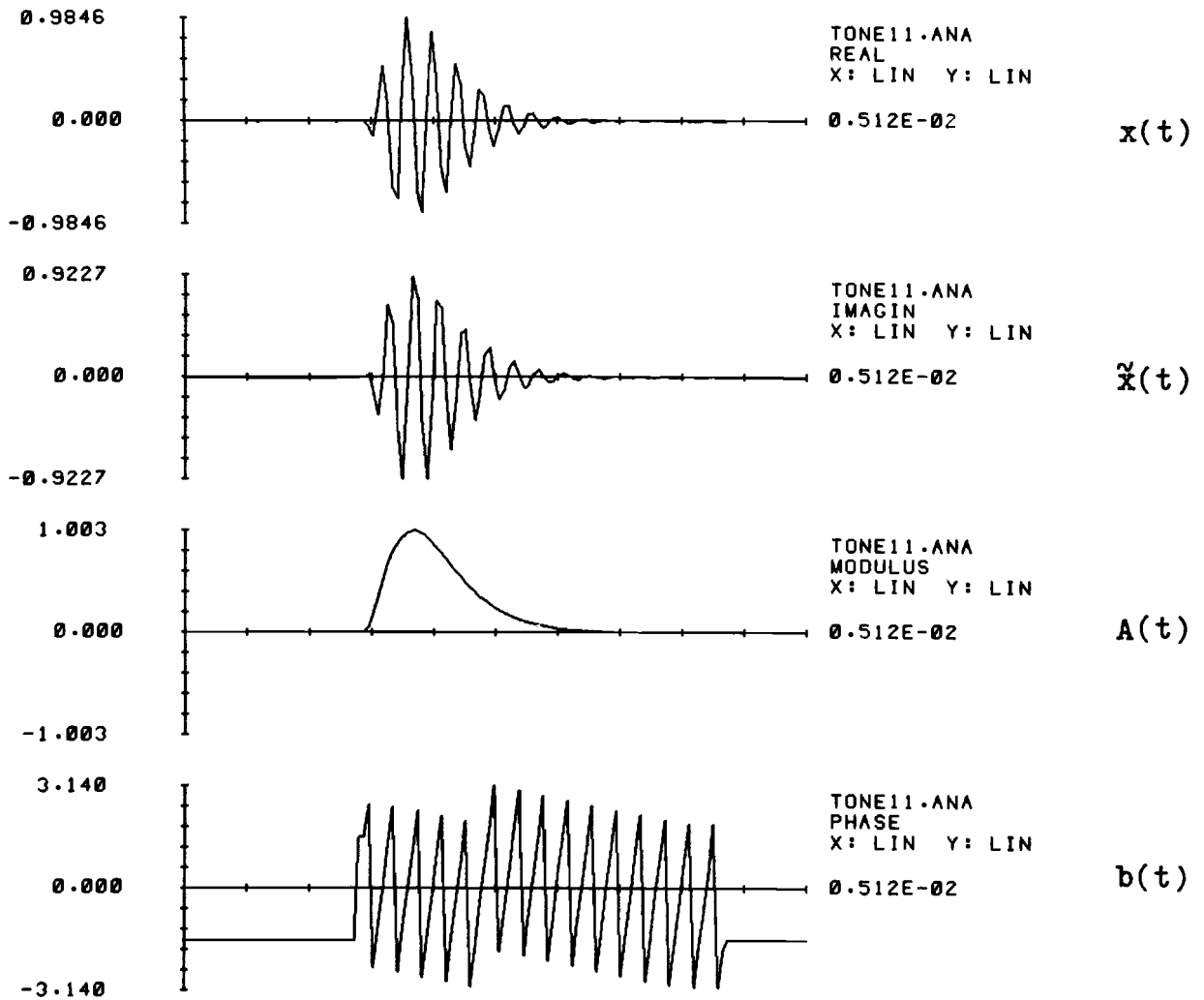


Fig. 4.3. The analytic signal of a single gamma-tone.

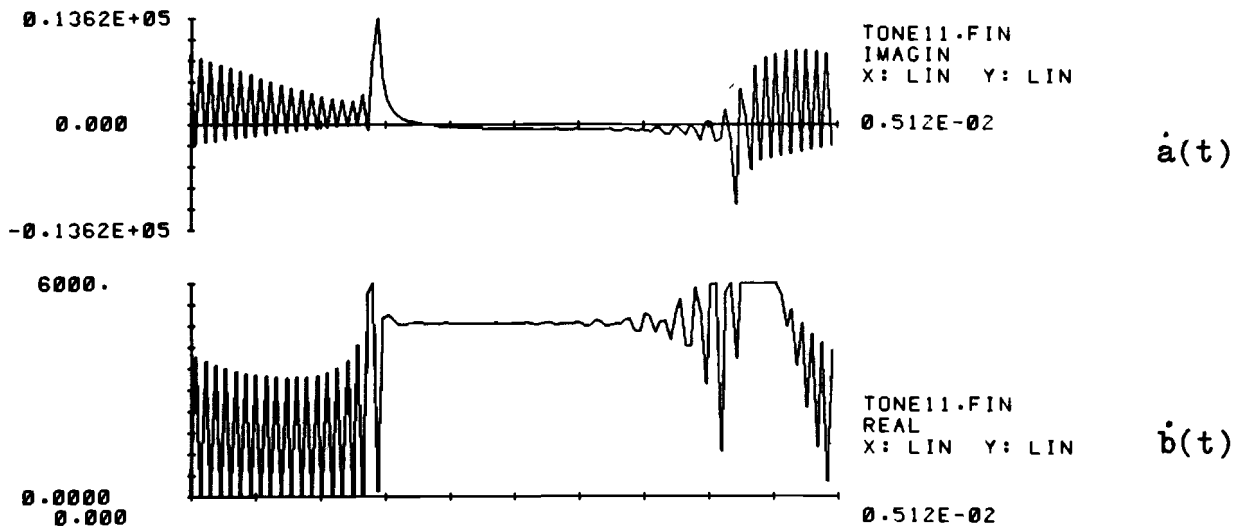


Fig. 4.4. The relative temporal amplitude change and instantaneous frequency of a single gamma-tone.



Frequency domain

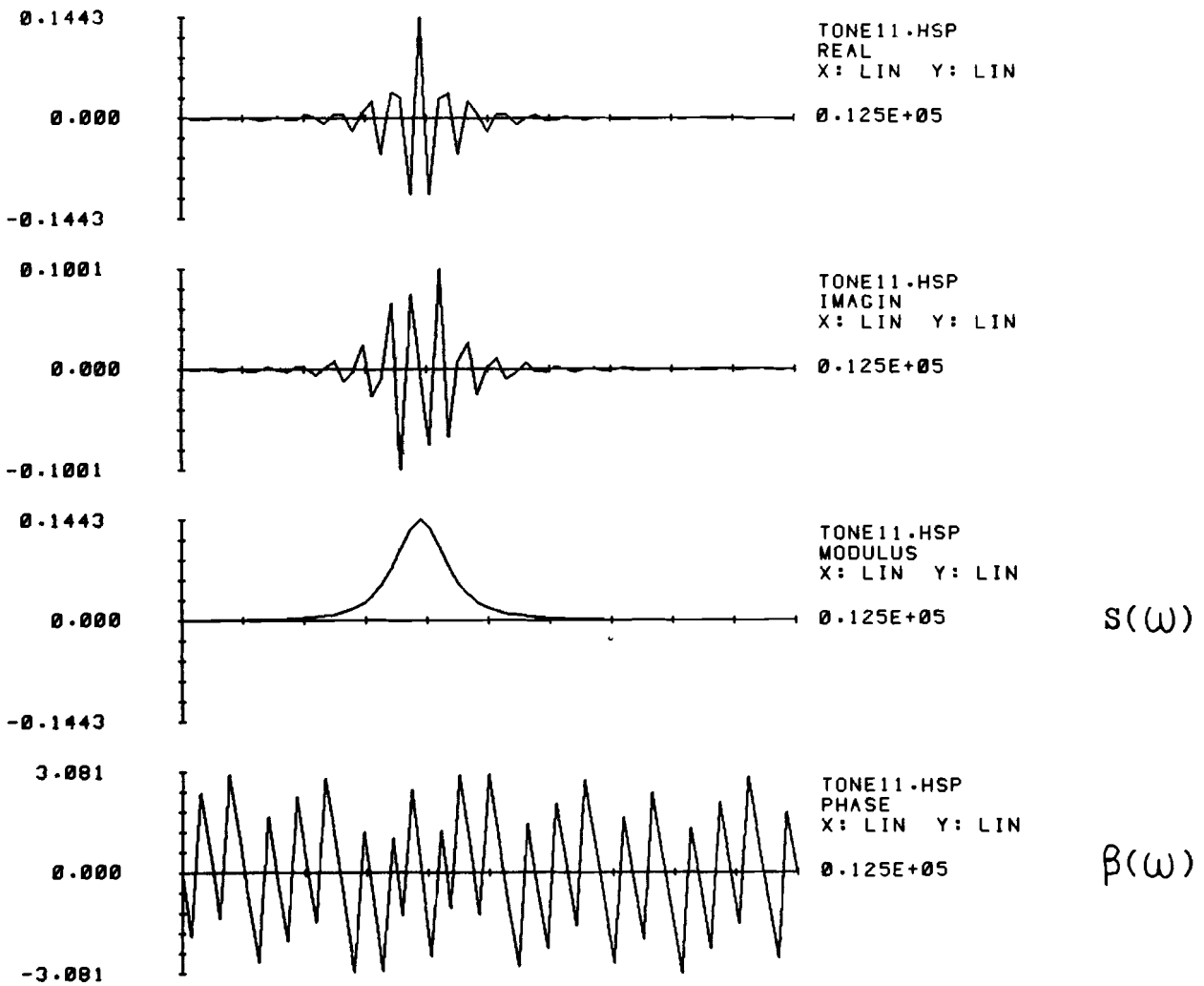


Fig. 4.5. The Fourier transform of the analytic signal of a single gamma-tone.

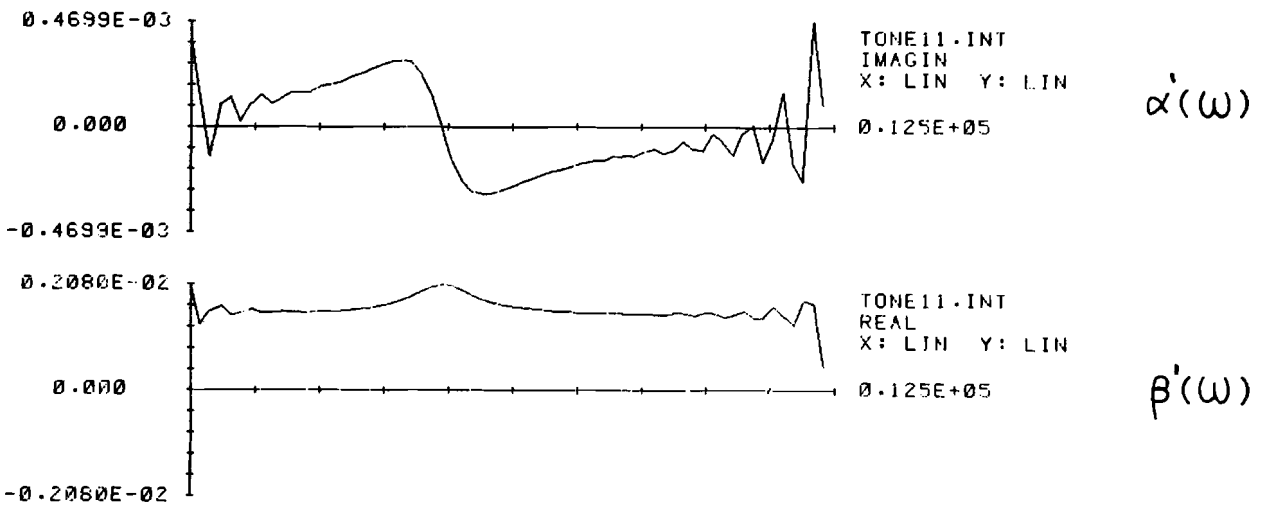


Fig. 4.6. The relative spectral amplitude change and spectral phase change of the single gamma-tone

Fig. 4.7. The COSTID-function of a single gamma-tone.  
time: from 0. to 5.12 msec; frequency: from 0. to 12500 Hz.

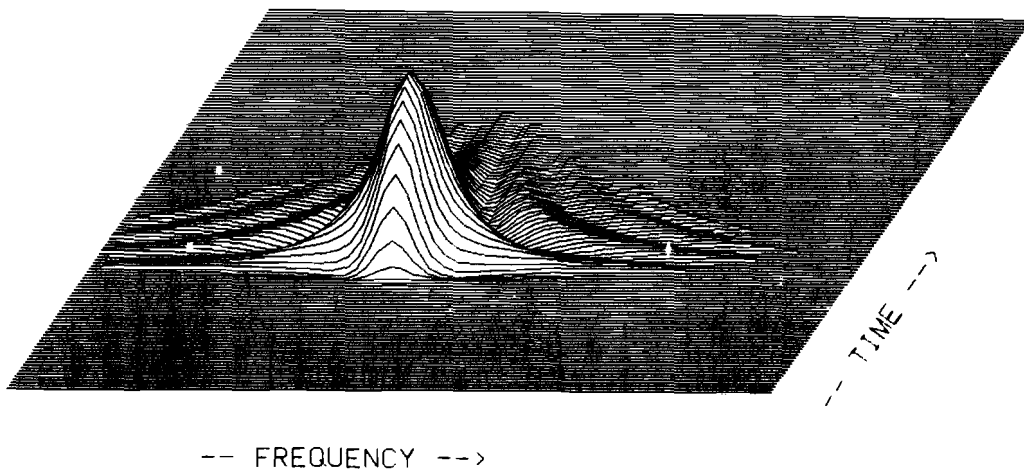


Fig. 4.7.a. The real part.

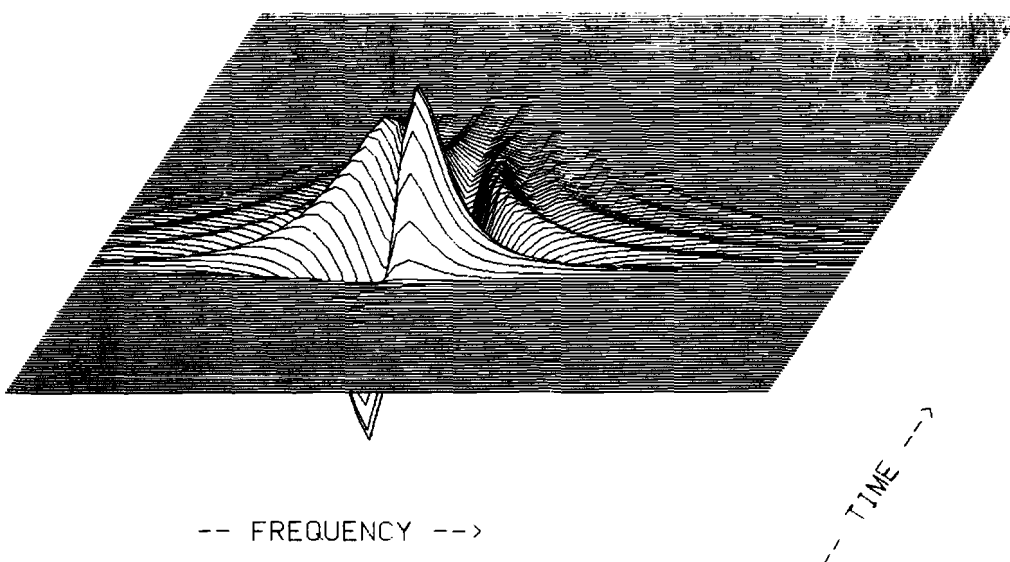


Fig. 4.7.b. The imaginary part.

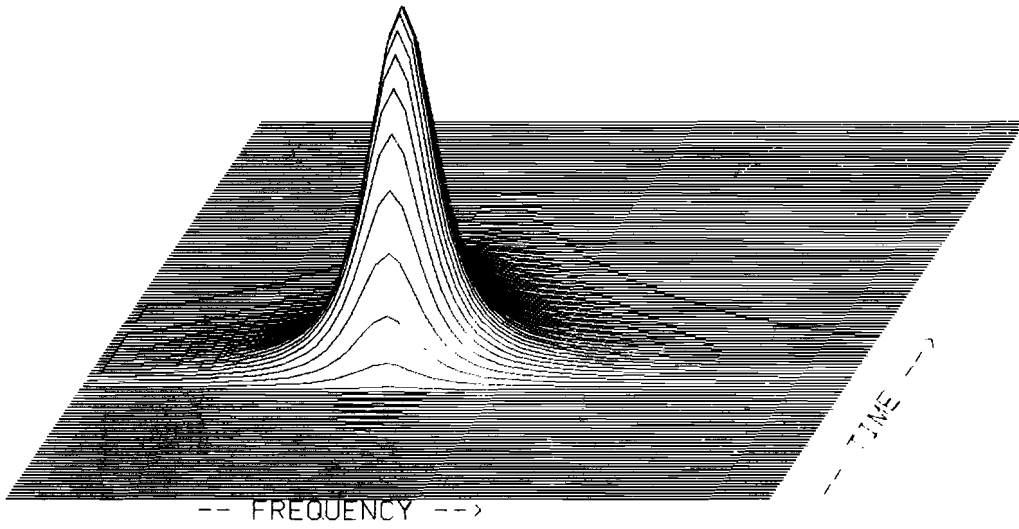


Fig. 4.7.c. The modulus.

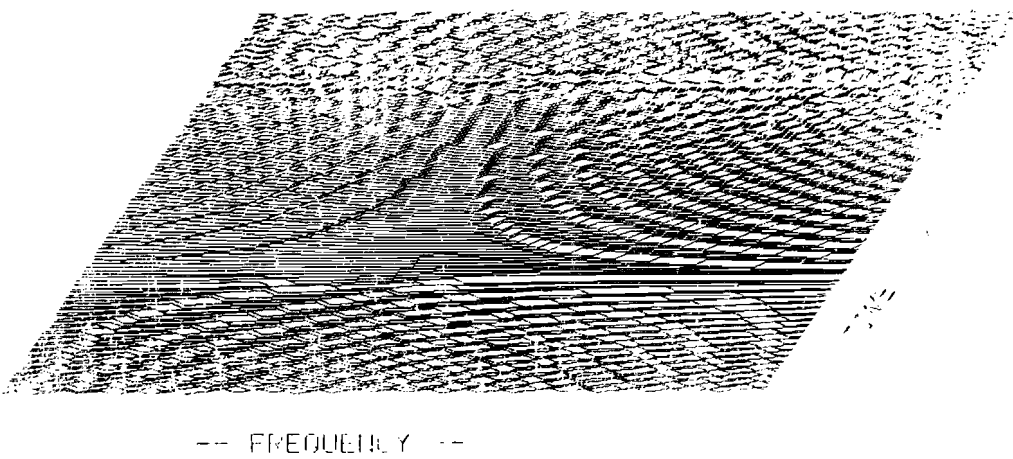


Fig. 4.7.d. The argument.

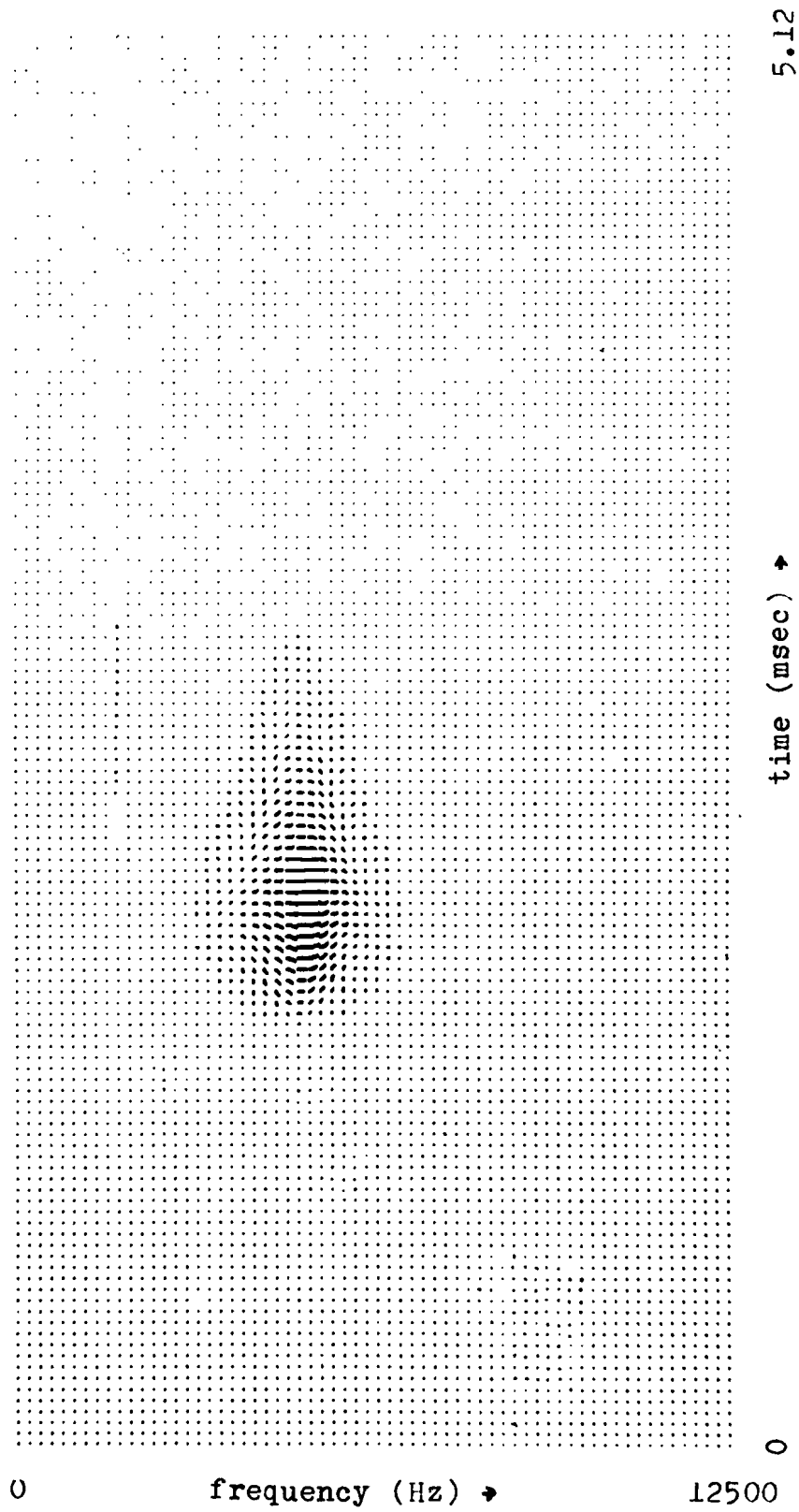


Fig. 4.8. The COSTID-function of a gamma-tone.

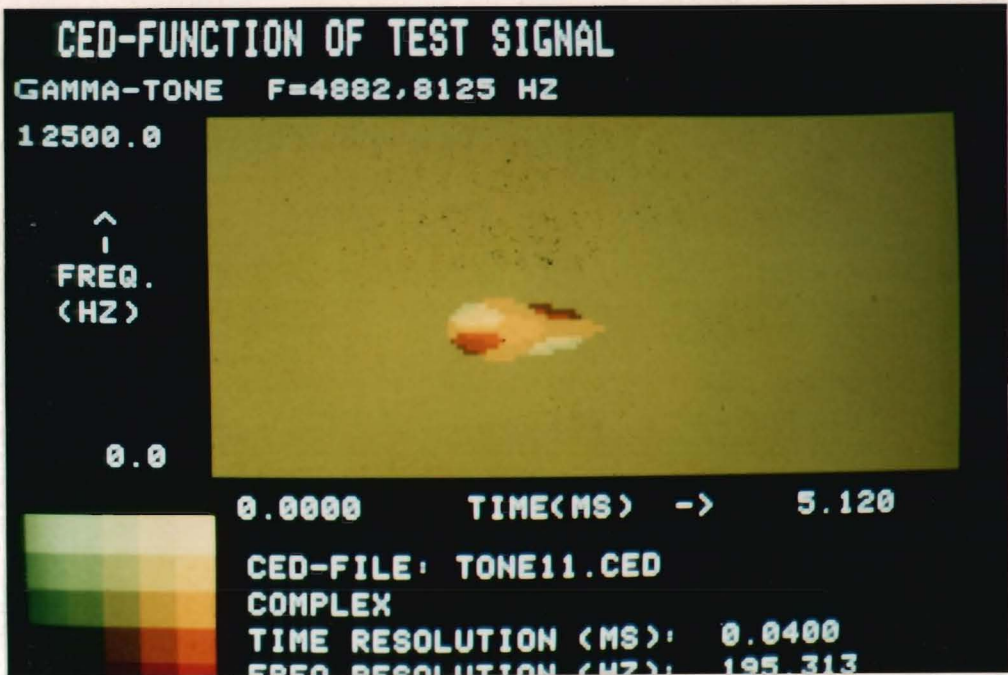


Fig. 4.9.a. The COSTID-function of a single gamma-tone with rectangular coding.

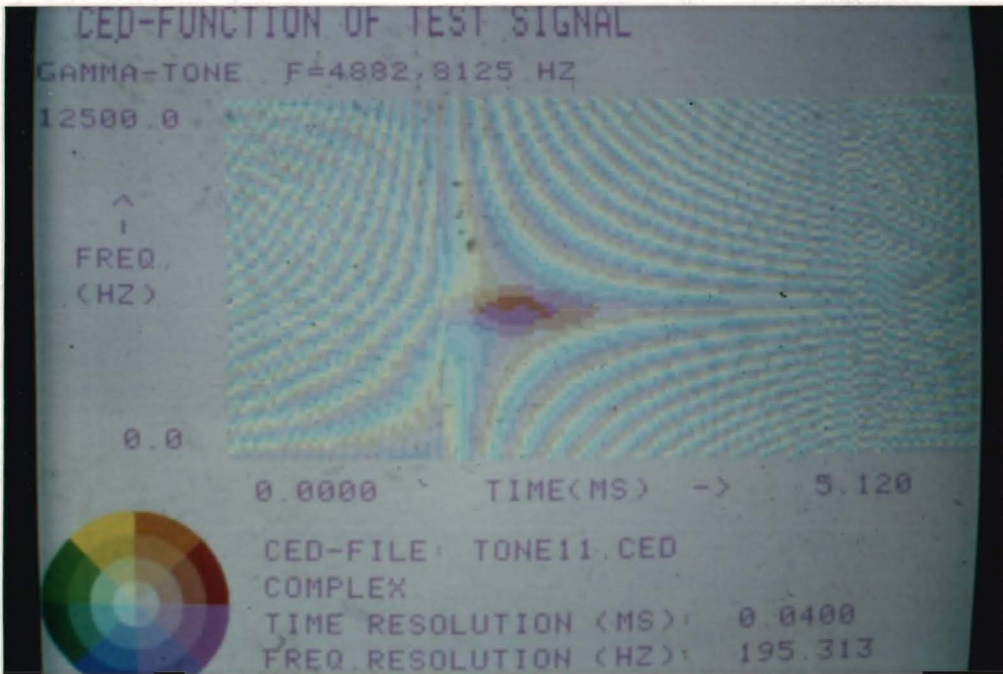


Fig. 4.9.b. The COSTID-function of a single gamma-tone with polar coding.

As seen from property e) of the COSTID - function this function is non linear. To investigate the effects that result from this property when the COSTID - function is calculated for the sum of two gamma tones we will shift the gamma tone, discussed before, in the time-frequency plane. We will consider three cases :

- 1) the sum of two time shifted gamma-tones
- 2) the sum of two frequency shifted gamma-tones
- 3) the sum of two time and frequency shifted gamma-tones.

With respect to a hardware spectral-analyzer or calculation of short-time spectrum the COSTID - function has a number of advantages. For the purpose of comparing the COSTID with these other methods we will give also the results of these methods for the next three examples.

For the spectral analyzer we converted the computer generated signals digital to analogue and analyzed the signals with the hardware real-time spectral-analyzer. (Conditions : sampling time 0.12 msec and averaging over 64 repetitions of the signal).

In the calculation of the short-time power spectrum we used a time window of duration 5.12 msec to get the same frequency resolution as we had for these signals in the COSTID- function, this implies however that the window is not optimum for the gamma-tones of the next examples. One can even say that it is very bad to take this window duration, because we can have two tones within the same window and so in the spectral representation it is not possible to distinguish between the two tones.

Time domain

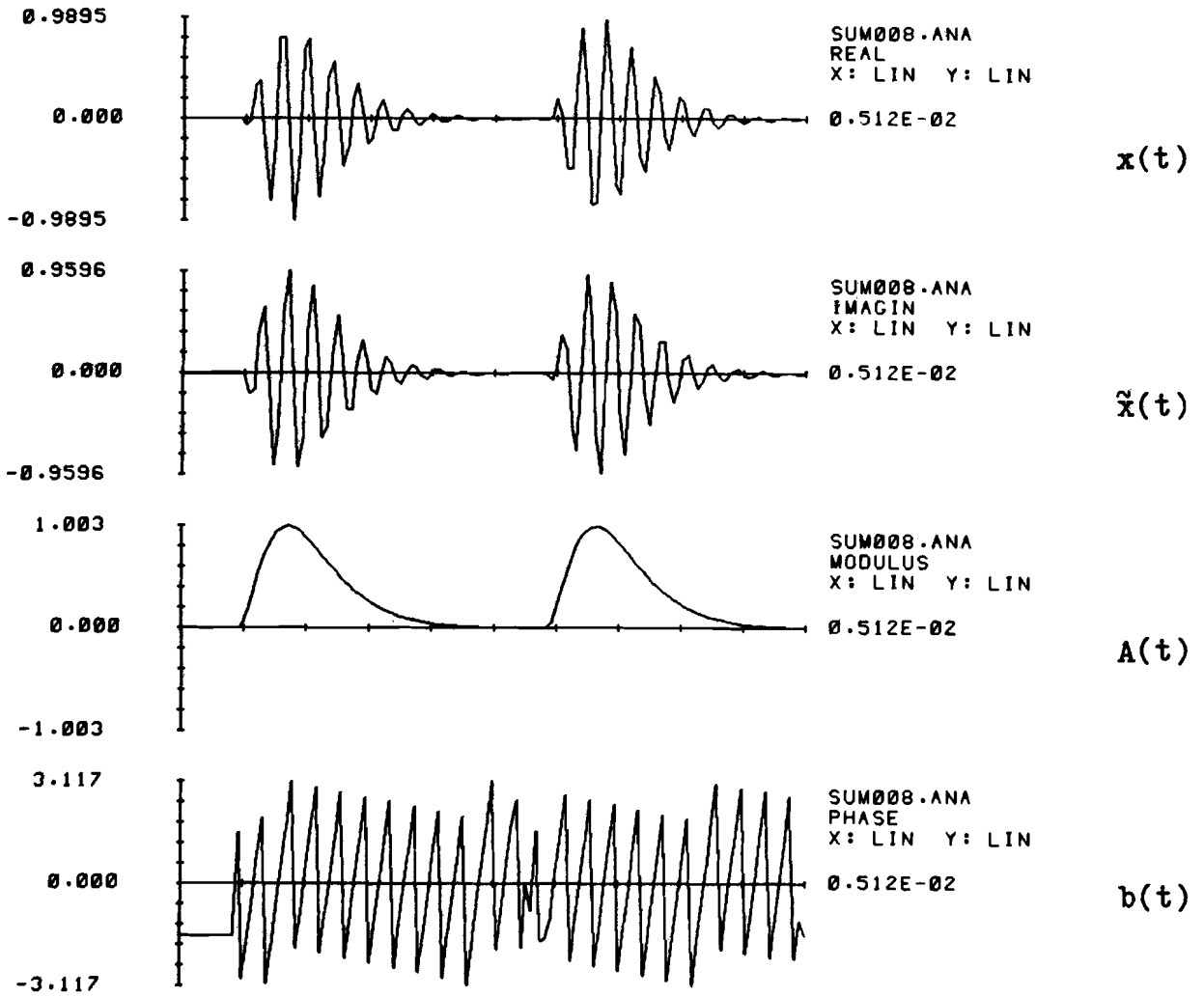


Fig. 4.10. The analytic signal of two time shifted gamma-tones.

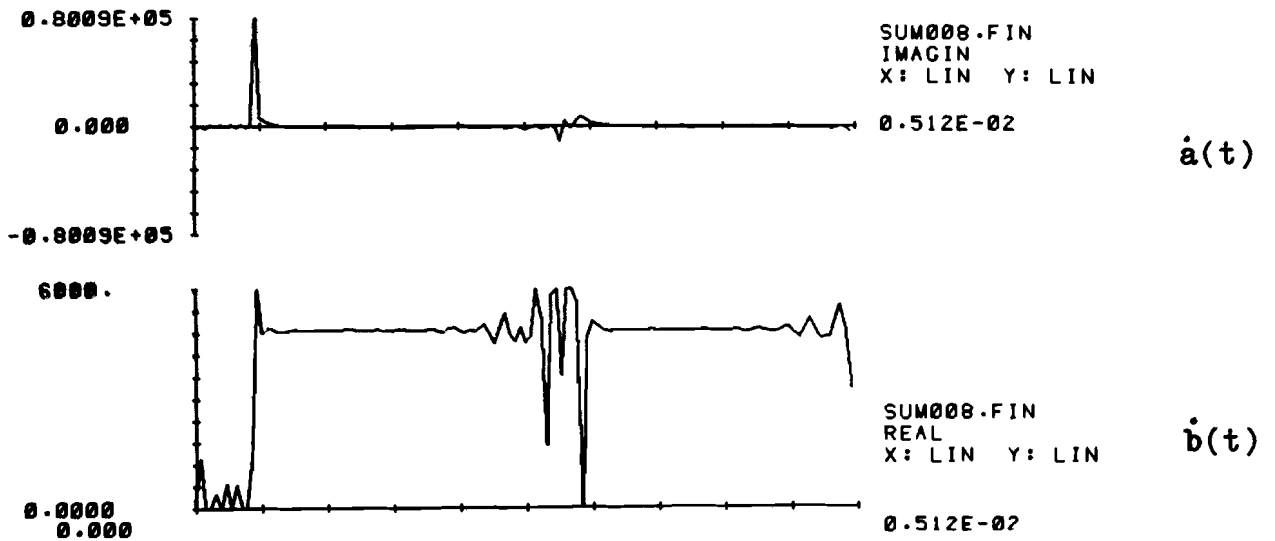


Fig. 4.11. The relative temporal amplitude change and instantaneous frequency of two time shifted gamma-tones.

Frequency domain

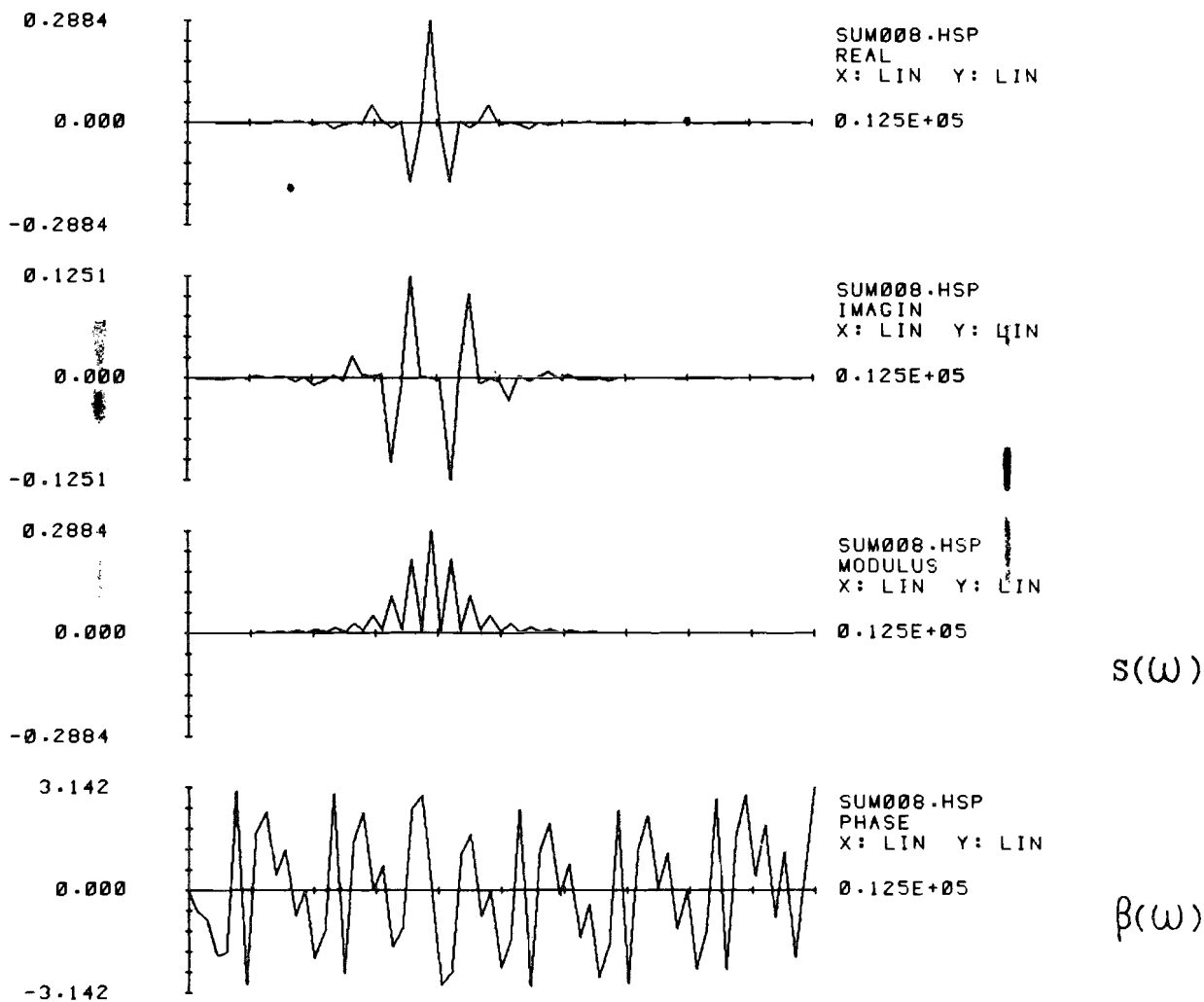


Fig. 4.12. The Fourier transform of the analytic signal of two time shifted gamma-tones.

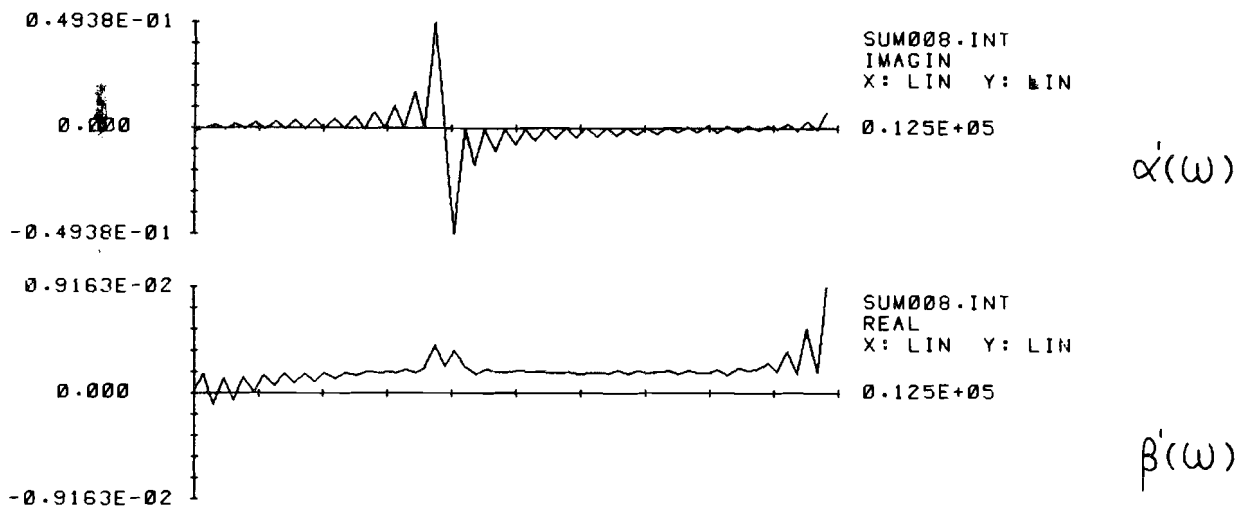


Fig. 4.13. The relative spectral amplitude change and spectral phase change of two time shifted gamma-tones.



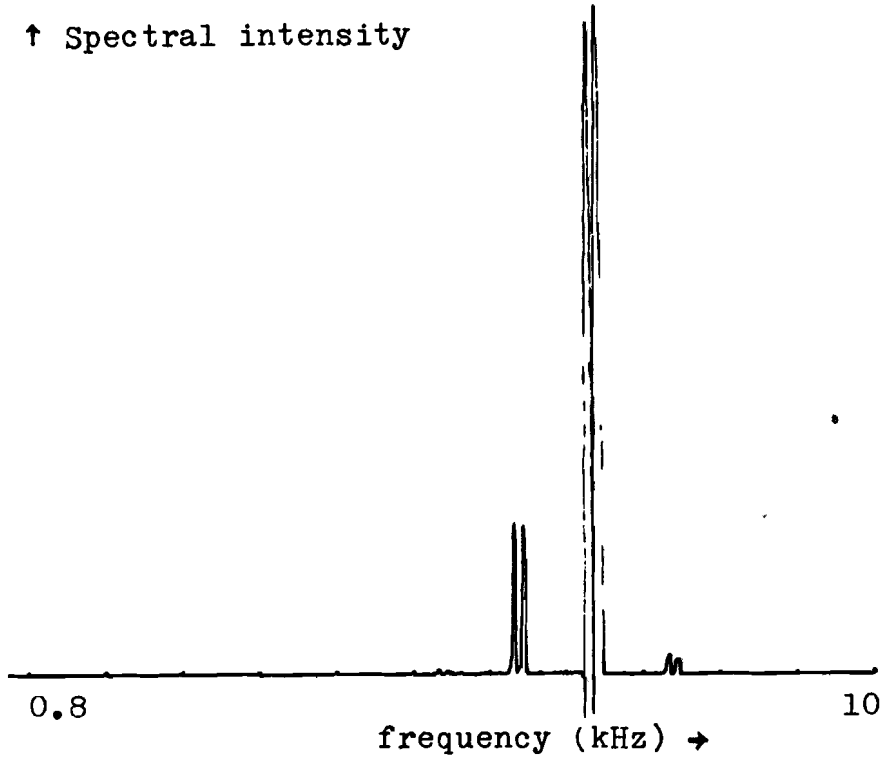


Fig. 4.14.a. Output of spectral analyzer: Static display of two gamma-tones shifted in time

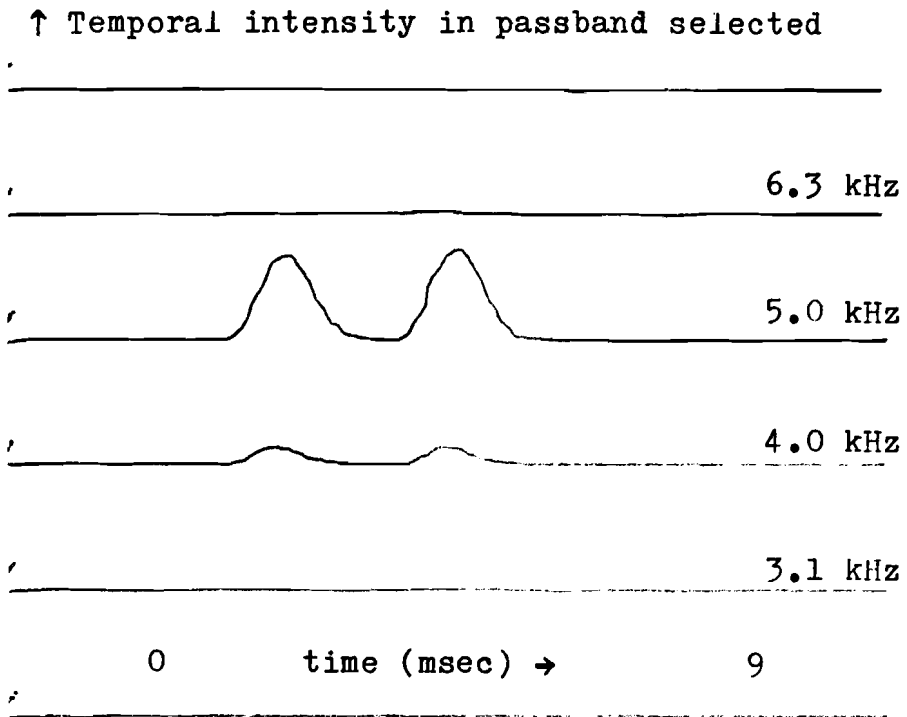


Fig. 4.14.b. Output of spectral analyzer: Dynamic display of two gamma-tones shifted in time.

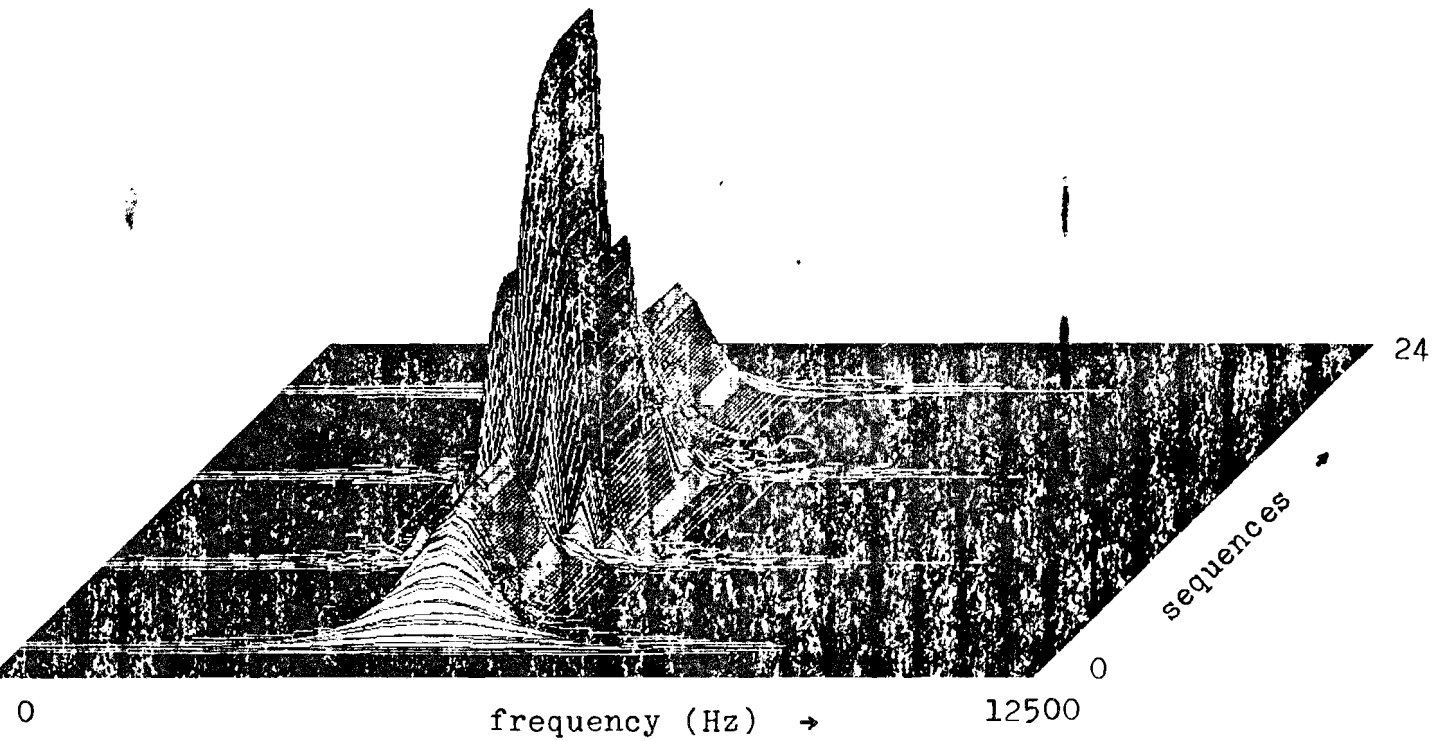


Fig. 4.15.a. The short-time power spectrum of two gamma-tones shifted in time; windowlength: 5.12 msec, windowshift: 40  $\mu$ sec.

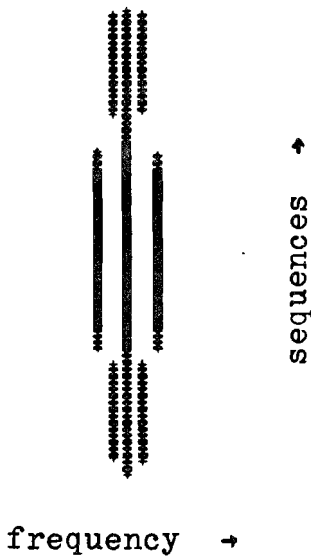


Fig. 4.15.b. Part of the corresponding "sonogram".

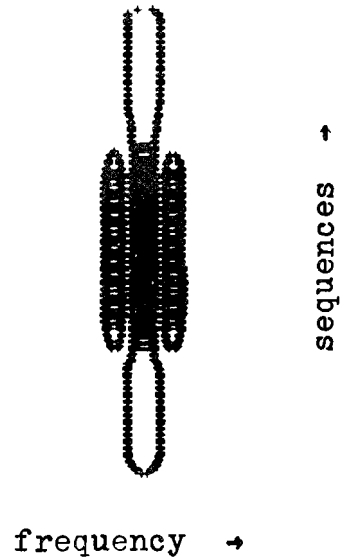


Fig. 4.15.c. Part of the corresponding level-display.

Fig. 4.16. The COSTID-function of  
two gamma-tones shifted in time.

time: from 0. to 5.12 msec; frequency: from 0. to 12500 Hz.

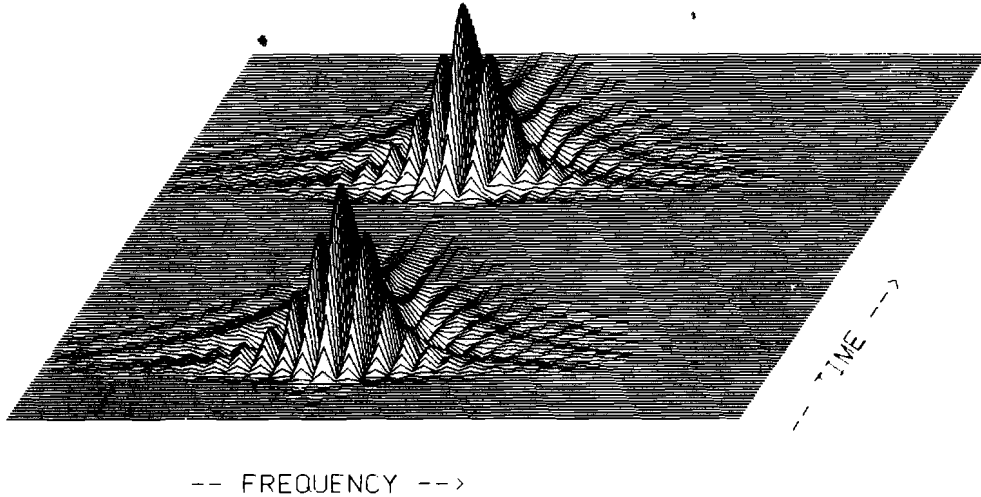


Fig. 4.16.a. The real part.

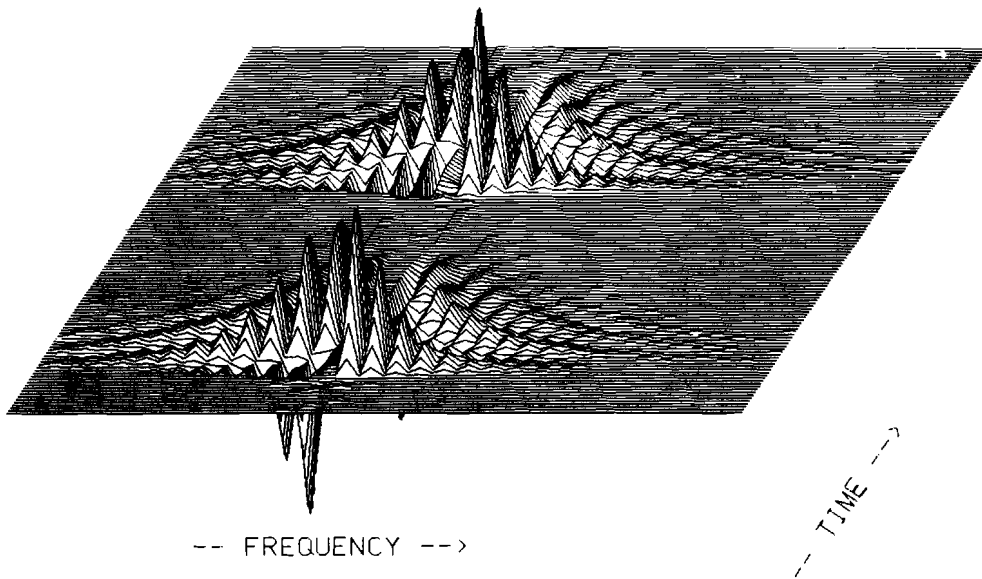


Fig. 4.16.b. The imaginary part.

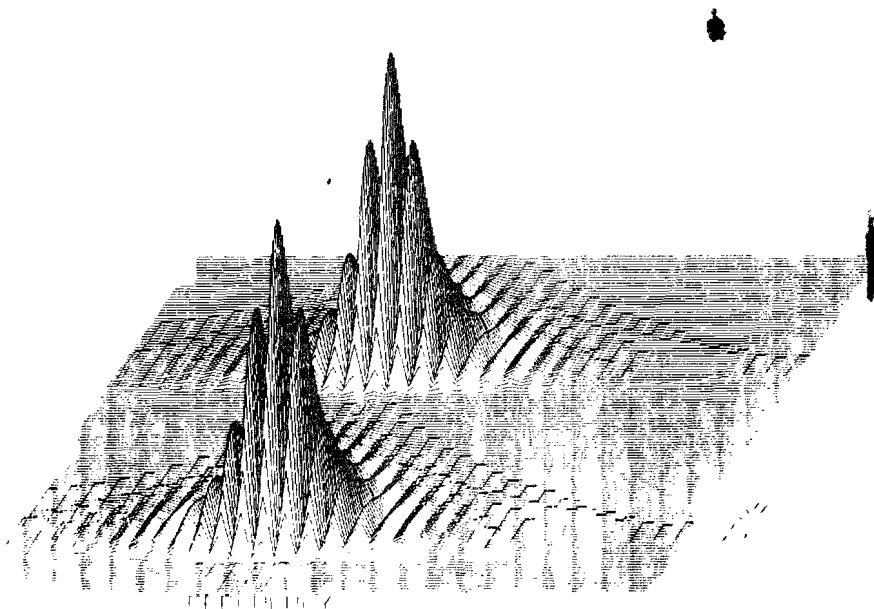


Fig. 4.16.c. The modulus.

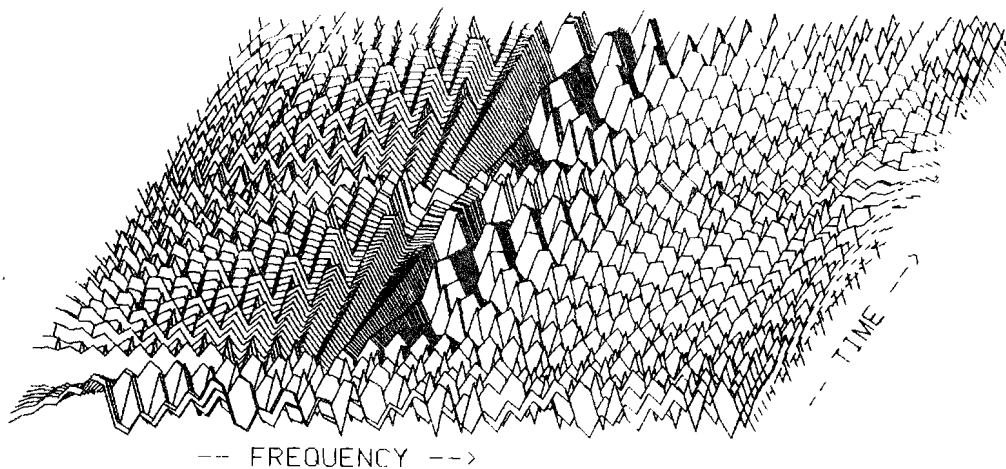


Fig. 4.16.d. The argument.

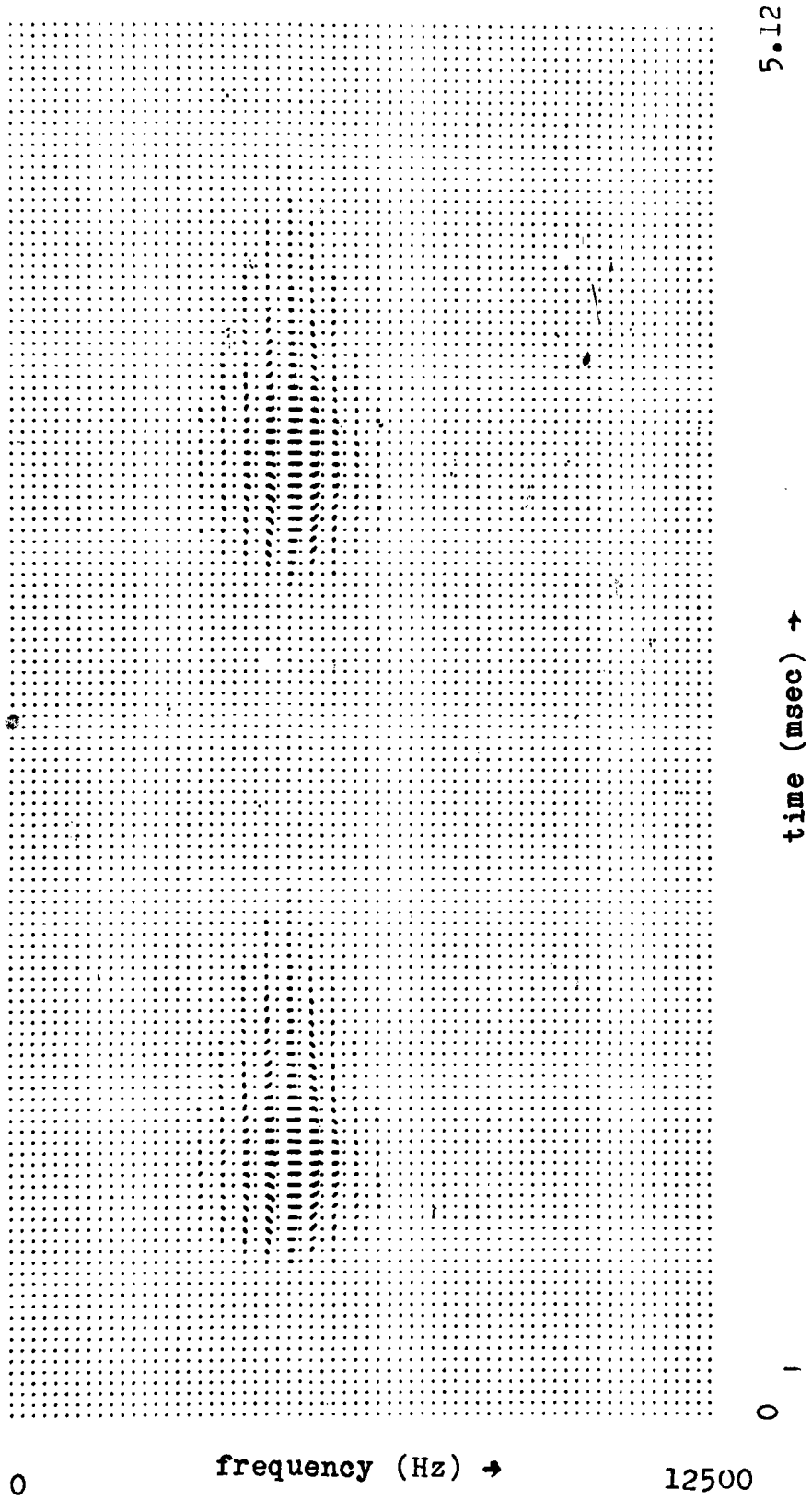


Fig. 4.17. The COSTID-function of two time shifted gamma-tones.



Fig. 4.18.a. The COSTID-function of two time shifted gamma-tones with rectangular coding.

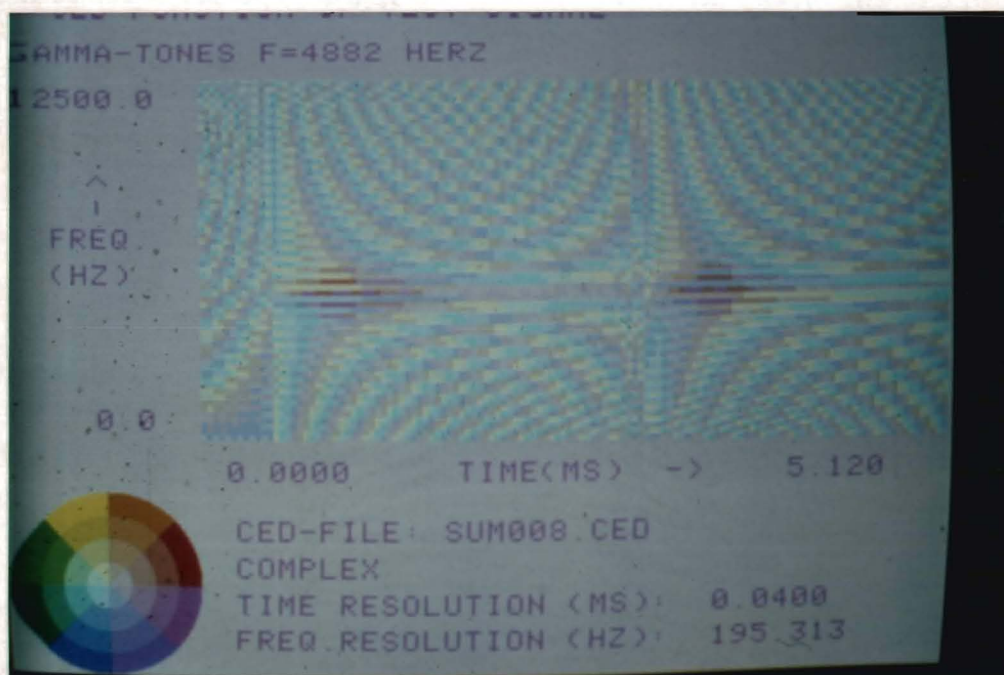


Fig. 4.18.b. The COSTID-function of two time shifted gamma-tones with polar coding.

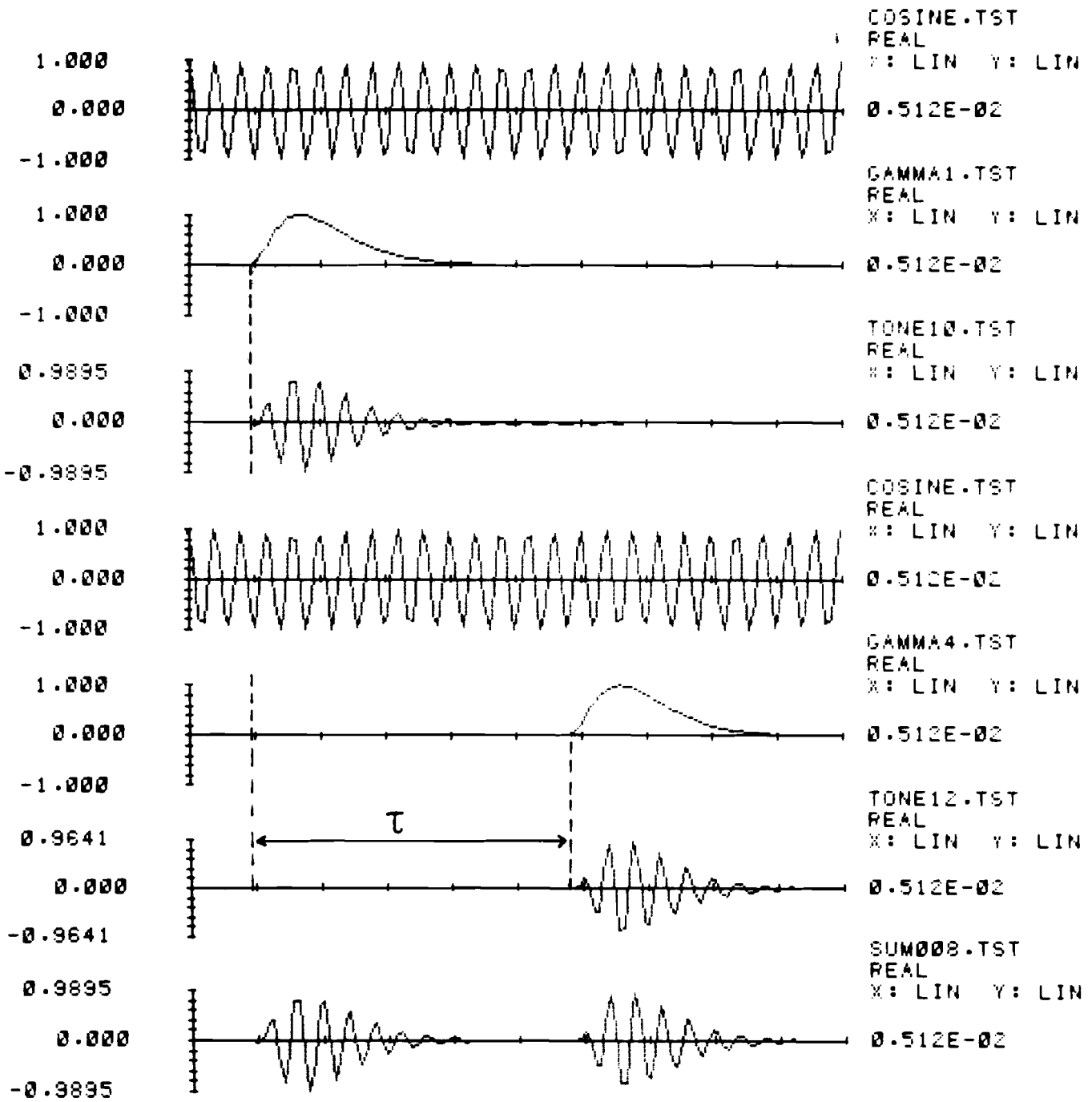


Fig. 4.19. The construction of two gamma-tones shifted in time by addition of two single gamma-tones.

The COSTID - function for two time-shifted gamma-tones.

Given  $x_1(t) = A(t) \cos \omega_0 t$   
 $x_2(t) = A(t - \tau) \cos \omega_0 t$

and the bandwidth of  $A(t)$  less than and below that of  $\cos \omega_0 t$  we can write

$$x_1(t) = A(t) \cos \omega_0 t \rightarrow \xi_1(t) \approx A(t) e^{i\omega_0 t}$$

$$x_2(t) = A(t - \tau) \cos \omega_0 t \rightarrow \xi_2(t) \approx A(t - \tau) e^{i\omega_0 t}$$

The sum signal  $x_3(t) = x_1(t) + x_2(t)$  leads to an analytic signal  $\xi_3(t)$

$$\xi_3(t) = \{ A(t) + A(t - \tau) \} e^{i\omega_0 t}$$

with spectrum  $\check{\xi}_3(\omega) = \{ 1 + e^{-i\tau(\omega - \omega_0)} \} \check{\xi}_1(\omega)$

The COSTID - function of this sum-signal is

$$\Xi(\omega, t) = \left\{ 1 + e^{i\tau(\omega - \omega_0)} \right\} \Xi_1(\omega, t) + \left\{ 1 + e^{-i\tau(\omega - \omega_0)} \right\} \Xi_1(\omega, t - \tau)$$

where  $\Xi_1(\omega, t)$  is the COSTID- function of  $\xi_1(t)$ . Note that the complex factor  $\left\{ 1 + e^{i\tau(\omega - \omega_0)} \right\}$  depends on the time-shift.



Time domain

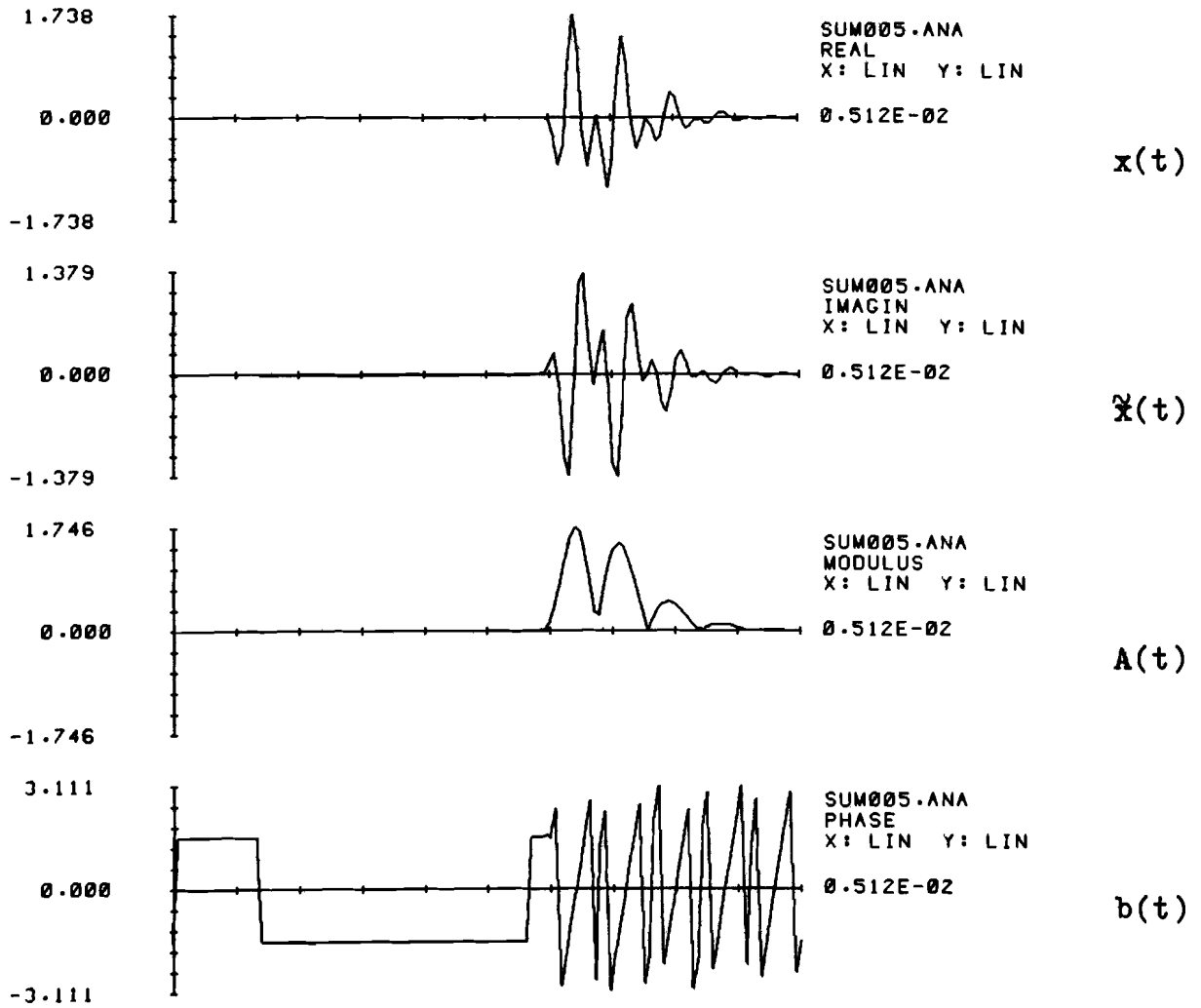


Fig. 4.20. The analytic signal of two frequency shifted gamma-tones.

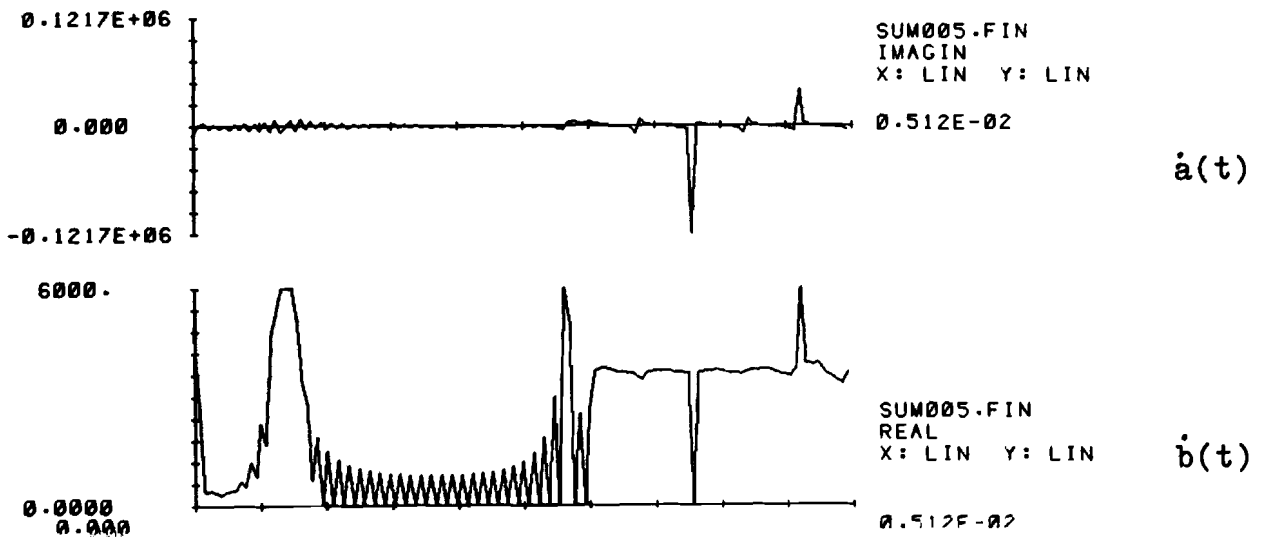


Fig. 4.21. The relative temporal amplitude change and instantaneous frequency of two frequency shifted gamma-tones.

Frequency domain

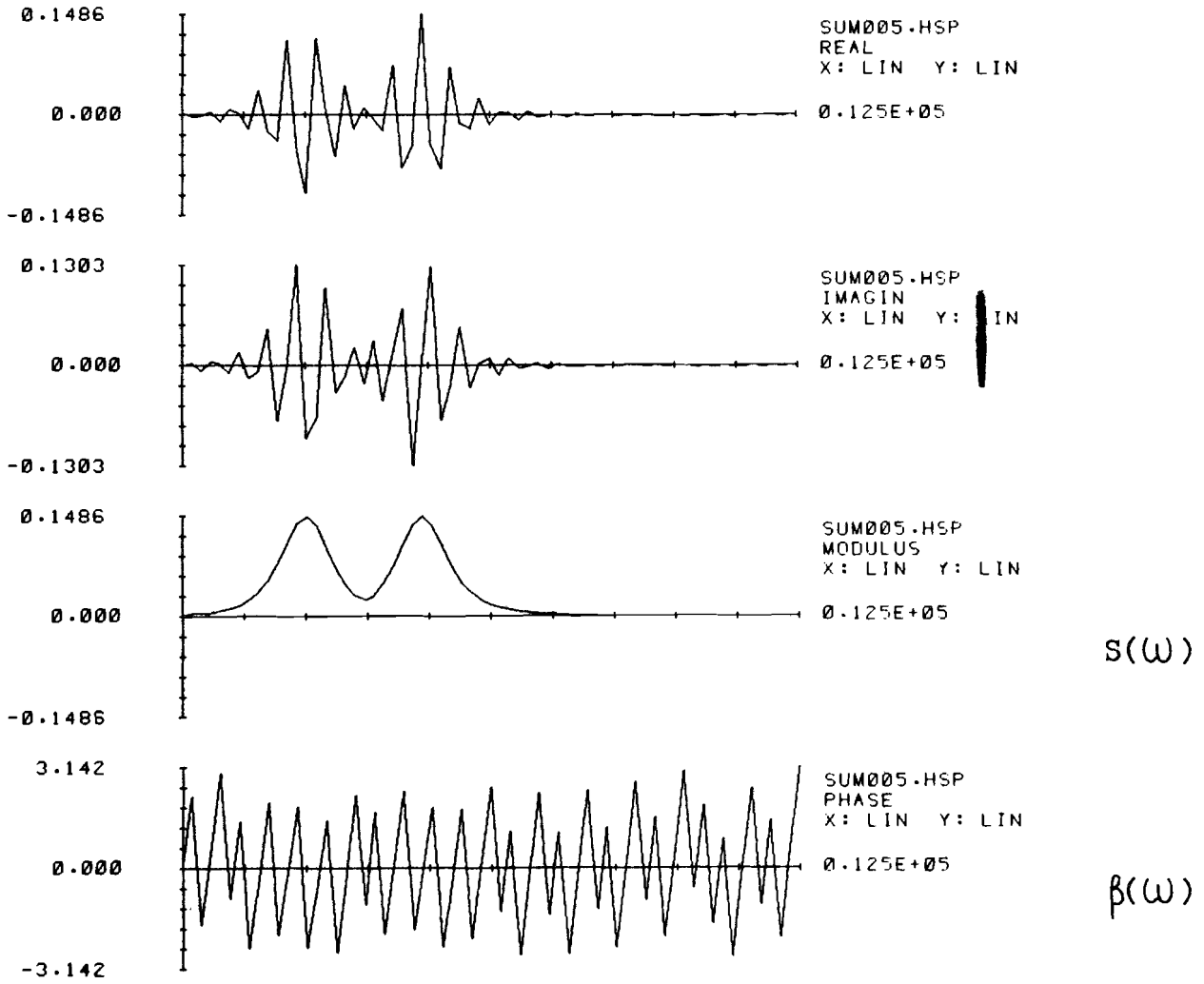


Fig. 4.22. The Fourier transform of the analytic signal of two frequency shifted gamma-tones.

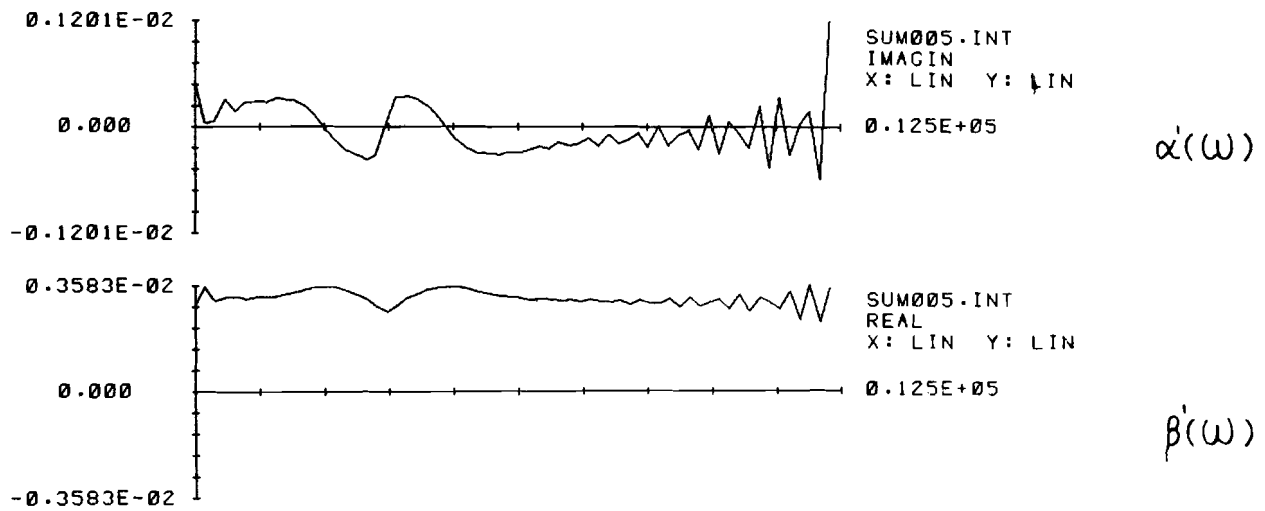


Fig. 4.23. The relative spectral amplitude change and spectral phase change of two frequency shifted gamma-tones.

↑ Spectral intensity

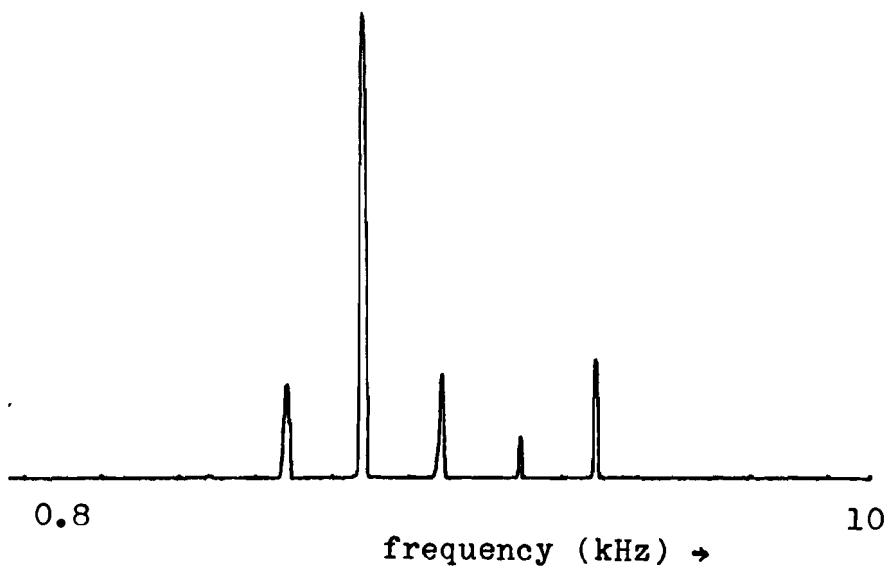


Fig. 4.24.a. Output of spectral analyzer: Static display of two gamma-tones shifted in frequency.

↑ Temporal intensity in passband selected

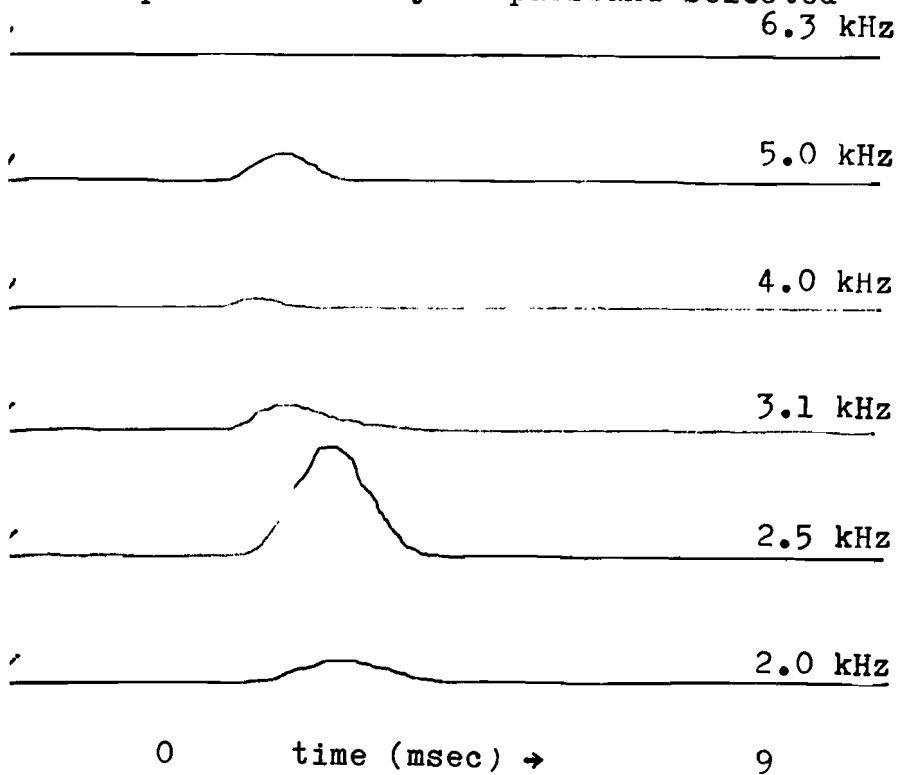
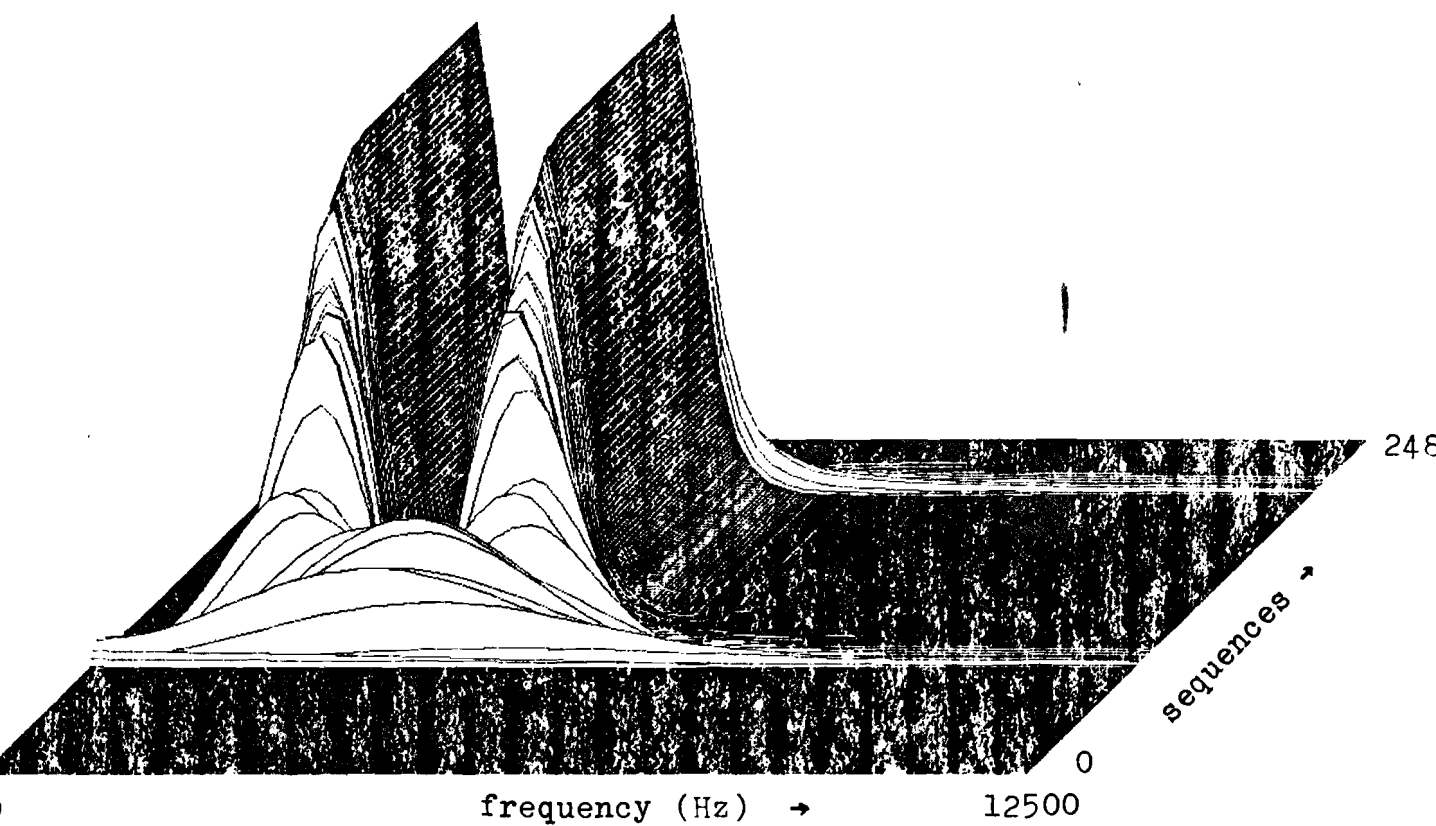


Fig. 4.24.b. Output of spectral analyzer: Dynamic display of two gamma-tones shifted in frequency.



248

Fig. 4.25.a. The short-time power spectrum of two gamma-tones shifted in frequency; windowlength: 5.12 msec, windowshift: 40  $\mu$  sec.

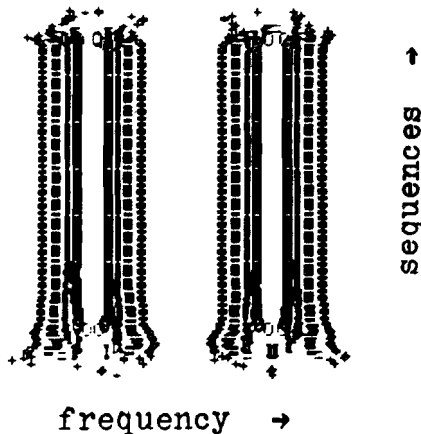
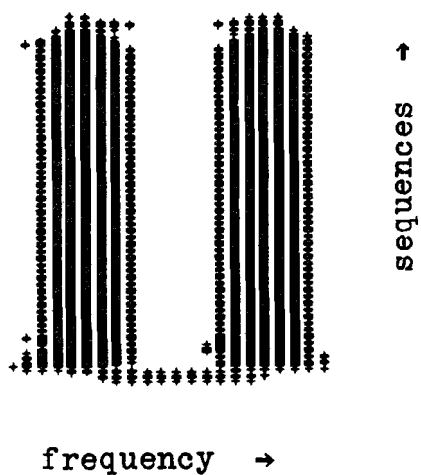


Fig. 4.25.b. Part of the corresponding "sonogram".

Fig. 4.25.c. Part of the corresponding level-display.

Fig. 4.26. The COSTID-function of two gamma-tones shifted in frequency.

time: from 0. to 5.12 msec; frequency: from 0. to 12500 Hz.

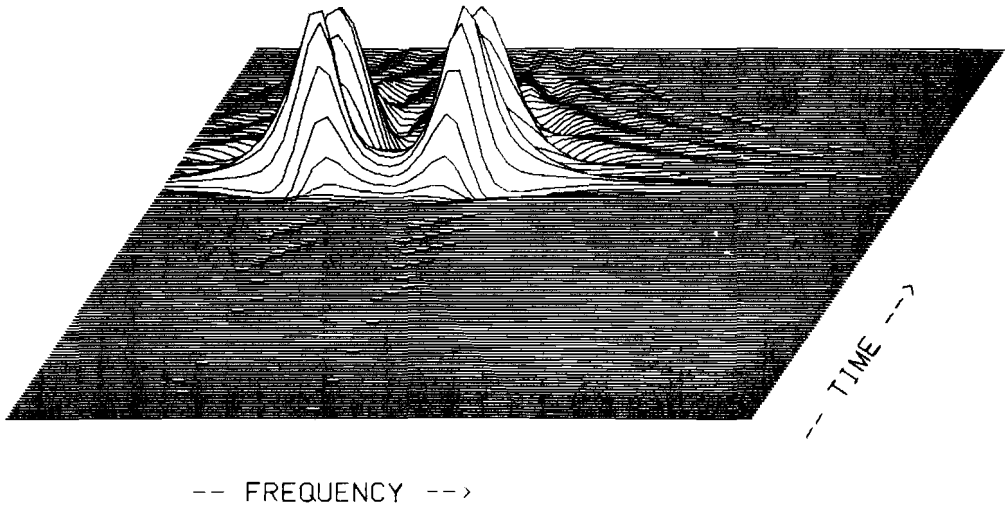


Fig. 4.26.a. The real part.

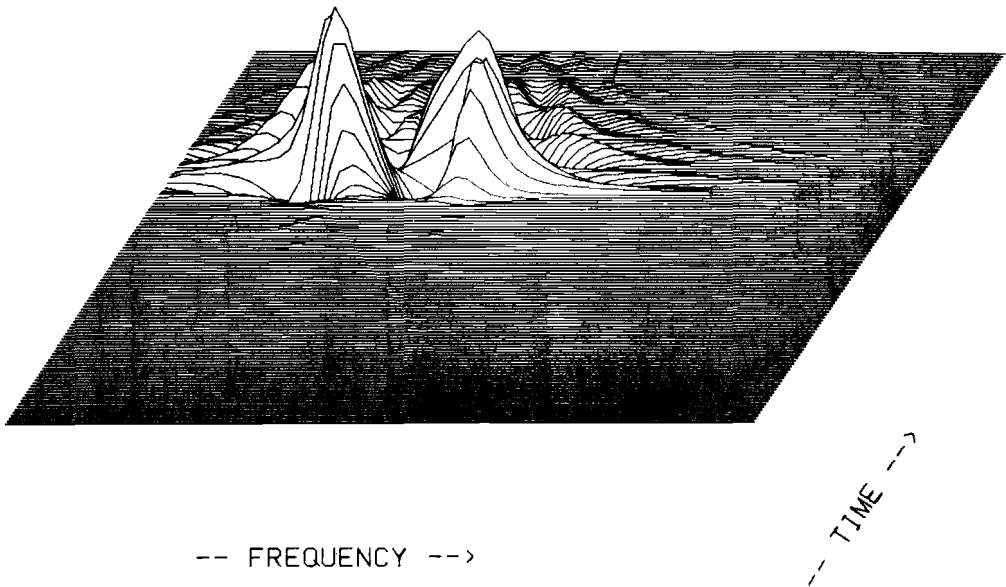


Fig. 4.26.b. The imaginary part.

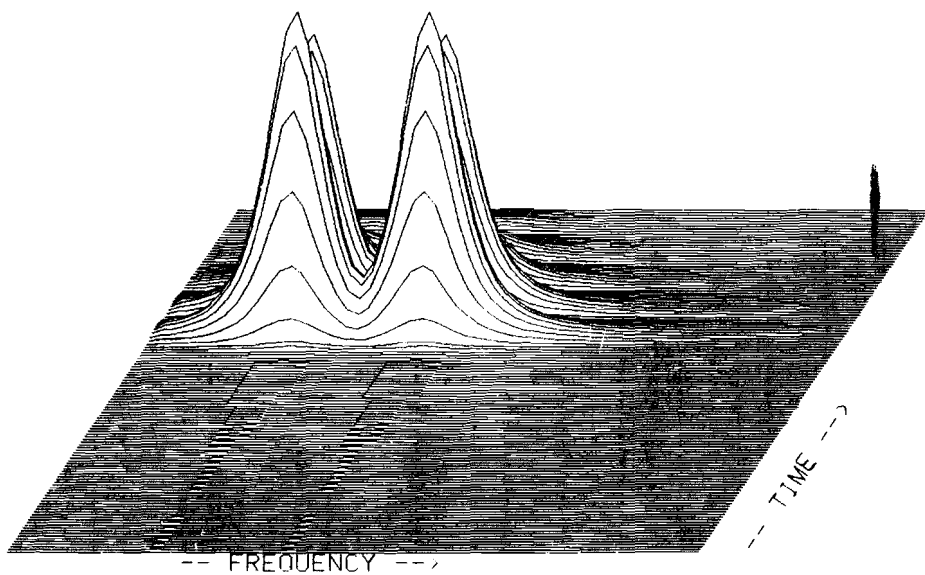


Fig. 4.26.c. The modulus.

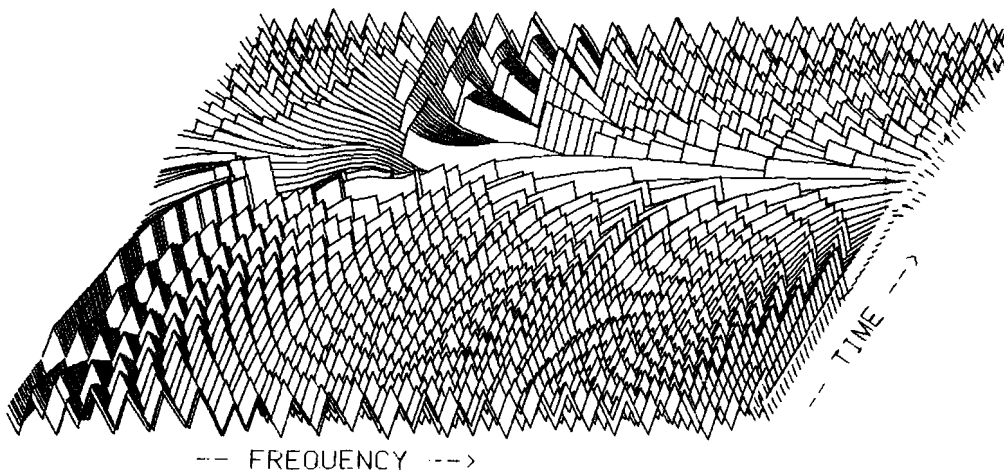


Fig. 4.26.d. The argument.

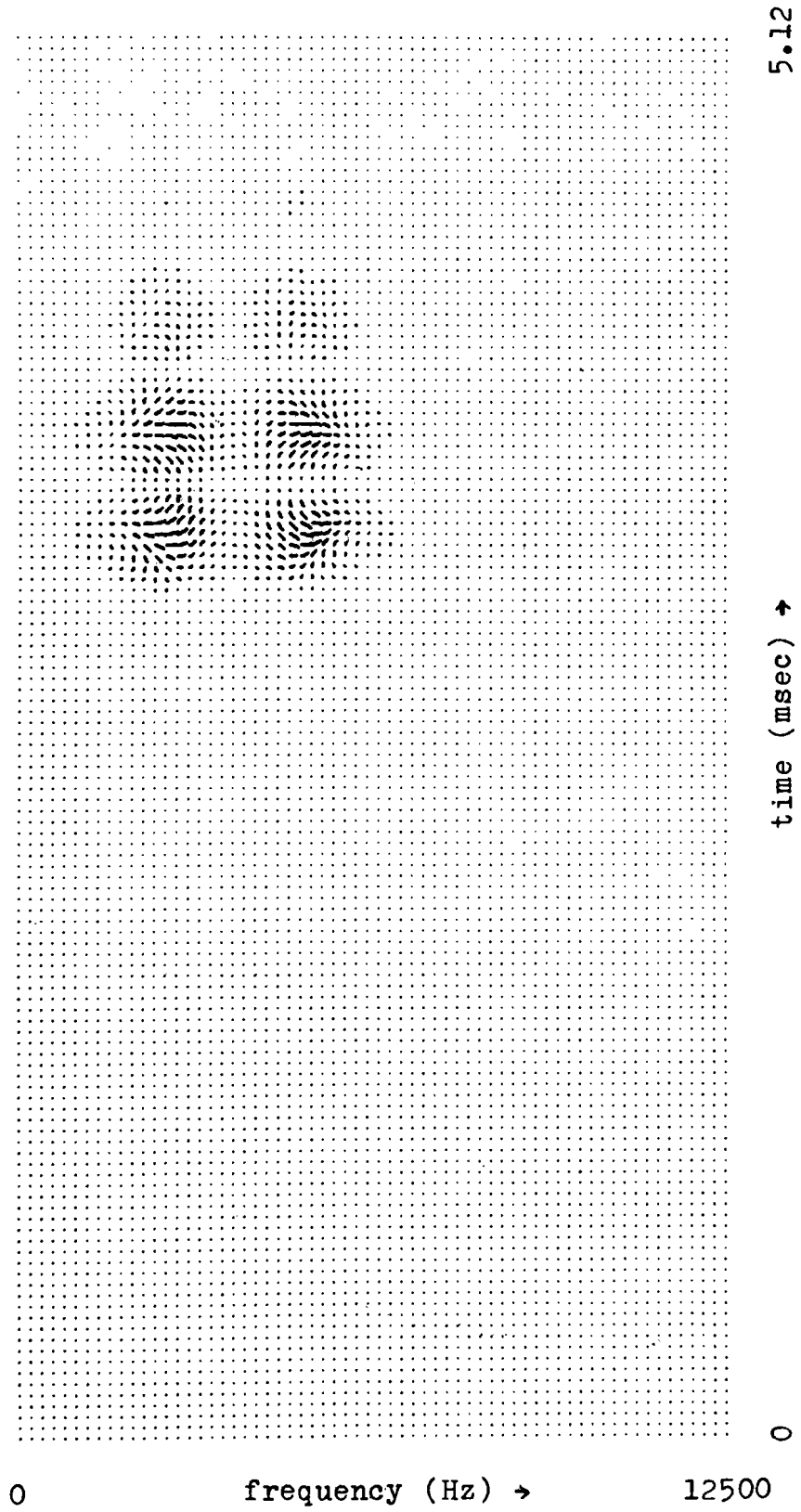


Fig. 4.27. The COSTID-function of two frequency shifted gamma-tones.

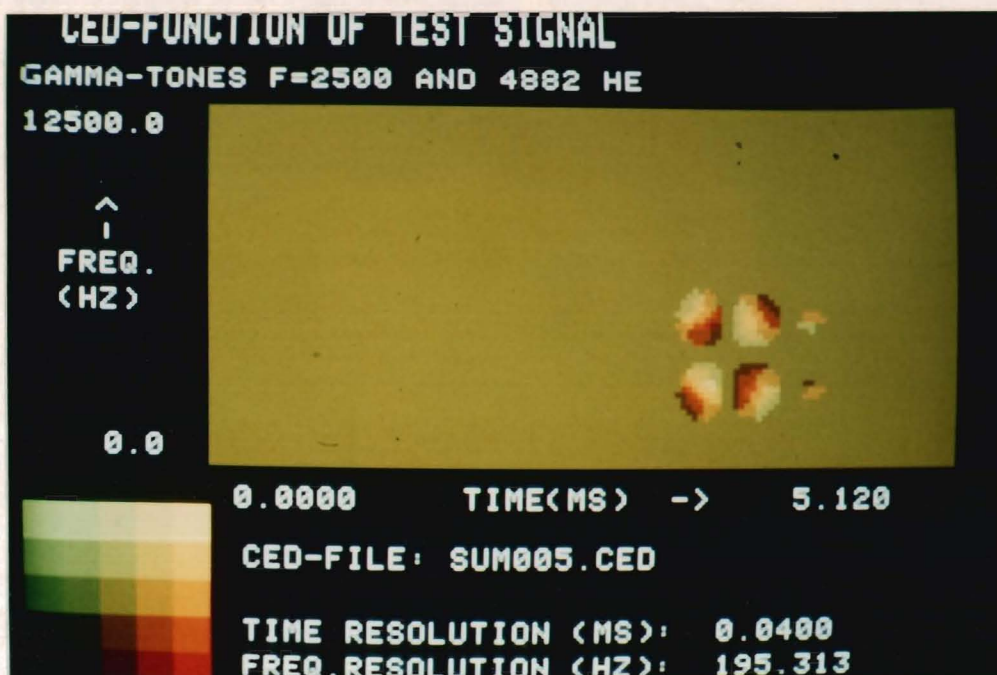


Fig. 4.28.a. The COSTID-function of two frequency shifted gamma-tones with rectangular coding.

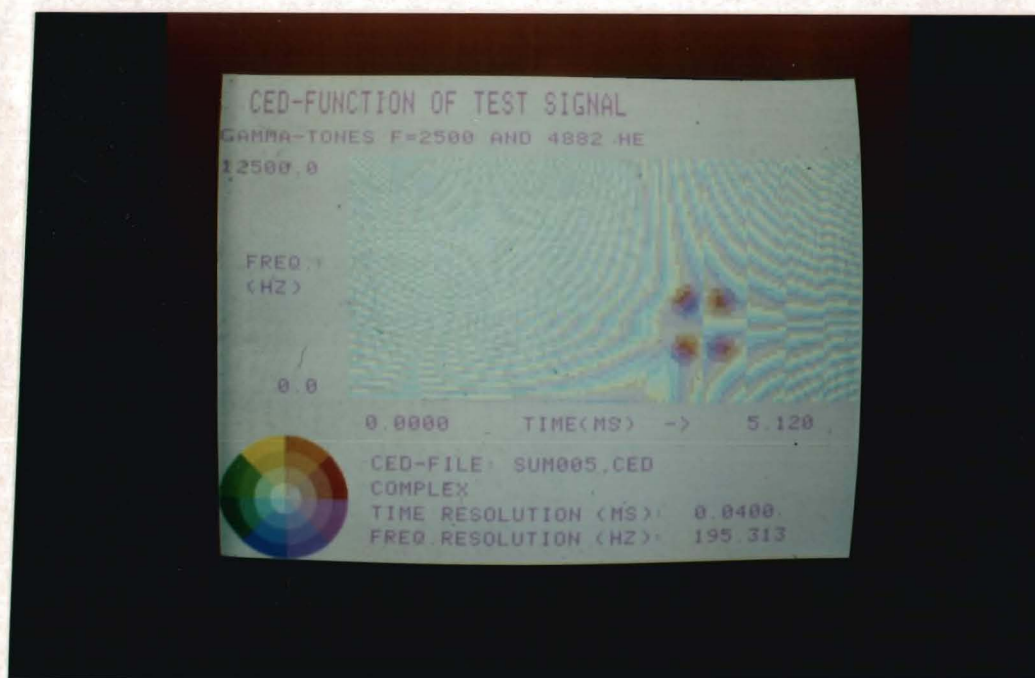


Fig. 4.28.b. The COSTID-function of two frequency shifted gamma-tones with polar coding.



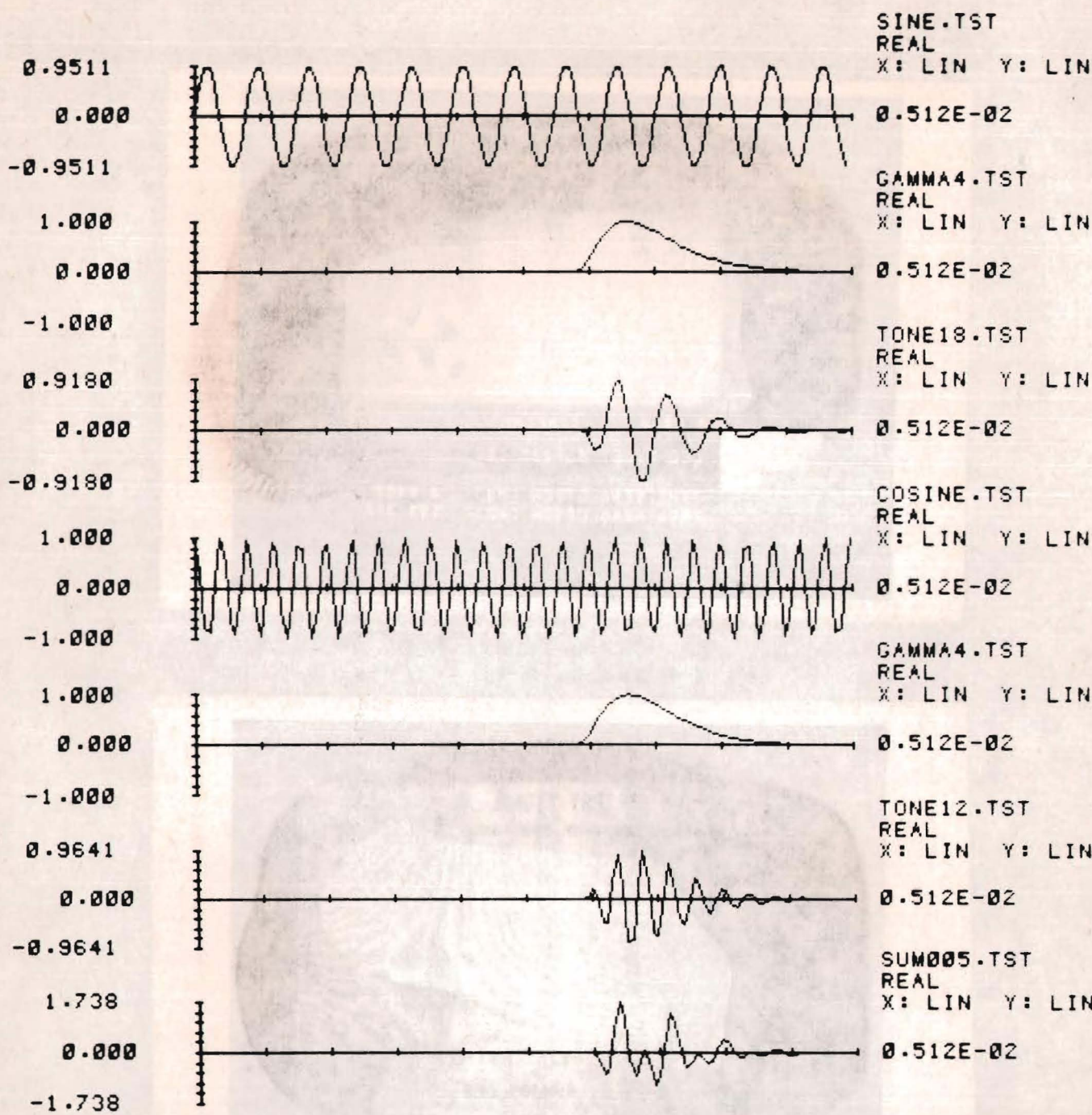


Fig. 4.29. The construction of two gamma-tones shifted in frequency by addition of two single gamma-tones.

The COSTID - function for two frequency-shifted gamma-tones.

Given  $x_1(t) = A(t) \sin(\omega_0 t)$

$x_2(t) = A(t) \cos(\omega_1 t) \quad ; \quad \omega_1 > \omega_0$

and the bandwidth of  $A(t)$  less and below that of  $\sin(\omega_0 t)$  or  $\cos(\omega_1 t)$  (fig.4.30), we can write

$$\begin{aligned} x_1(t) &\longrightarrow \xi_1(t) \approx A(t) e^{i\omega_0 t - i\frac{\pi}{2}} \\ x_2(t) &\longrightarrow \xi_2(t) \approx A(t) e^{i\omega_1 t} \end{aligned}$$

The sum signal  $x_3(t) = x_1(t) + x_2(t)$  leads to an analytic signal  $\xi_3(t)$

$$\xi_3(t) = A(t) e^{i\omega_1 t} \left\{ e^{-i\frac{\pi}{2}} e^{-i\Delta\omega t} + 1 \right\}; \Delta\omega = \omega_1 - \omega_0$$

with spectrum

$$\check{\xi}_3(\omega) = \check{\xi}_1(\omega) + e^{i\frac{\pi}{2}} \check{\xi}_1(\omega - \Delta\omega)$$

The COSTID- function of this sum signal

$$\begin{aligned} \Xi(\omega, t) &= \left\{ 1 + e^{i(\Delta\omega t + \frac{\pi}{2})} \right\} \Xi_1(\omega, t) \\ &+ \left\{ 1 + e^{-i(\Delta\omega t + \frac{\pi}{2})} \right\} \Xi_1(\omega - \Delta\omega, t) \end{aligned}$$

Time domain

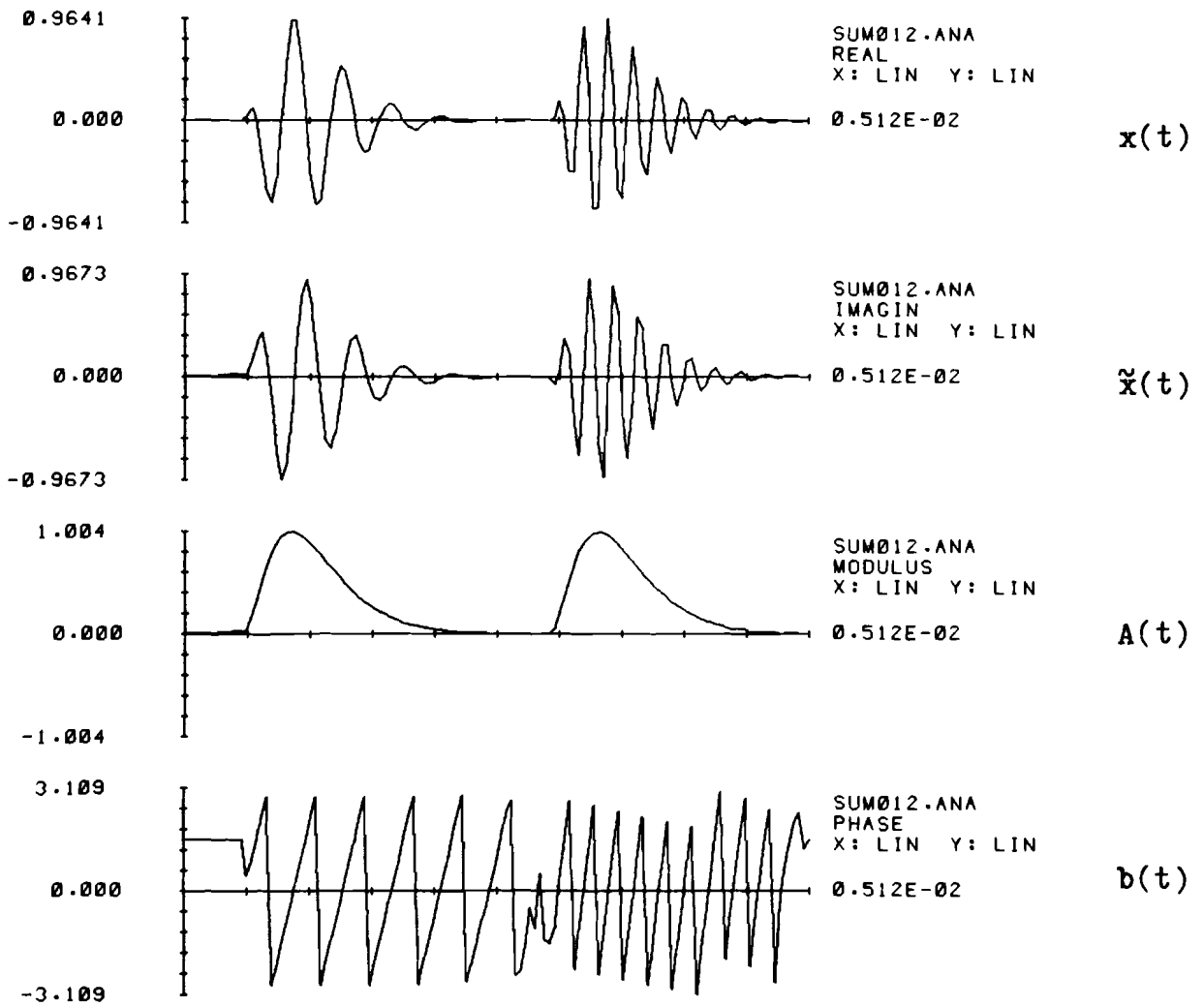


Fig. 4.30. The analytic signal of two time and frequency shifted gamma-tones.

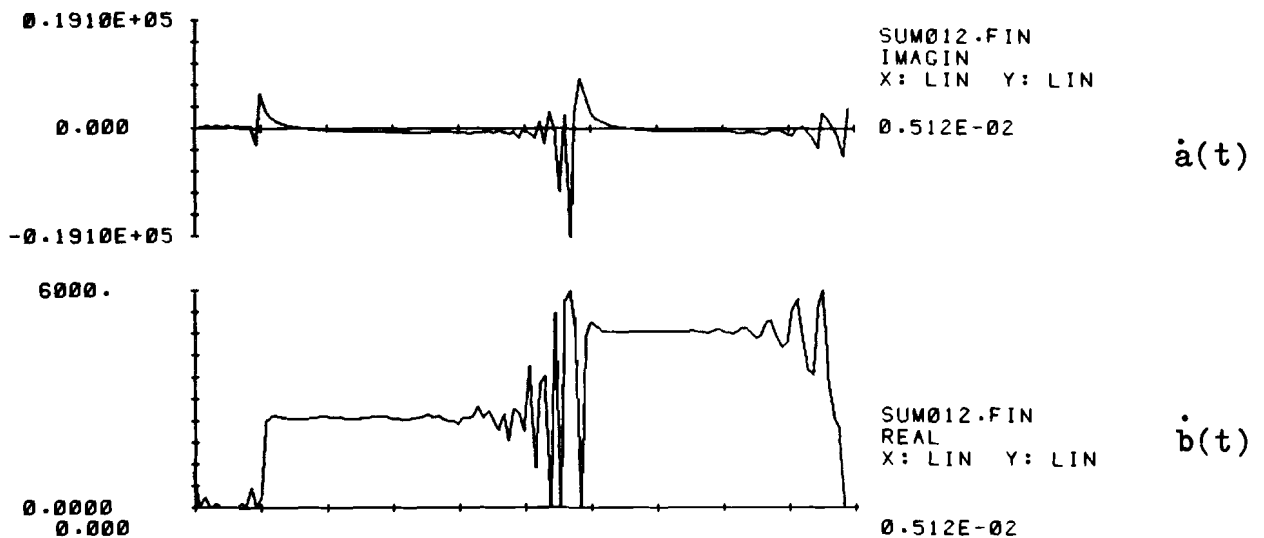


Fig. 4.31. The relative temporal amplitude change and instantaneous frequency of two time and frequency shifted gamma-tones.

Frequency domain

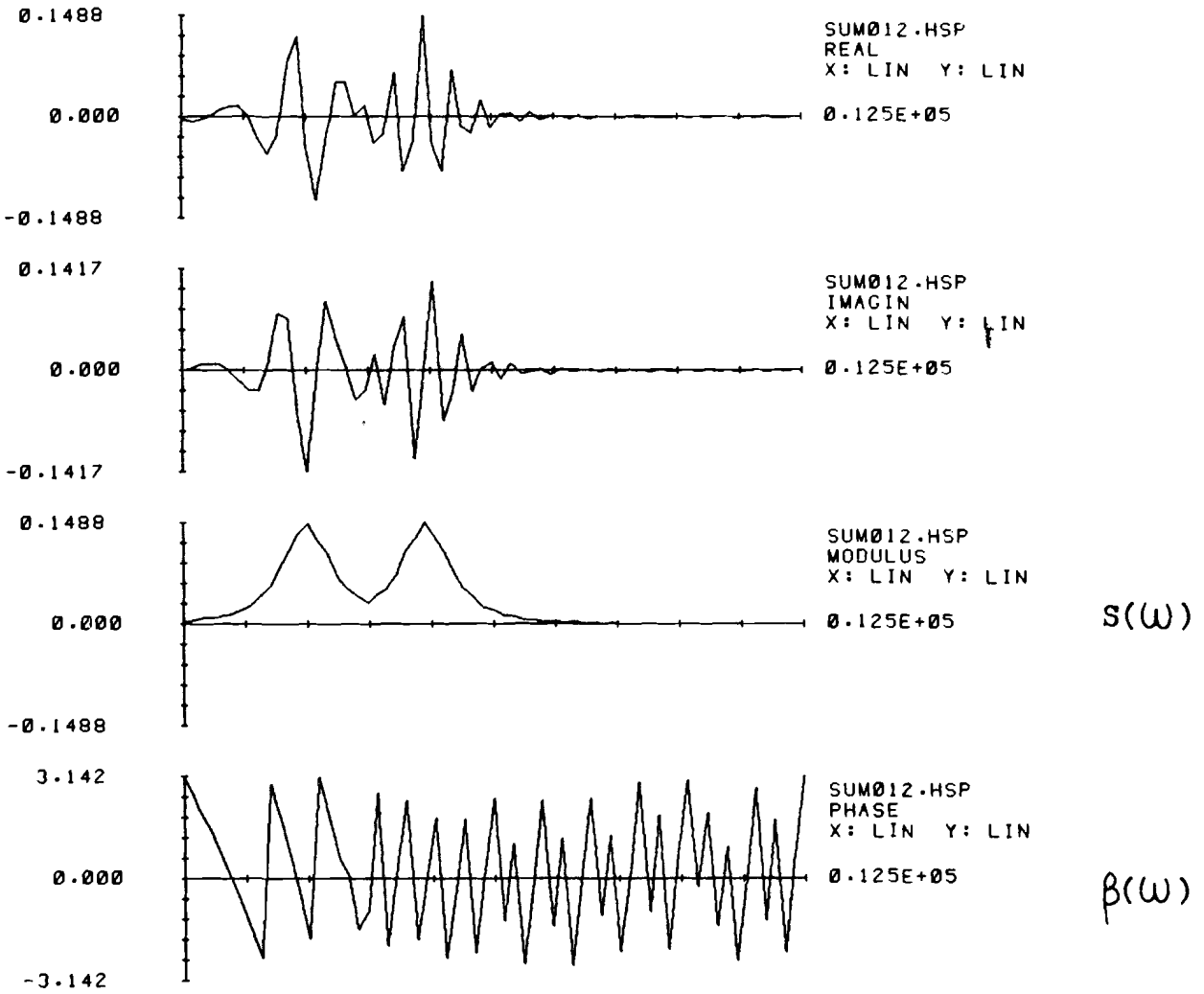


Fig. 4.32. The Fourier transform of the analytic signal of two time and frequency shifted gamma-tones.

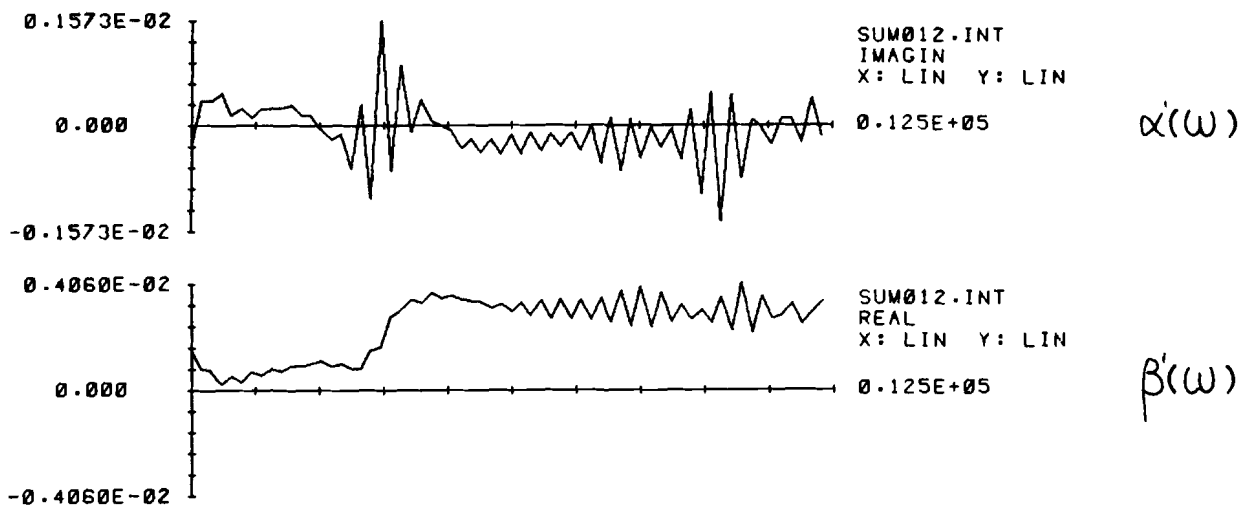


Fig. 4.33. The relative spectral amplitude change and spectral phase change of two time and frequency shifted gamma-tones.

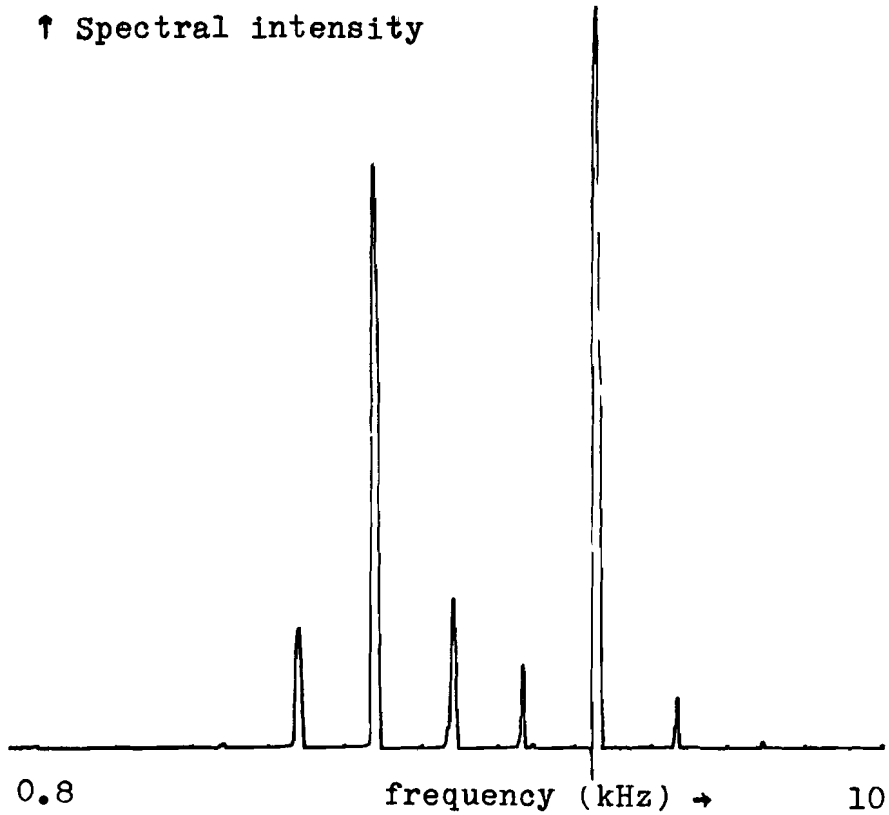


Fig. 4.34.a. Output of spectral analyzer: Static display of two gamma-tones shifted in time and frequency.

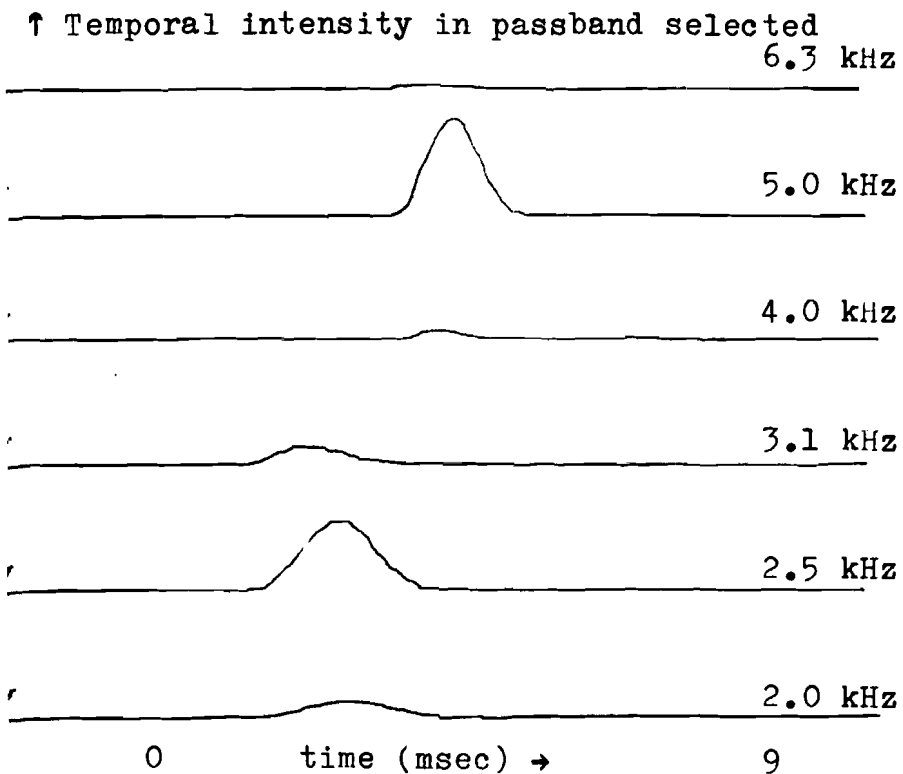


Fig. 4.34.b. Output of spectral analyzer: Dynamic display of two gamma-tones shifted in time and frequency.

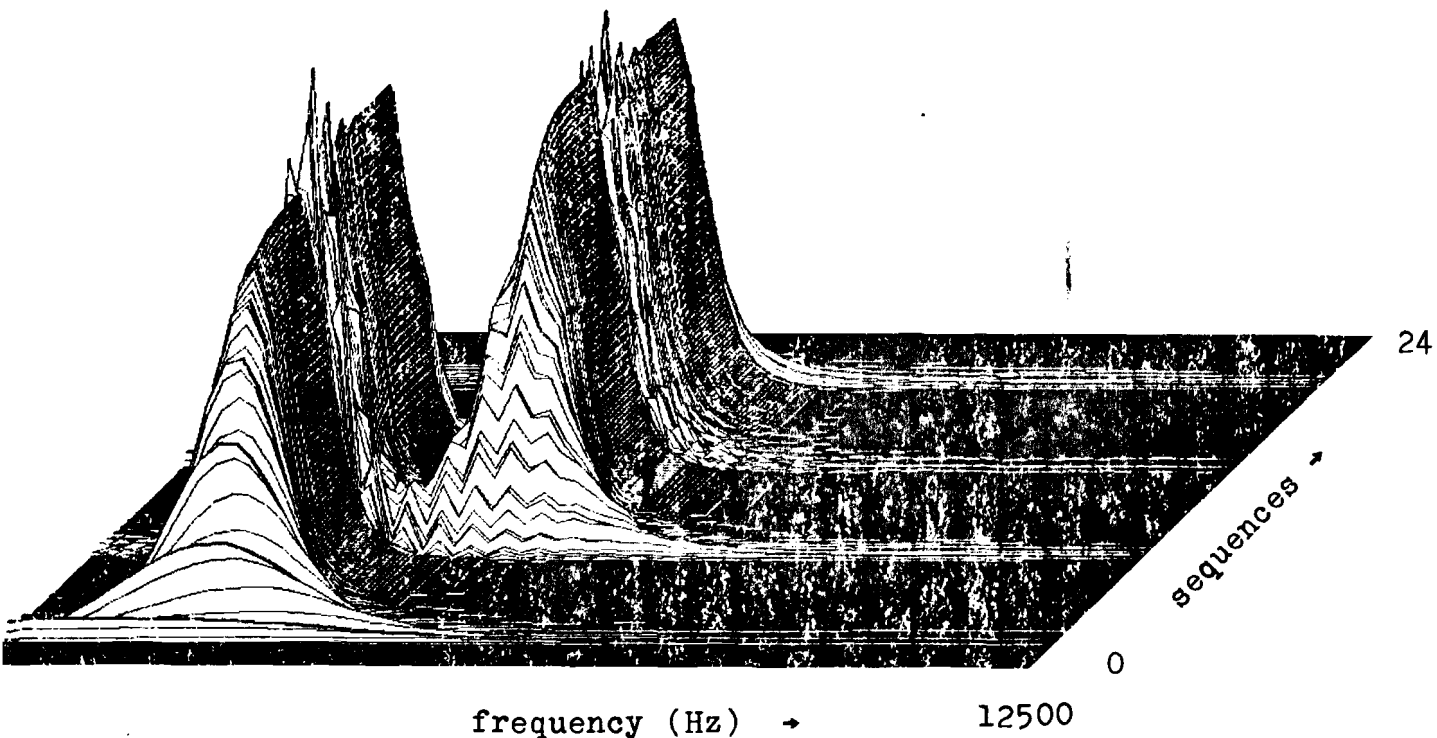


Fig. 4.35.a. The short-time power spectrum of two gamma-tones shifted in time and frequency. windowlength: 5.12 msec, windowshift: 40 sec.

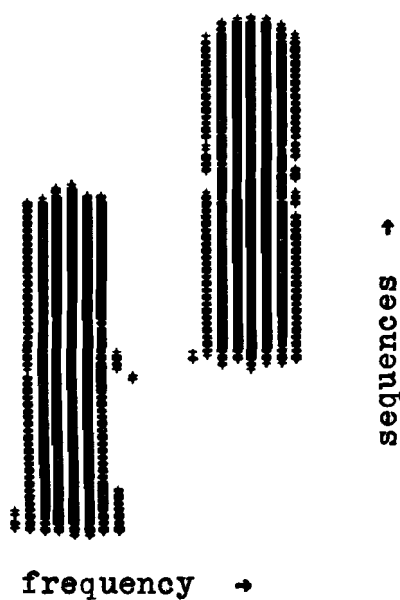


Fig. 4.35.b. Part of the corresponding "sonogram".

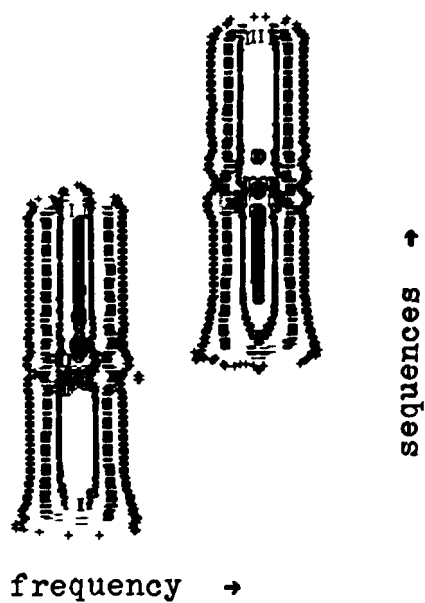


Fig. 4.35.c. Part of the corresponding level-display.

Fig. 4.36. The COSTID-function  
of two gamma-tones shifted in time and frequency.

time: from 0. to 5.12 msec; frequency: from 0. to 12500 Hz.

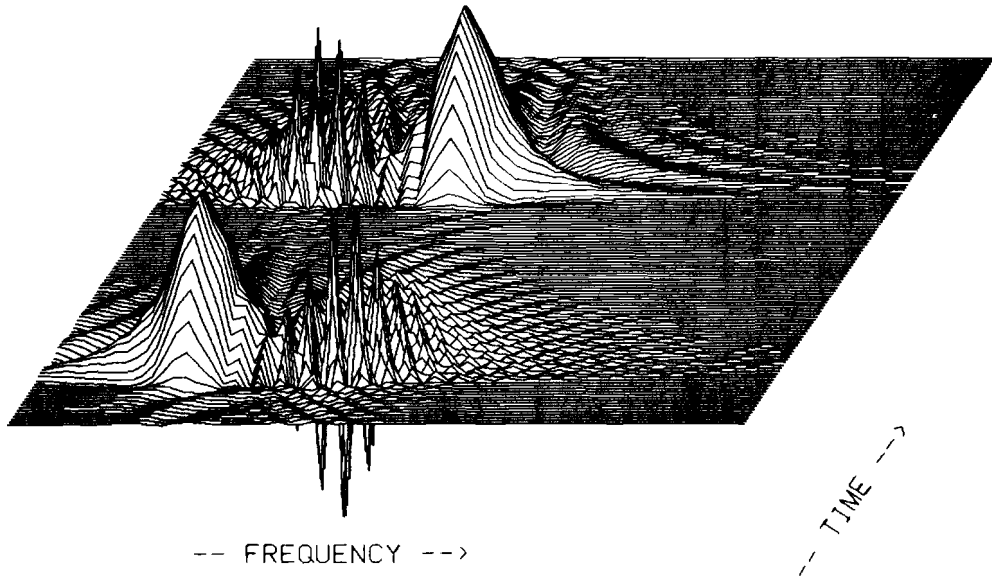


Fig. 4.36.a. The real part.

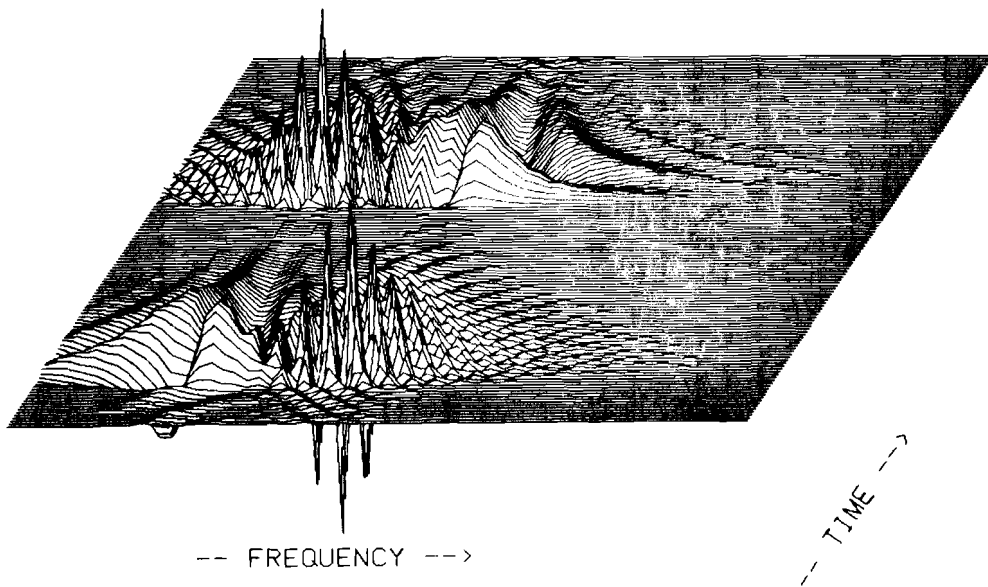


fig. 4.36.b. The imaginary part.

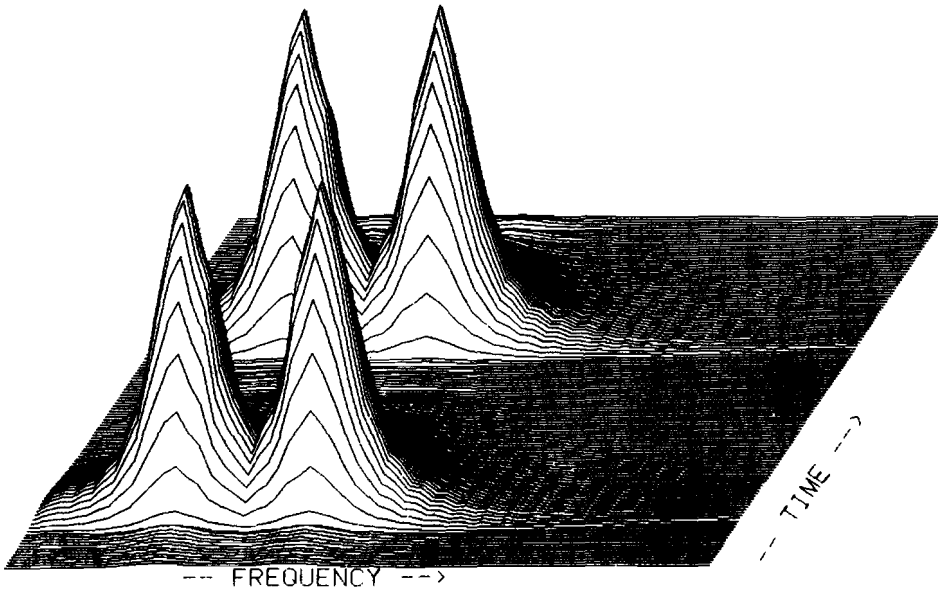


Fig. 4.36.c. The modulus.

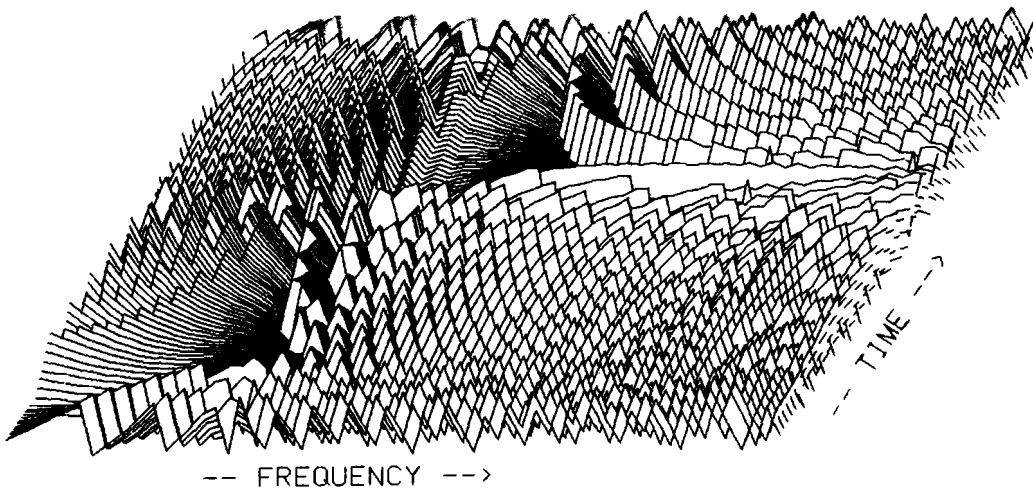


Fig. 4.36.d. The argument.



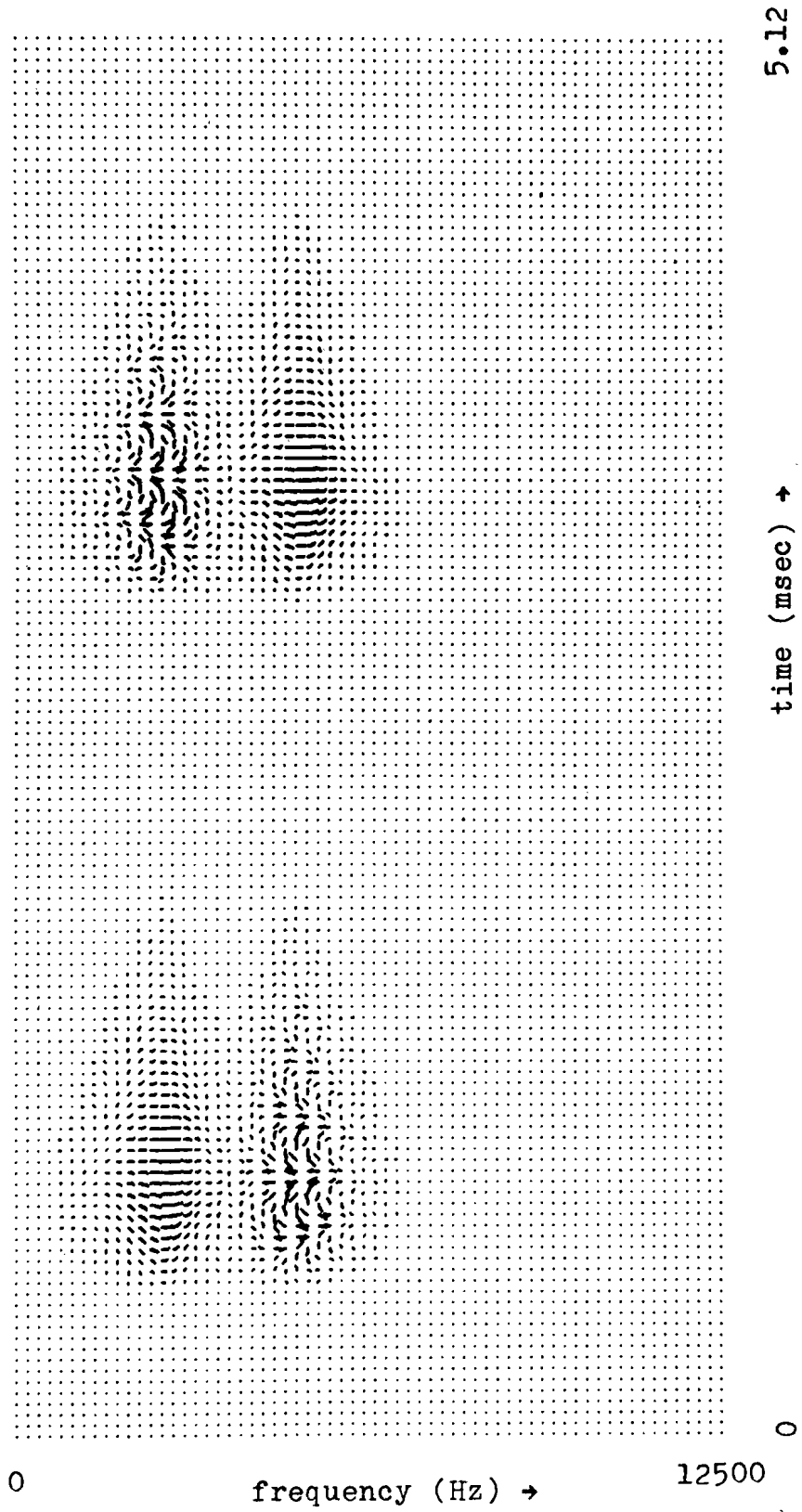


Fig. 4.37. The COSTID-function of two time and frequency shifted gamma-tones.

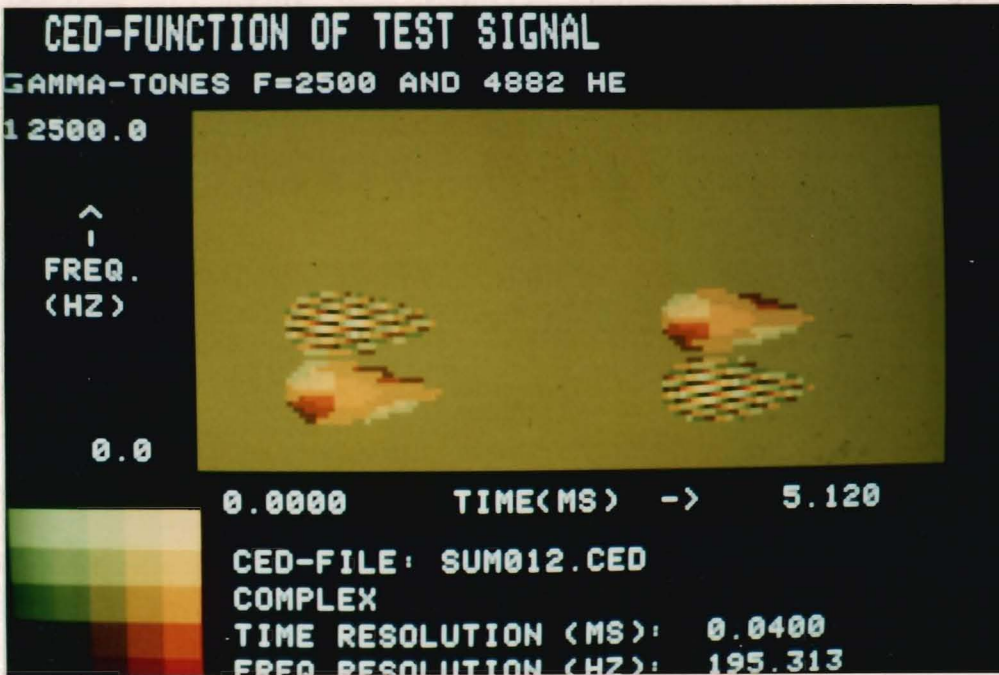


Fig. 4.38.a. The COSTID-function of two time and frequency shifted gamma-tones with rectangular coding.

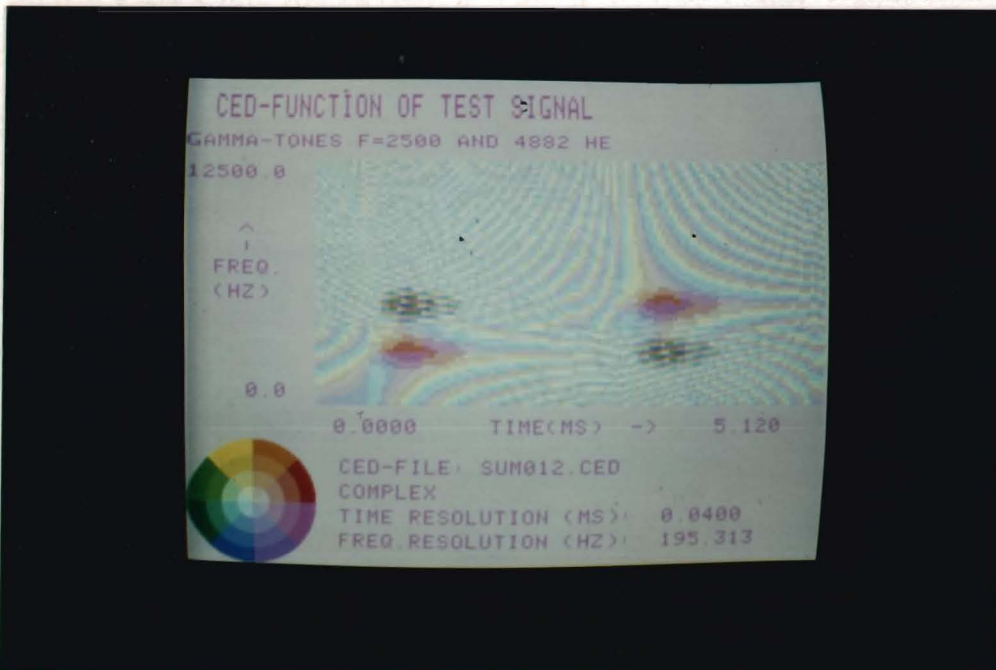


Fig. 4.38.b. The COSTID-function of two time and frequency shifted gamma-tones with polar coding.

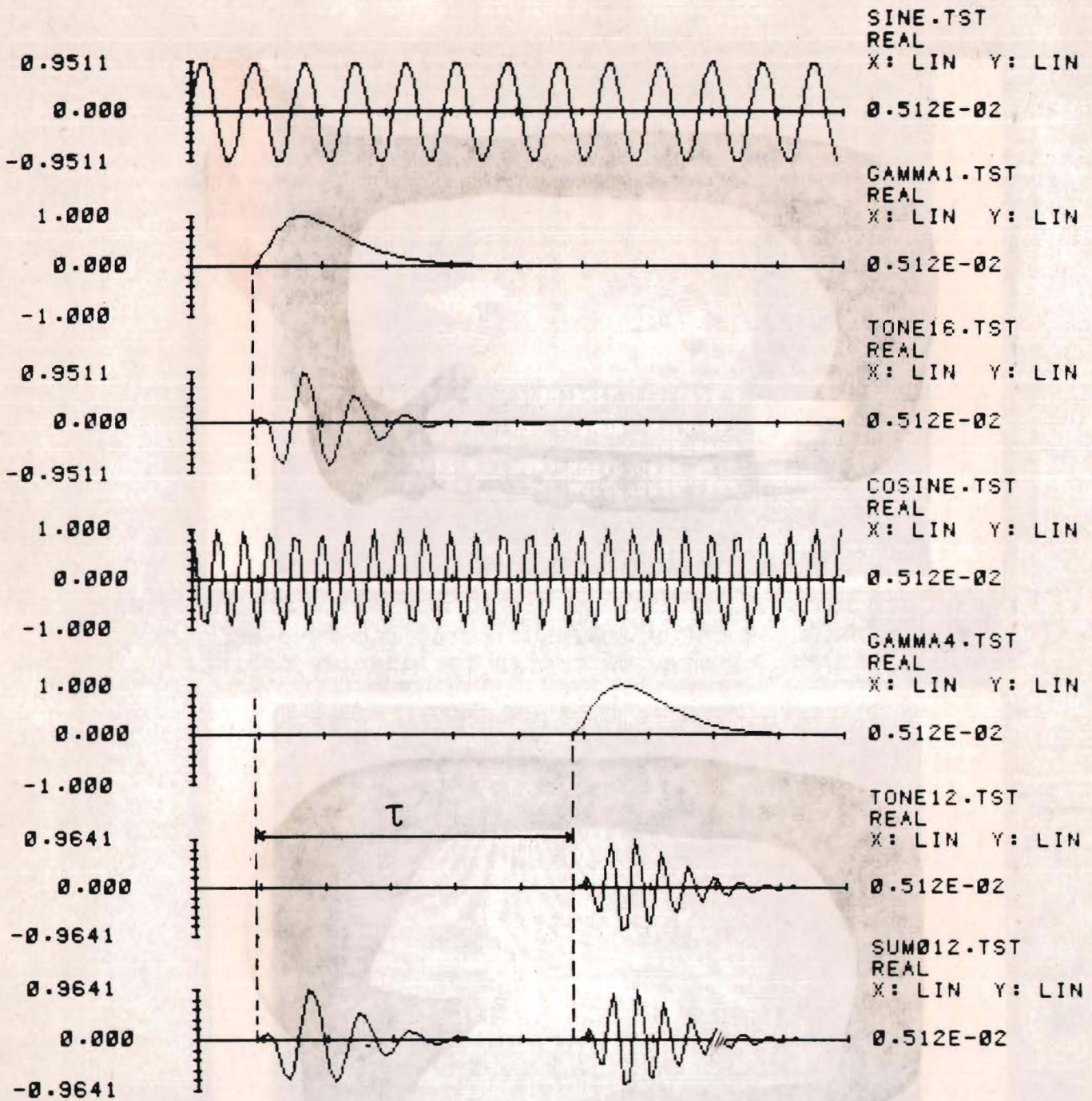


Fig. 4.39. The construction of two gamma-tones shifted in time and frequency by addition of two single gamma-tones.

The COSTID - function for two gamma-tones shifted in time and frequency

$$\begin{aligned} \text{Given } x_1(t) &= A(t) \sin(\omega_0 t) \\ x_2(t) &= A(t-\tau) \cos(\omega_1 t) \quad ; \quad \omega_1 > \omega_0 \end{aligned}$$

and the bandwidth of  $A(t)$  less and below that of  $\sin(\omega_0 t)$  and  $\cos(\omega_1 t)$  (fig.4.41), we can write

$$\begin{aligned} x_1(t) &\longrightarrow \xi_1(t) \simeq A(t) e^{i\omega_0 t} e^{i\frac{\pi}{2}} \\ x_2(t) &\longrightarrow \xi_2(t) \simeq A(t-\tau) e^{i\omega_1 t} \end{aligned}$$

The sum signal  $x_3(t) = x_1(t) + x_2(t)$  leads to an analytic signal

$$\xi_3(t) = \left\{ A(t) + A(t-\tau) e^{i\Delta\omega t} e^{-i\frac{\pi}{2}} \right\} e^{i\omega_0 t} e^{i\frac{\pi}{2}},$$

where  $\Delta\omega = \omega_1 - \omega_0$ . The spectrum of this analytic signal is

$$\check{\xi}_3(\omega) = \check{\xi}_1(\omega) + e^{i\frac{\pi}{2}} \check{\xi}_1(\omega - \Delta\omega) e^{-i(\omega - \omega_0)\tau}$$

So the COSTID - function of this sum-signal results in

$$\begin{aligned} \Xi_3(\omega, t) &= \Xi_1(\omega, t) \\ &+ \Xi_1(\omega, t - \tau) e^{i(\Delta\omega t - \omega\tau + \omega_0\tau + \frac{\pi}{2})} \\ &+ \Xi_1(\omega - \Delta\omega, t) e^{-i(\Delta\omega t - \omega\tau + \omega_1\tau + \frac{\pi}{2})} \\ &+ \Xi_1(\omega - \Delta\omega, t - \tau) \end{aligned}$$

Again we find a complex factor that changes the original COSTID - function, but this time there appear also two cross-terms. Note that the two COSTID - functions that we find for the gamma-tones apart can be recovered unaffected from the

COSTID-function of the summation of these tones shifted in time and frequency.

To conclude this part some additional remarks on the displays of the calculated functions of the combinations of two time and/or frequency shifted gamma-tones. From the output of the spectral analyzer it can be seen that the gamma-tone with carrier-frequency closest to the central-frequency of a passband selected is favoured with respect to the other (fig. 4.24 and 4.34). In the displays of the short-time power spectrum it can be seen that there cannot be distinguished between them if they are within the time-window at the same time. Besides that, we see how signal values, which are unequal zero at the edges of the time-window, introduce higher frequency components. Finally we see from the displays of the COSTID-function, that the real -, imaginary part and modulus can lead to misinterpretations if they are considered separately (fig. 4.36; there are only two tones !)

#### 4.2. Natural Signals.

To conclude this report the COSTID-function was calculated for the fourth element of the B-call of the *Rana temporaria* (fig. 4.1). In this case we calculated the COSTID-function for a time-signal four times as long as the preceding signals, because of the duration of this element. This is also the largest sequence we can handle at this moment (512 points or samples). As we will see in the displays it is not necessary for these elements to consider frequencies over 3000 Hz. So the sample frequency can be reduced (skipping of time samples) without aliasing effects. Doing so it will be possible to calculate the COSTID over longer time.

Time domain

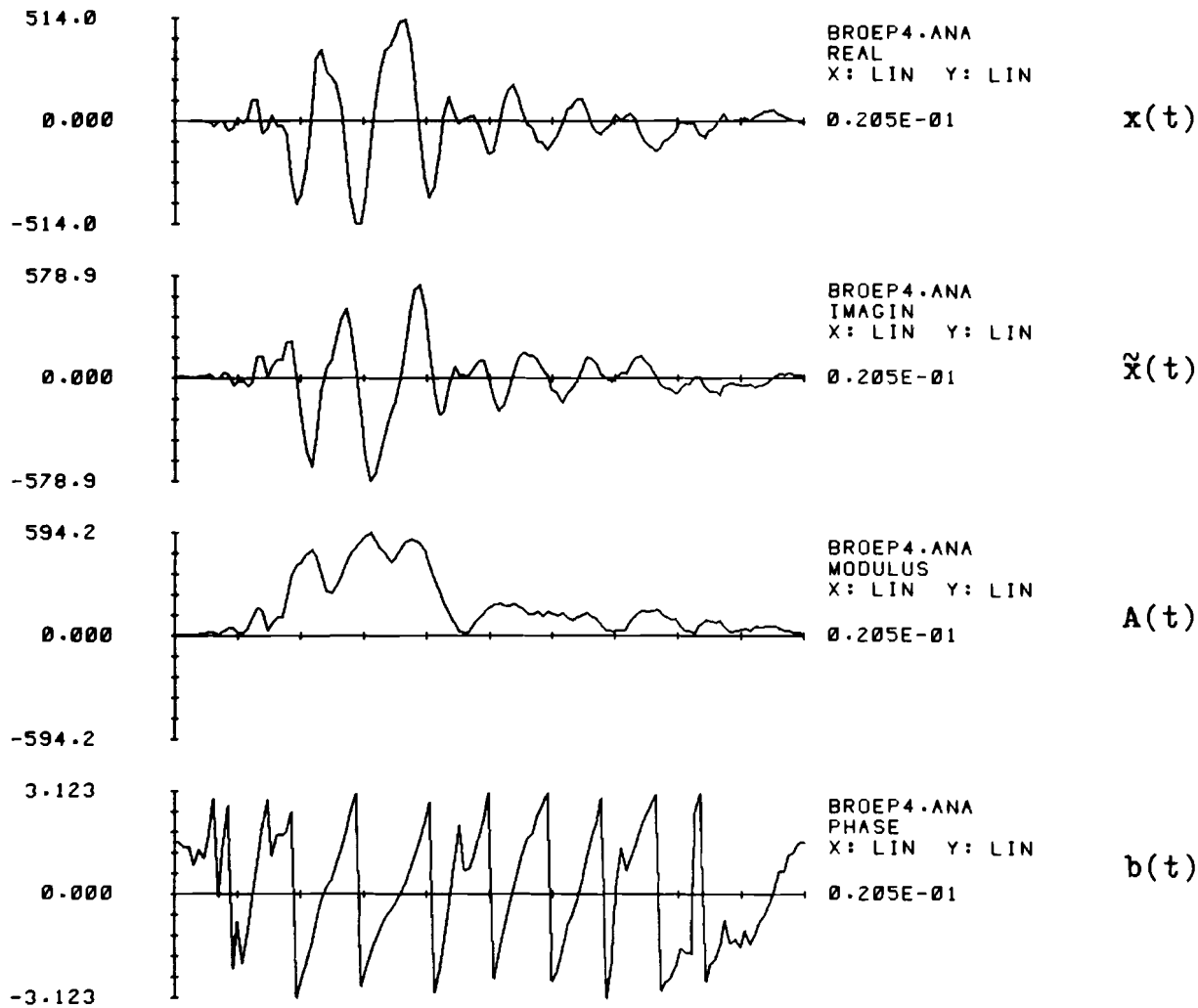


Fig. 4.40. The analytic signal of an element from a B-call of the Irish frog *Rana temporaria*.

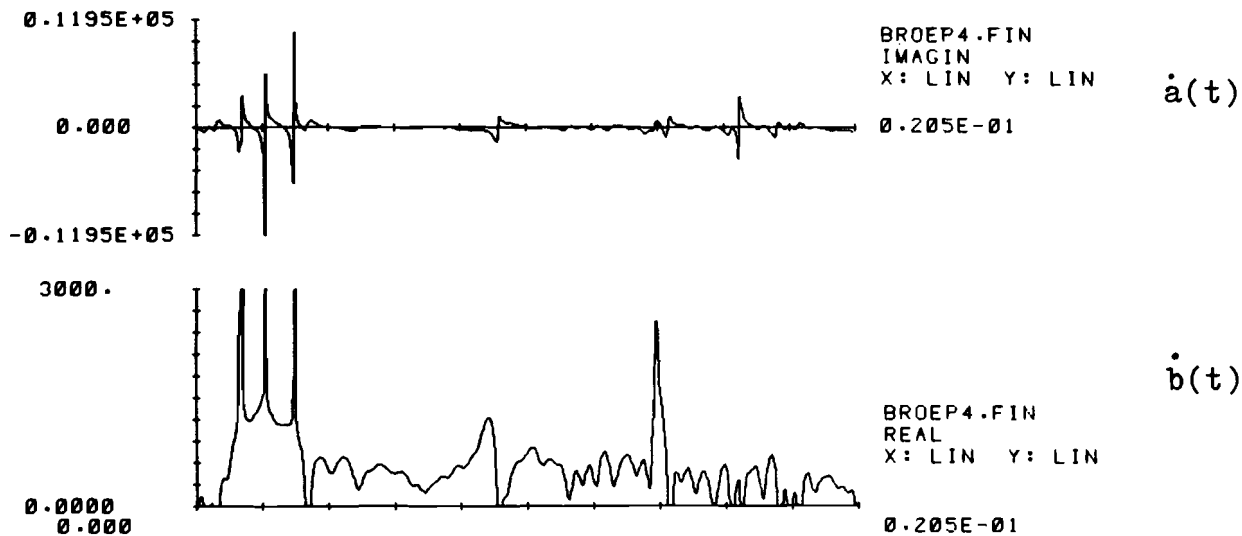


Fig. 4.41. The relative temporal amplitude change and instantaneous frequency of an element from the B-call of the *Rana temporaria*.

Frequency domain

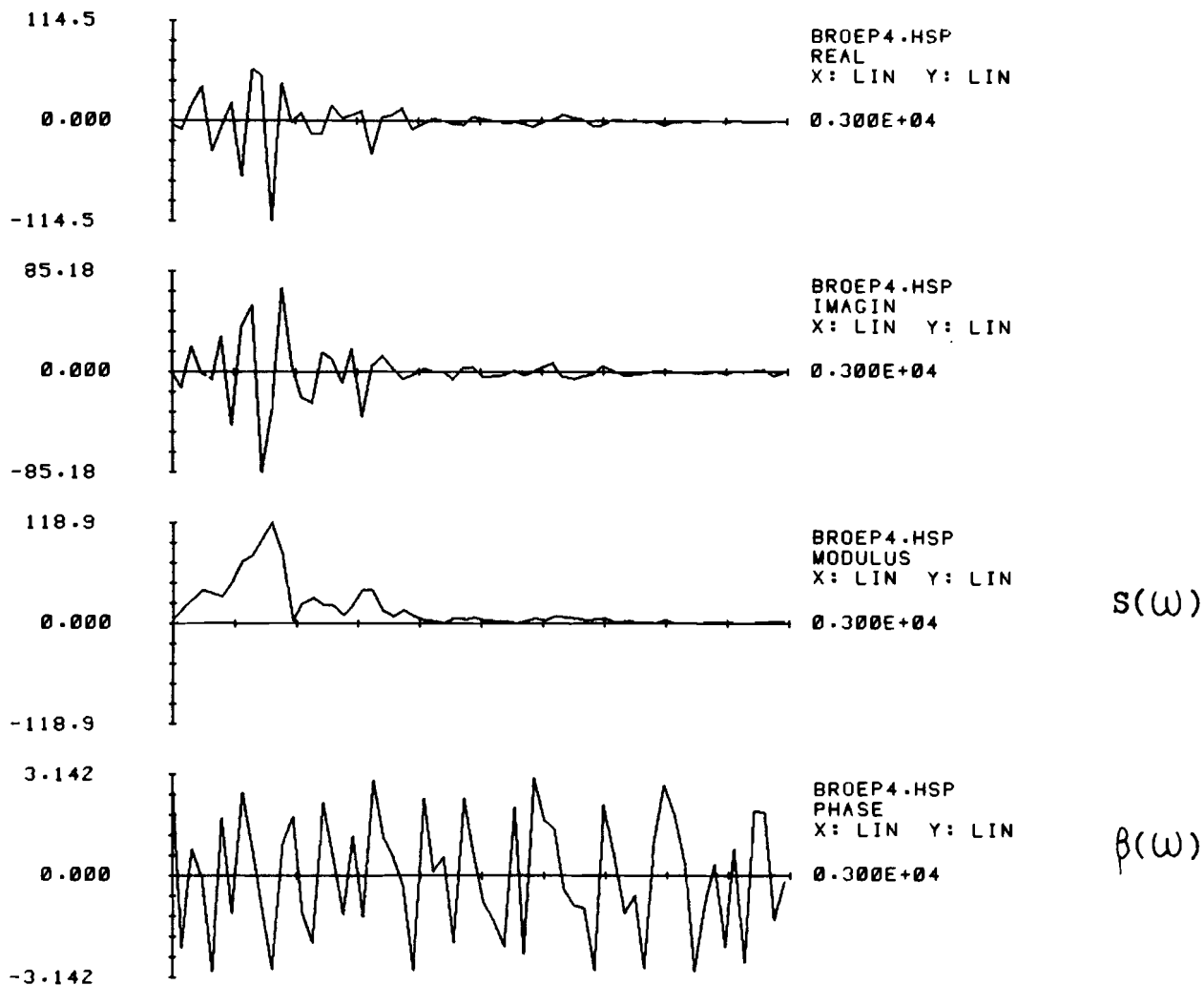


Fig. 4.42. The Fourier transform of the analytic signal of an element from a B-call of the frog *Rana temporaria*.

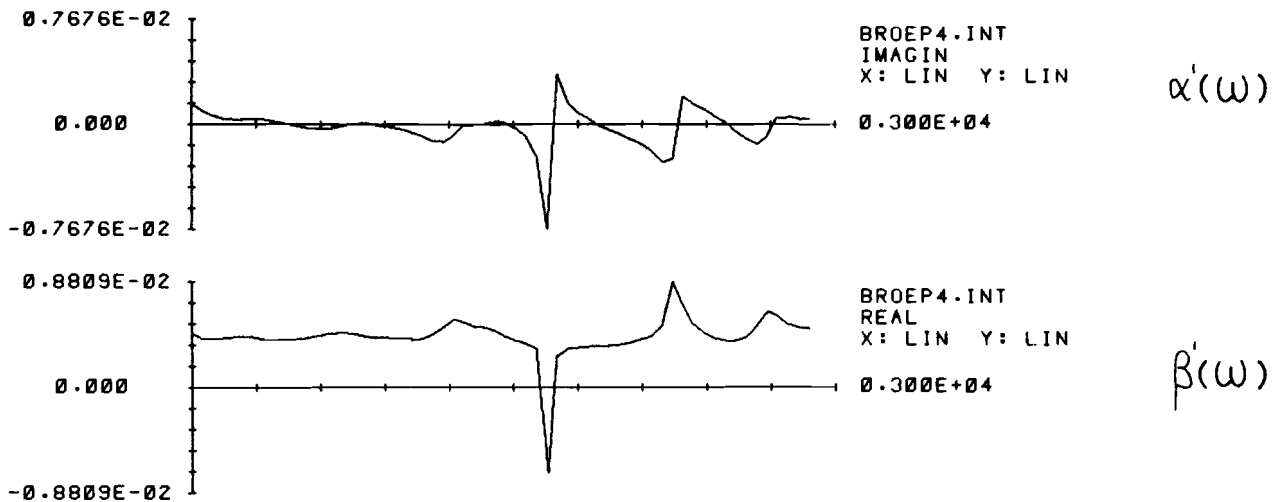


Fig. 4.43. The relative spectral amplitude change and spectral phase change of an element from a B-call of the *Rana temporaria*.

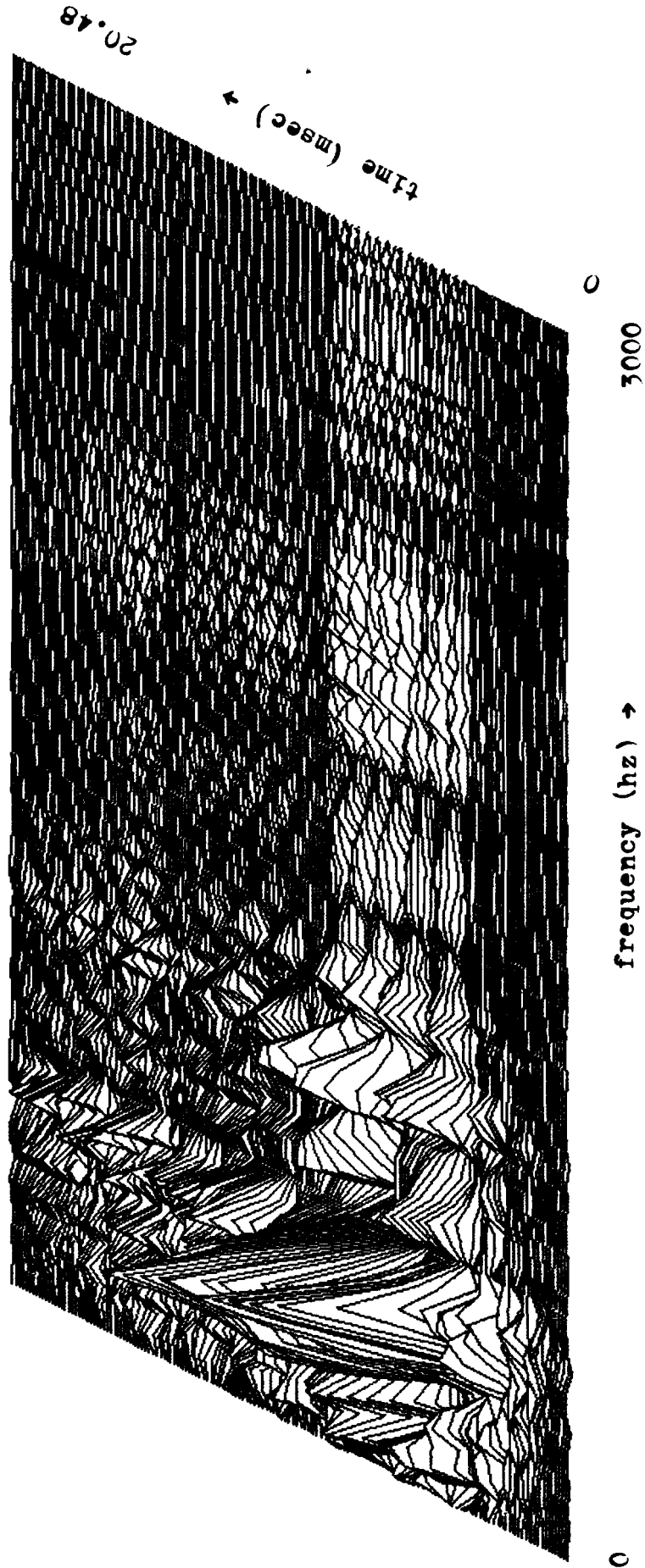


Fig. 4.44. The real part of the COSTID-function of an element from a B-call of the frog *Rana temporaria*.



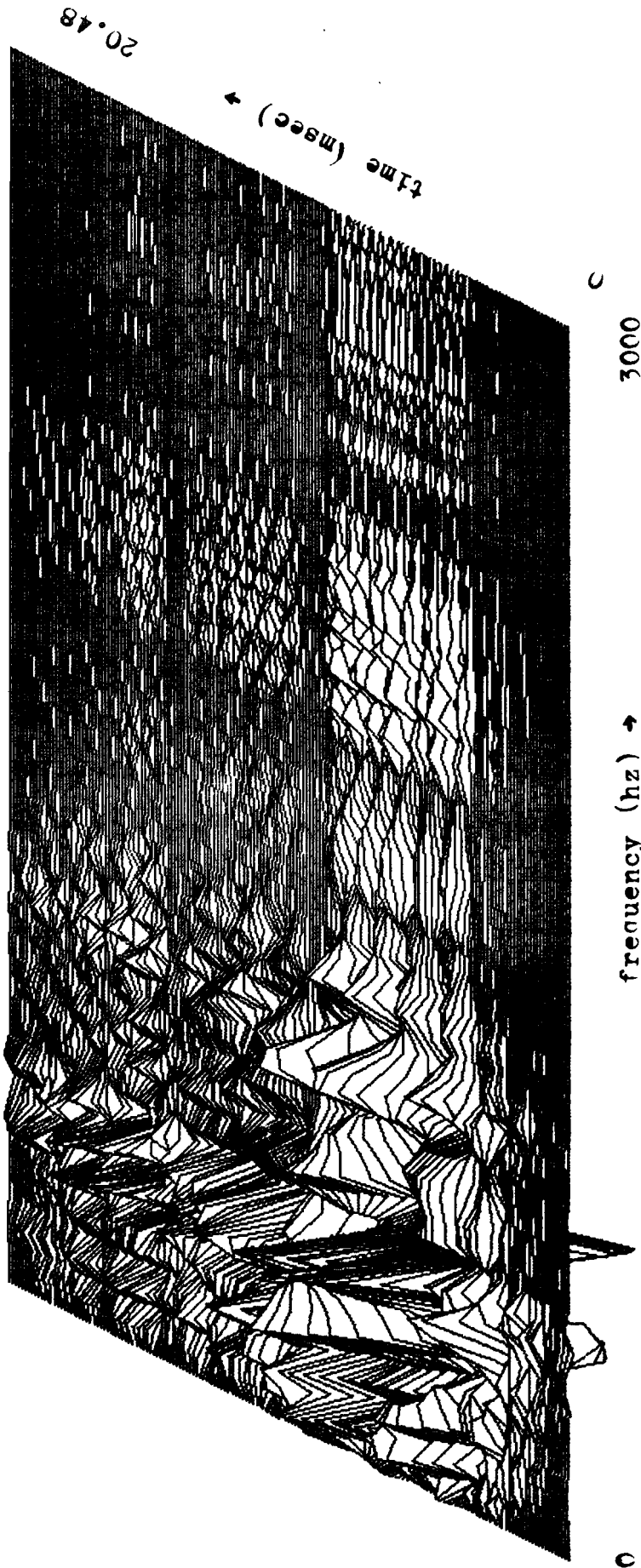


Fig. 4.45. The imaginary part of the COSTID-function of an element from a B-call of the frog *Rana temporaria*.

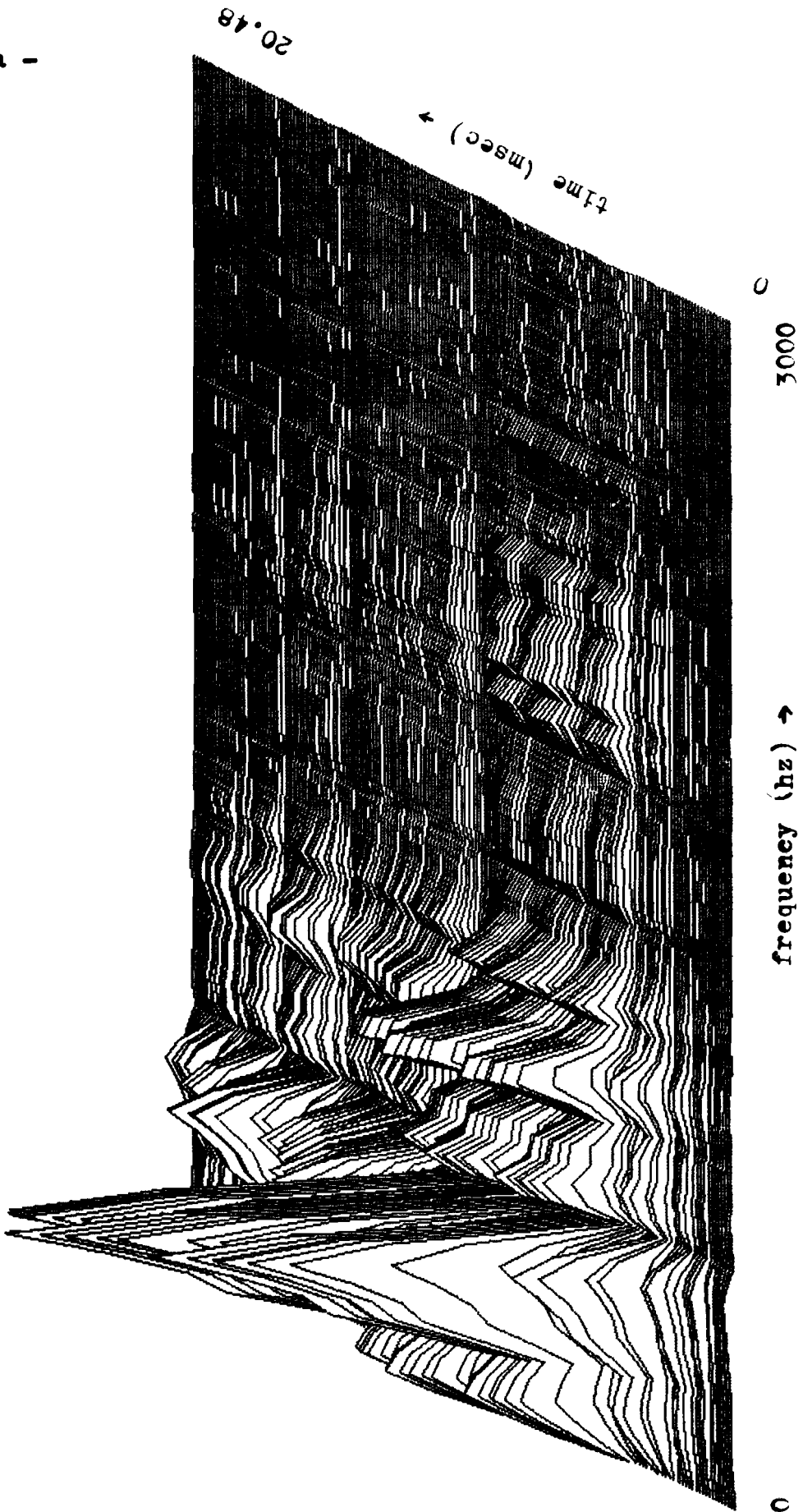


Fig. 4.46. The modulus of the COSTID-function of an element from a B-call of the frog *Rana temporaria*.

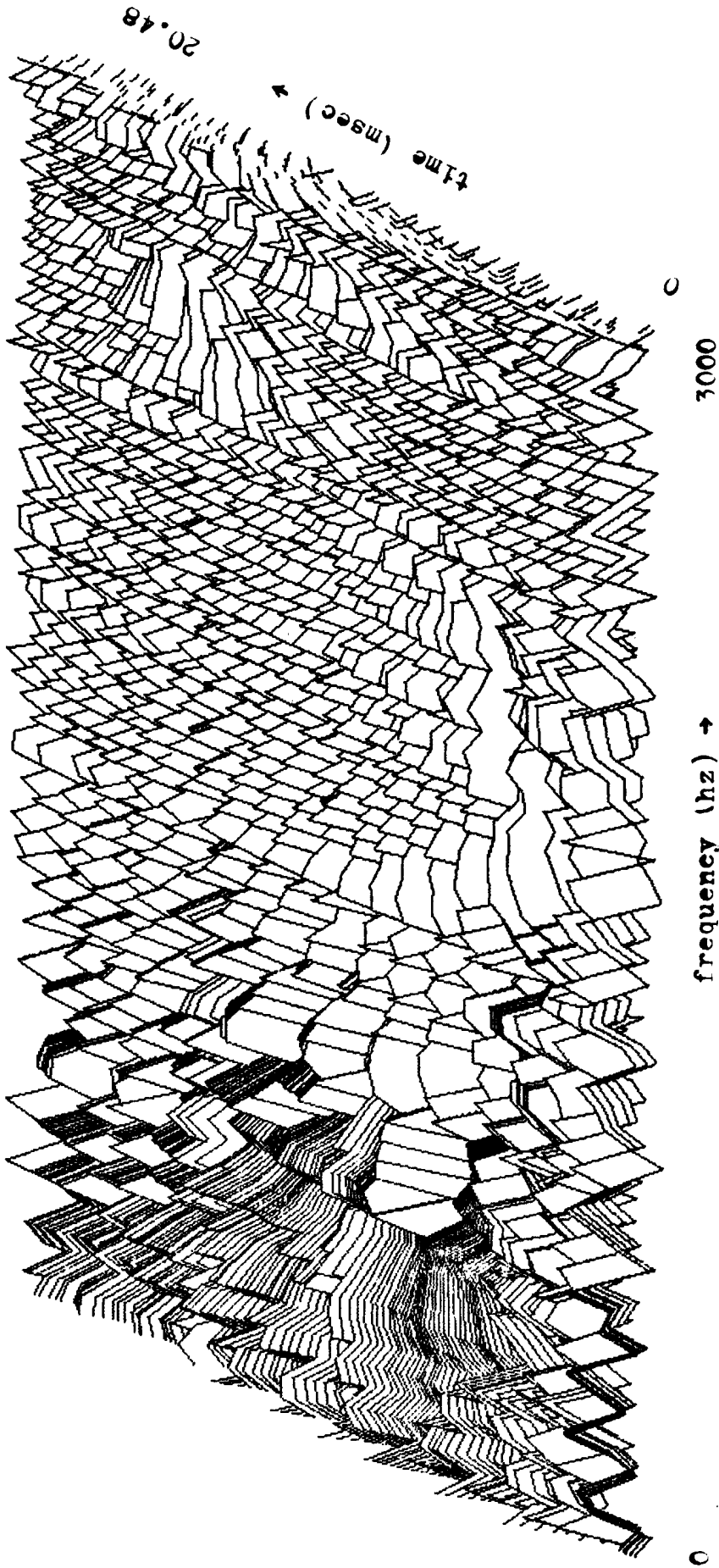
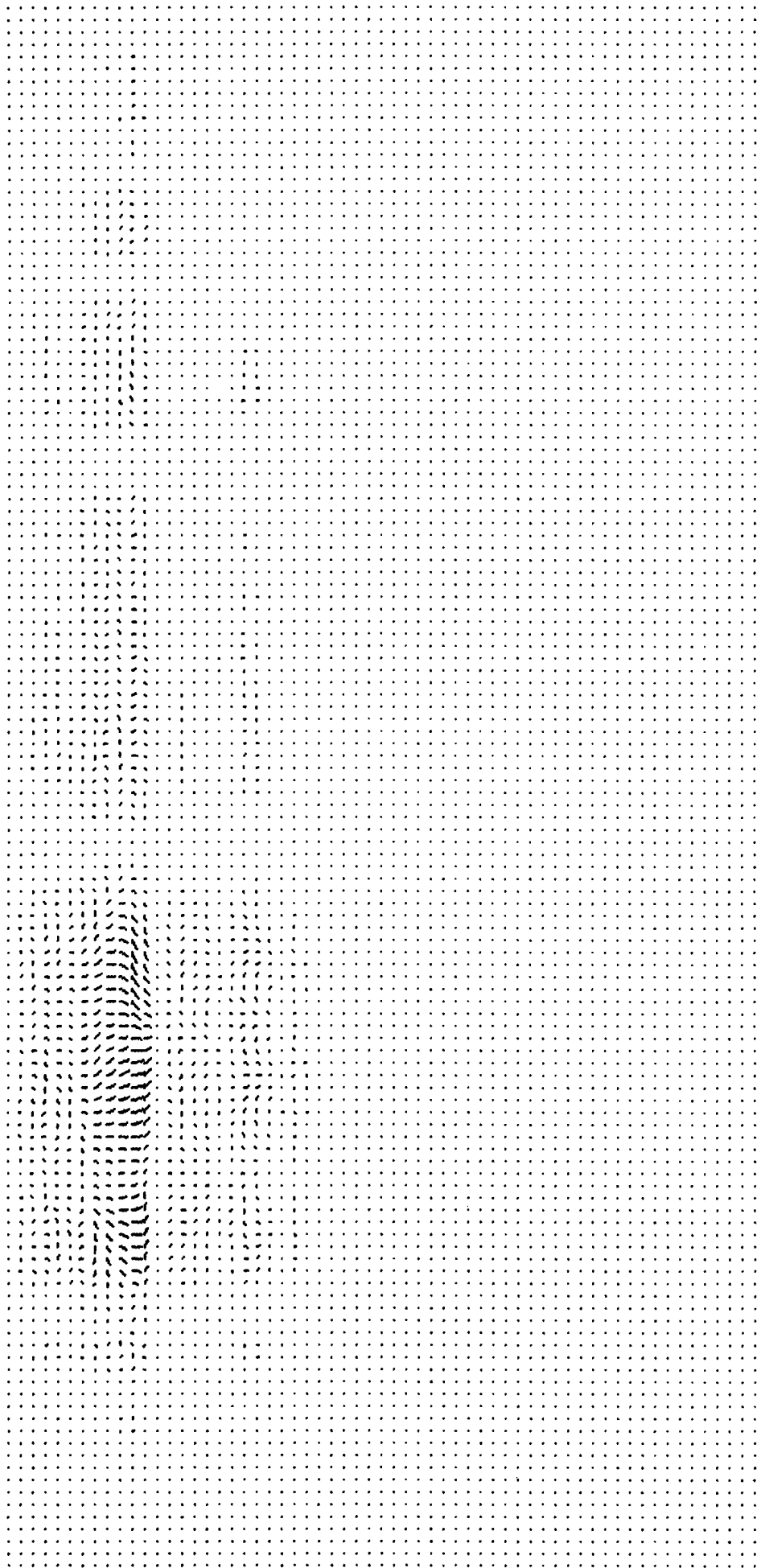


Fig. 4.47. The argument of the COSTID-function of an element from a B-call of the frog *Rana temporaria*.

- 61a -



20.48

time (msec) →

0

frequency (Hz) →

3000

0

Fig. 4.48.  
Vector-display  
of the COSTID-  
function of an  
element from a  
B-call of the  
Irish frog *Rana  
temporaria*.



Fig. 4.49.a. The CoSTID-function of an element from a B-call of the frog *Rana temporaria* with rectangular coding.

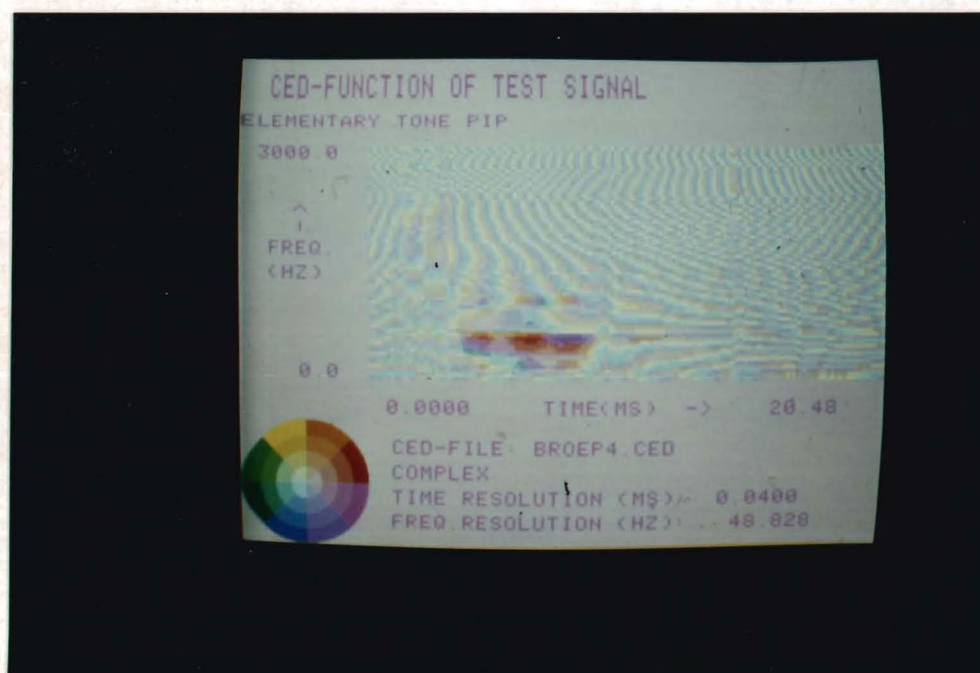


Fig. 4.49.b. The CoSTID-function of an element from a B-call of the frog *Rana temporaria* with polar coding.

## Discussion.

In this report we have described a new method to represent signals in time and frequency. The COSTID - function preserves the phase relations that exist between the spectral components. From the theory we have seen that the COSTID - function, although it has rather elegant properties is nonlinear . In the displays of the COSTID - function of two time and/or frequency shifted gamma-tones we saw that the COSTID - functions of the separate tones were multiplied by a complex factor. It should be noted, that the COSTID - function itself has no physical meaning, but that a number of functionals on it do have.

The relations between the COSTID - function and other second-order signal representations, as well as the properties of the COSTID - functions averaged over a stochastic ensemble of signals will be further evaluated by L. Cranen [21] .

While applications of the averaging of COSTID - functions of pre-neural-event stimuli for cat and frog are done by

A. Aertsen.

From the results for the summation signals of gamma-tones, of spectral analyzer, short-time spectrum and COSTID - function method one can see, that with the COSTID - function, there is no need for window-selection matched to the signal phenomenon under investigation.

A remarkable difference between the  $xy$ - and  $r\phi$  colour-

coding is found because of the implicit threshold of the xy-coding. All points within the square around the origin of the complex plane get the same colour. This in contrast to the  $r\varphi$ -coding, where all points with modulus unequal to zero, get different colours depending on their argument and modulus size. The question arises in howfar the data in the region of very small modulus is relevant. So an analysis of the accuracy limits has to be done and this will lead to further improvement of the colour-coding.

As for the choice of the colours we can say that by changing the colour configuration certain signal features may be enhanced, but are difficult to interpret. An optimal selection cannot be given here. With respect to the perceptive effects of the colour-display we can say that we have the impression that one can learn to examine the colour displays.

Concluding we can say that it is expected that the COSTID-function method will contribute to better insight in the signal properties in cases where the phase relation between the frequency components may be of interest.

References.

1. Olders, J.H.J. (1977), The Auditory System of the Frog. Report, Laboratory of Medical Physics and Biophysics, University Nijmegen.
2. Smolders, J. (1975), Neural representation of sounds from the acoustic biotope of the cat. Doctoral report, Laboratory of Medical Physics and Biophysics, University Nijmegen.
3. Eykhoff, P. (1974), System Identification, John Wiley Sons, London, New York, Sydney, Toronto.
4. Burgers, C.J.M. (1977), Spectral analysis of sound signals from the acoustic biotope of the Cat. Doctoral report, Laboratory of Medical Physics and Biophysics, University Nijmegen.
5. Koldewijn, C.J.R. (1973), Modelstudy of the peripheral auditory system. Doctoral report, University of Technology, Eindhoven.
6. Ville, J. (1948), Theorie et applications de la notion de signal analytique. Câbles et Transmission 2, pp 61 - 74.
7. Dijk, B. van (1971), Telecommunication I, class notes, University of Technology, Eindhoven.



8. Bedrosian, E. (1962), The analytic signal Representation of Modulated Waveforms. Proc. IEEE, october, pp 2071-2076.
9. Oswald, J.R.V. (1956), The theory of analytic Bandlimited signals applied to carrier systems. IRE translations on Circuit Theory, dec., pp 244-250.
10. Bedrosian, E. (1963), A Product Theorem for Hilbert Transforms, Proc. IEEE, vol.51, pp 868-869.
11. Gabor, D. (1946), Theory of Communication, Proc. IEEE (London) vol.93, pt.III, november, pp 429-445.
12. Rihaczek, A.W. (1969), Principles of high resolution radar (Chapter 2) Mc Graw-Hill Bookcompany, New York.
13. Ackroyd, M.H. (1970), Instantaneous and Time-varying Spectra (an Introduction). The radio and electronic engineer, vol.39 no.3, pp 145-152.
14. Page, C.H.(1952), Instantaneous power spectra. Journal of appl.physics, no.1, pp 103-106.
15. Rihaczek, A.W.(1968), Signal energy distribution in time and frequency. Trans. IEEE IT-14, pp 369-374, may.
16. Wozencraft, J.M. and Jacobs, I.M.(1965), Principles of Communication Engineering, John Wiley Sons, Inc.

17. Sheich, H.(1977), Central processing of Complex Sounds and Feature Analysis. In : T.H.Bullock (Ed), Recognition of Complex Acoustic Signals, Life Sciences Research Report 5, Abakon Verlagsgesellschaft, Berlin 1977.
18. Aertsen, A.M.H.J. and Johannesma, P.I.M.(1979), Spectro temporal analysis of auditory neurons: the CoSTID-function. (in preparation)
19. Cranen, L.I.J.(1979), Second order representation of signals. Doctoral report, Laboratory of Medical Physics and Biophysics, University Nijmegen.
20. Beauchamp, K.G.(1973), Signal Processing Using Analog and Digital Techniques (chapter 11), Allen Unwin Ltd. Printed by William Clowes and Sons Ltd.
21. Hoeks, A.P.G. and Krijt, H.J.(1976), Hardware processing of non-stationary signals. Internal report, Lab. of Medical Physics and Biophysics, University Nijmegen.

## Curriculum Vitae

The author of this report was born May 1951 in Oss, The Netherlands. In 1969 he took his certificate of the Secondary Modern School.

Then he studied electrical engineering at the University of Technology Eindhoven. During his practical training periods he worked at a hardware parity checking device, the surface conditions of silicon after oxidation, software for an interactive signal analysis program and a device for an automatic location of His bundle in the heart (Centre d'Etude et de Technologie Appliquées à la Chirurgie, Lyon, La France). He completed his studies by the project described in this report and passed the doctoral examination in March 1979.

Since 1978 he is working at the Laboratory of Medical Physics and Biophysics of the University of Nijmegen, The Netherlands, in the group of Prof. Dr. A.J.H. Vendrik and Dr. Ir. H.J.M. Gerrits, on eye movement.